APPLICATION OF PHOTOCATALYSIS FOR THE TREATMENT OF GREY WATER

by

NAZMİYE CEMRE BİRBEN

B.S. in Environmental Engineering, Yıldız Technical University, 2008

Submitted to the Institute of Environmental Sciences in partial fulfillment of

the requirements for the degree of

Master of Science

in

Environmental Technology

Bogazici University

2012

Dedicated to my family...

ACKNOWLEDGEMENTS

I sincerely appreciate the precious guidance, support, opportunuties and supervision I have received from Prof. Dr. Miray BEKBÖLET. It was a pleasure to study with her and to have a chance of benefit from her scientific and personal experiences.

I would also like to express my appreciation to the members of my thesis jury; Prof. Dr. Orhan YENİGÜN and Prof. Dr. İdil ARSLAN ALATON for their valuable time and comments.

I would express my special thanks to Dr. Ayşe Tomruk, Dr. Ceyda Uyguner Demirel, research assistants Sibel Şen Kavurmacı and Asu Ziylan who helped me for the experimental part of this study.

I wish to thank my colleagues; Yeşim Ekici, Arın Küçükdoğan, Zeynep Akdoğan and Özlem Karataş for their support and friendship.

Finally, I would like to thank my family for their love, never-ending support, understanding and encouragement during my life.

APPLICATION OF PHOTOCATALYSIS FOR THE TREATMENT OF GREY WATER

Defined as the all wastewater coming from urban areas except any input from toilets, grey waters constitute the largest fraction of the total domestic wastewater consumption which may fluctuate in quality and quantity diversely. Since grey water is less contaminated by nutrients, inorganics and hazardous organic substances, it is a potential ‘’non-conventional’’ water resource. As a consequence, several treatment technologies to treat and reuse grey water have been studied widely. As one of these processes, photocatalytic oxidation, which relies upon the generation of highly reactive hydroxyl radicals under UV radiation, has become an innovative and effective technology for the treatment of grey water in terms of degradation of refractory organic matter and potential disinfection mechanism.

This study aimed to investigate applicability of photocatalytic oxidation process to treat grey water sources. In this manner, synthetically prepared grey water samples were subjected to photocatalytic oxidation in the presence of TiO_2 as the semiconductor photocatalyst. Further assessment of the system performance was observed by making compositional alterations of grey water samples in terms of organic matter loading, anion concentration, and microbiological content particularly. The results of photocatalytic oxidation experiments were deliberated by the determination of selected specified and specific UV-vis and fluorescence parameters. In addition to specified UV-vis parameters, DOC and bacterial content of samples were also evaluated in terms of removal efficiencies and photocatalytic degradation kinetics expressed by pseudo- first order kinetic modeling.

As a consequence, photocatalytic oxidation of low load grey water with microorganism and low anion content revealed the most effective results in terms of the removal of selected parameters whereas lowest removal efficiencies for the selected parameters were achieved by photocatalytic oxidation of high load grey water with high anion content indicating the impact of organic matter loading and anion strength on the performance of photocatalytic oxidation process.

GRİ SU ARITIMINDA FOTOKATALİTİK OKSİDASYON UYGULAMASI

Tuvalet girdisi dışındaki tüm evsel atıksular olarak tanımlanan gri su, kalite ve miktar bakımından değişiklikler göstermekle birlikte evsel atıksu tüketiminin büyük bir fraksiyonunu oluşturmaktadır. Gri su nütrientler, inorganikler ve tehlikeli organik maddeler açısından daha az kirlilik göstermesi dolayısıyla geleneksel olarak kullanılan su kaynaklarına alternatif olarak kullanım potansiyeli bulunmaktır. Dolayısıyla gri su artımı ve tekrar kullanımı amacıyla bir çok arıtma teknolojileri geniş ölçüde çalışılmıştır. Bu arıtma teknolojilerinden biri olan fotokatalitik oxidasyon prosesi UV ışığı altında yüksek reaktivitedeki hidroksil radikallerinin üretimi mekanizmasına dayanmakla beraber, gri suda bulunan dirençli organik maddeleri giderme ve dezenfeksiyon potansiyeli dolayısıyla gri su arıtımında yenilikçi ve etkili bir teknoloji halini almıştır.

Bu çalışma, fotokatalitik oskidasyon prosesinin gri su arıtımında uygulanabilirliğini araştırmayı amaçlamıştır. Bu amaçla sentetik olarak hazırlanan gri su numunleri TiO_2 ile fotokatalitik oksidasyona maruz bırakılmıştır. Sistem prefromansının daha ileri seviyede değerlnedirilmesi gri su kompozisyonlarında organic madde yükü, anyon konsantrasyonu ve mikrobiyolojik içerik açısından değişikliklere gidilerek gözlemlenmiştir. Fotokatalitik oksidasyonun deneysel sonuçlarının tartışılması amacıyla tayin edilen spesifik UV görünür bölge ve floresans parametreleri saptanmıştır. UV görünür bölge parametrelerine ilave olarak gri suda bulunan çözünmüş organik karbon ve bakteriyolojik parametreler de giderim verimleri ve fotokatalitik degradasyon kinetikleri açısından incelenmiştir.

Sonuç olarak mikroorganizma ve düşük anyon konsantrasyonu içeren düşük yüklü gri suyun fotokatalitik oksidasyonu seçilen parametrelerin giderimi açısından en etkili sonuçları göstermiştir öte yandan seçilen aynı parametrelerin en düşük giderim verimlerini yüksek anyon konsantrasyonuna sahip yüksek yüklü gri suyun fotokatalitik oksidasyonu ile vermesiyle organik madde yükü ve anyon konsantrasyonunun fotokatalitik oksidasyon prosesinin performansı üzerindeki etkisi belirtilmiştir.

TABLE OF CONTENTS

LIST OF FIGURES

LIST OF TABLES

LIST OF SYMBOLS/ABBREVIATIONS

Symbol	Explanation	Units used
AOPs	Advanced Oxidation Processes	
BET	Brunauer, Emmett and Teller	m^2g^{-1}
BLF	Black Light Fluorescent Lamp	
BOD	Biochemical Oxygen Demand	mg O_2 L^{-1}
BOD_5	5 Days Biochemical Oxygen Demand	mg O_2 L^{-1}
CB	Conductance Band	
CBOD	Carbonaceous Biochemical Oxygen Demand	mg O_2 L^{-1}
COD	Chemical Oxygen Demand	mg O_2 L^{-1}
$Color_{436}$	Absorbance at 436 nm	m^{-1} or cm^{-1}
DOC	Dissolved Organic Carbon	mg OrgC L^{-1}
EC	Electrical Conductance	µS cm^{-1}
E.coli	*Escherichia coli*	CFU mL^{-1}
FE	Faecal Enterococci	CFU mL^{-1}
FS	Faecal Streptococci	CFU mL^{-1}
HLGW	High Load Grey Water with microorganism and low anion content	
HLGWHIC	High Load Grey Water with High Anion Content	
HLGWLIC	High Load Grey Water with Low Anion Content	
HRT	Hydraulic Retention Time	
LLGW	Low Load Grey Water with microorganism and low anion content	
LLGWHIC	Low Load Grey Water with High Anion Content	
LLGWLIC	Low Load Grey Water with Low Anion Content	
MCR	Membrane Chemical Reactor	
MBR	Membrane Bioreactor	
NASA	National Aeronautics and Space Administration	
NBOD	Nitrogenous Biochemical Oxygen Demand	mg O_2 L^{-1}
NO_2^-	Nitrite Nitrogen	mg L^{-1}

NO_3^-	Nitrate Nitrogen	mg L^{-1}
PAC	Powdered Activated Carbon	
PO_4^{3-}	Phosphate Phosphorus	mg L^{-1}
RBCs	Rotating Biological Contactor	
ROS	Reactive Oxygen Species	
SCOA	Specific color absorbance	m^{-1} $mg^{-1}L$
$SCOA_{436}$	Specific color absorbance at 436 nm	m^{-1} $mg^{-1}L$
SM-SBR	Submerged membrane sequencing batch reactor	
SRT	Solids Retention Time	
SUVA	Specific UV absorbance	m^{-1} $mg^{-1}L$
$SUVA_{254}$	Specific UV absorbance at 254 nm	m^{-1} $mg^{-1}L$
$SUVA_{280}$	Specific UV absorbance at 280 nm	m^{-1} $mg^{-1}L$
$SUVA_{365}$	Specific UV absorbance at 365 nm	m^{-1} $mg^{-1}L$
TC	Total Coliform	CFU mL^{-1}
TKN	Total Kjeldahl Nitrogen	mg TKN L^{-1}
TN	Total Nitrogen	mg N L^{-1}
TOC	Total Organic Carbon	mg OrgC L^{-1}
TP	Total Phosphorus	mg P L^{-1}
TS	Total Solids	mg L^{-1}
TSS	Total Suspended Solids	mg L^{-1}
UASB	Up flow Anaerobic Sludge Blanket	
UV_{254}	Absorbance at 254 nm	m^{-1} or cm^{-1}
UV_{280}	Absorbance at 280 nm	m^{-1} or cm^{-1}
UV_{365}	Absorbance at 365 nm	m^{-1} or cm^{-1}
UVC	Ultraviolet-C	
VB	Valence Band	
WHO	World Health Organization	
XOCs	Xenobiotic Organic Compounds	

1. INTRODUCTION

Grey waters are defined as the all domestic wastewater coming from households excluding any discharge from toilet flushing, thus constituting the largest portion of total domestic wastewater consumption. Grey water is comparatively less contaminated by nutrients, inorganics and hazardous organic substances which makes it favorable for non-potable reuse purposes. Consequently, evaluation and application of several processes to treat grey water sources comprising a wide range of alternatives from a simple filtration process to sophisticated systems based on physical, biological and chemical/advanced oxidation technologies have been studied by many researchers widely.

Considered as one of the advanced oxidation processes (AOPs), heterogeneous TiO_2 photocatalysis relies on the generation of highly reactive oxygen radicals as strong and non-selective oxidants that are able to degrade organic pollutants effectively to carbon dioxide, water and mineral acids. Due to its tremendous advantages e.g. degradation of recalcitrant organic pollutants, bactericidal activity and elimination of chemical use, photocatalytic oxidation process has become an innovative technology for the treatment of water and wastewater.

The overall objective of this research is to investigate the potential application of TiO_2 photocatalysis as a novel alternative to treat grey water. In this manner, synthetically prepared grey water samples with compositional differences in terms of organic matter loading (low load organic matter and high load organic matter), anion strength (low anion content and high anion content) and bacteriological content were subjected to photocatalytic oxidation in the presence of TiO_2 as the photocatalyst in order to assess the performance of process specifically. The results of the experimental studies were evaluated in terms of the specified ($Color_{436}$, UV_{365}, UV_{280} and UV_{254}) and specific UV-vis ($SCoA_{436}$, $SUVA_{365}$, $SUVA_{280}$ and $SUVA_{254}$) and fluorescence parameters (SFI_{emis} and SFI_{sync}), DOC values and microbiological contents (Total Coliforms, Faecal Coliforms and Faecal Streptococci) concomitantly.

2. THEORETICAL BACKGROUND

The aim of this chapter is to give detailed information about grey water. Firstly, definition of grey water and its characteristics are explained elaborately. Secondly, explanatory information of grey water reuse, its importance, and its applications are demonstrated. Thirdly, different grey water treatment technologies and their applications are mentioned specifically. Following an introduction to advanced oxidation processes, the fourth chapter is concluded with the summary of several literature studies performed for photocatalytic oxidation of grey water.

2.1. Grey Water Definition and Characteristics

2.1.1. Grey Water

Grey waters are defined as the all low polluted domestic wastewater coming from showers, hand washing basins, laundry facilities, kitchen sinks and washing machines. In other words, grey water is known to be all wastewater originating from domestic sources except toilet flushing called as ‘black water’ (Nolde, 1999; Eriksson et al., 2002; Hourlier et al., 2010; Chaillou et al., 2011). Moreover, grey water can be divided into two groups in terms of its organic matter and solid content. While kitchen grey water is classified as ‘high load’ grey water due to its high organic and solid content as well as surface active compounds e.g. detergents, the rest of the grey water sources are defined as ‘low-load’ grey water that are poor in organic matter and solids (Al-Jayyoushi, 2003). Grey water constitutes 75% of the combined residential sewage and 50-80% of total domestic wastewater consumption that can reach up to 90% if vacuum toilets are installed (Eriksson et al., 2003; Friedler and Hadari, 2006; Hernández Leal et al., 2011). Percentage change in domestic water consumption for several purposes is displayed in Table 2.1 according to studies conducted in some of the selected countries.

Table 2.1. Percentage change in domestic water consumption for several purposes.

	Water Demand (%)						
Country	Toilet Flushing	Laundry	Kitchen	Shower	Cleaning	Other	Reference
UK	33	12	18	25	9	3	UK Rainwater Harvesting Association
USA*	27	22	-	17	-	5	AWWA, 1999
Oman	19	23	6	46	-	6	Jamrah et al., 2008
India	15	20	23	18	3	11	Mandal et al., 2011

*15% defined as faucet and 14% defined as leaks

2.1.2. Grey Water Characteristics

Characteristics of grey water may depend on several factors, but there are three main factors directly affect the quality and quantity of grey water. Quality of the water supply, the type of distribution network for both drinking water and grey water and activities of households comprise the most important factors contributing to the compositional differences in grey water. Moreover, customs, life styles, installations, and use of chemical household products are other crucial factors that influence presence of different substances in grey water (Eriksson et al., 2002). Due to the presence of perishable food waste, kitchen wastewater generally contains more organic matter loading than other grey water sources (Donner et al., 2010). In addition, use of variety of chemical products causes presence of xenobiotic organic compounds (XOCs) in bathroom grey waters. Conventional wastewater parameters observed for different grey water sources are classified according to their physical, chemical, bacteriological and nutrient properties and presented in tables 4.1, 4.2, 4.3 and 4.4 respectively.

Compositional differences of different grey water sources are presented in Table 2.2 and Table 2.3 in terms of their physical and chemical constituents. Total suspended solids concentrations and turbidity values of grey water compositions vary from 12 to 76 mg L^{-1} and from 20 to 92 NTU pointing out that grey waters have considerably lower suspended solid content compared to domestic wastewaters (Table 2.2). Grey water originating from bath/showers displayed considerably higher turbidity and TSS (Surendran and Wheatley, 1998).

Table 2.2. Physical properties of grey water originating from different sources.

Source	Parameter			Reference
	Turbidity (NTU)	TS (mg L^{-1})	TSS (mg L^{-1})	
Bath/Shower	92	631	76	Surendran and Wheatley, 1998
Hotel Bathroom	20	-	44	March et al., 2004
Synthetic	24	-	72	Hourlier et al., 2010
Mixed	20.6	-	12	Mandal et al., 2011

Compared to domestic wastewater, the pH range of grey water is more likely to be alkaline (pH~10) which comes from detergents and shampoos used in laundries and baths (Chin et al., 2009; Schäfer et al., 2006). On the other hand, kitchen grey water may differ from others by having an acidic composition with regard to its constituents (Halalsheh et al., 2008). When considering the other traditional wastewater parameters, COD and BOD loadings of grey water samples may be similar to domestic wastewater, but their chemical nature may be quite different. BOD_5/COD ratio (~0.45) is one of the parameters taken into account by various researchers for determining the chemical nature of grey water samples and their biodegradability either aerobically or anaerobically (Jefferson et al., 1999; Li, 2009; Hernández Leal et al., 2011; Weitao et al., 2011). Reported COD and BOD values vary from 170 to 2244 mg L^{-1} and from 76 to 1100 mg L^{-1} indicating the diversified concentrations of selected parameters for several grey water sources.

Table 2.3. Chemical properties of grey water originating from different sources.

Source	Parameter				
	pH	EC ($\mu S\ cm^{-1}$)	BOD_5 ($mg\ O_2\ L^{-1}$)	COD ($mg\ O_2\ L^{-1}$)	Reference
Bath and Shower	7.6	-	216	424	Surendran and Wheatley, 1998
Shower	7.5	1241	78	170	Ramon et al., 2004
Kitchen Sink	5.6	1066	1100	2244	Halalsheh et al., 2008
Bathroom	10.0	1088	76	225	Chin et al., 2009
Bathroom	7.3	421	200	421	Chaillou et al., 2011

Other than traditional wastewater parameters, grey water may contain a variety of different compounds originating from use of several different products in kitchen, bathroom and laundries. One of these compounds are xenobiotic organic compounds (XOCs), constituting a heterogeneous group of compounds coming from use of chemicals in households (Eriksson et al., 2002; Eriksson et al., 2009; Donner and Eriksson, 2010; Gulyas et al., 2011). Hazardous substances also another serious topic related to grey water due to the possibility of their presence in grey water. 22 of the 105 selected hazardous substances were detected in ordinary Swedish households (Palmquist and Hanaeous, 2005). Classified as hazardous substances, sources, presence and fate of metals in grey waters have also been studied in order to get detailed information about this component of grey water specifically. Although annual metal loadings from bathroom grey waters are comparatively lower than typical municipal wastewater loadings, they still have difficulties in meeting environmental quality standards for surface waters (Eriksson and Donner, 2009). Although grey waters do not contain feces and urine, they may contain a variety of bacterial cultures with particular concentrations.

Some of the bacterial content of real and synthetic grey water samples are displayed in Table 2.4 specifically. According to literature studies displayed in Table 2.4, it is revealed that bacterial content of grey water samples are comparatively lower than domestic wastewaters, however their existence is still a problem due to their potential risk to health when considering grey water reuse for potable and non-potable purposes (Dixon et al., 1999). Total Coliform (TC), E.coli and Faecal Enterococci (FE) are some of bacterial cultures observed in grey water sources specifically (Table 2.4).

Table 2.4. Microbiological properties of grey water originating from different sources.

Source	Microorganism (CFU 100 mL^{-1})			Reference
	TC	*E. coli*	FE	
Bathroom	500-2.4 x 10^7	170-3.3 x 10^3	-	Christova-Boal et al., 1996
Laundry	10^4-10^5	-	-	Nolde, 1999
Mixed	8.1	6	4.4	Ottoson and Strensöm, 2003
Synthetic	> 2400	67	> 100	Toifl et al., 2008
Synthetic	3.8 x 10^5	9.6 x 10^3		Hourlier et al., 2010

Table 2.5. Nutrients observed for grey water samples originating from different sources.

Source	Nutrients (mg L^{-1})					Reference
	TN	TP	NO_2^-	NO_3^-	PO_4^{3-}	
Synthetic	5	0.047	-	-	-	Jefferson et al., 2001
Shower	-	1.6	-	-	1	Merz et al., 2007
Mixed	7.6	-	-	3.9	0.5	Pidou et al., 2008
Mixed	26.3	7.2	0.84	0.77	2.36	Hernandez Leál et al., 2011
Bathroom	9.5	0.42	-	-	-	Chaillou et al., 2011

A comparative demonstration for the nutrient content of different grey water samples is shown in Table 2.5. Grey water is quite poor in nutrient content in contrast to domestic wastewater because it does not contain feces and urine which are the main sources of nitrogen and phosphorus. As a result, nutrient addition is taken into account for process efficiency when considering biological treatment of grey water (Jefferson et al., 2001). When considering the nutrient content of several grey water compositions, some of the literature studies revealed total nitrogen concentrations in the range of 5-26 mg N L^{-1} and total phosphorus concentrations in the range of 0.047-7.2 mg P L^{-1}. Diversity of the nutrient content of grey water samples can be attributed to the factors affecting the characteristics of grey water mentioned previously.

2.2. Grey Water Reuse

Water demand management has gained a great deal of interest due to emerging problems in relation to water scarcity especially for arid and semi-arid regions, avoiding use of fresh water sources, reducing pollutant loading into the environment and overall supply costs. All these problems revealed the idea of recycling and reuse of different wastewater sources (i.e. domestic, industrial, and grey wastewater) in order to prevent use of high quality fresh water thus, reducing pollutants in the environment and last but not least reducing overall supply costs (Burkhard et al., 2000; Al-Jayyoushi, 2003 and 2004). Moreover, improving access to water and sanitation has the potential to prevent global disease burdan.

Grey water recycling and reuse for non-potable purposes is more likely to become an attractive topic due to its advantageous properties compared to domestic wastewater recycling and reuse, such as comprising the largest volume of the waste flow from households (50 to 80 %), having poor nutrient and pathogen content, and reasons that have mentioned before in water demand management section (WHO, 2006). However, classified as a wastewater, recycled grey water should also fulfill four important criteria: technical and economical feasibility, environmental tolerance, hygienic safety, and aesthetics to prevent several risks while reusing grey water (Nolde, 1991; Eriksson, 2002).

Multi-storey buildings have a potential for application of grey water treatment and reuse in order to overcome problems related to potable water savings and cost-effectiveness. Several researchers have studied this topic in terms of sustainable water management. Most of the studies concluded that by choosing appropriate technologies, treated grey water may be used for non-potable purposes, such as toilet flushing, irrigation, and car washing beneficially (Nolde, 1999; Friedler and Galil, 2003; Garland, 2006; Ghisi and Ferreira, 2007).

Hotels are other places where grey water treatment and reuse systems have been studied to overcome seasonal demand of fresh water that exceeds the capacity of reservoirs. Simple physical treatment processes of sedimentation and filtration followed by a disinfection unit have been studied for the treatment of bathroom and laundry grey waters in different hotels in different countries. They concluded that satisfactory results would be obtained in terms of sustainability and cost effectiveness (March et al., 2004; Friedler and Galil, 2005; Gual et al., 2008; Li et al., 2010).

Having only desirable results for recycled grey water that meets quality requirements would not be enough to implement such a system in any place. Economical feasibility is another most important factor on deciding and applying grey water treatment and reuse systems. As a result, internal and external benefits, risks and costs of these systems have also been studied widely in order to decide whether using these systems will bring economical benefits too (Gulyas et al., 2007; Godfrey et al., 2009; Henriques and Louis, 2011; Mandal et al., 2011).

2.3. Grey Water Treatment Technologies

There are several technologies applied for grey water treatment comprise a wide range of alternatives, such as physicochemical, biological and advanced treatment technologies. Characteristics of grey water and reuse purposes are the main factors taken into consideration on deciding the appropriate grey water treatment technology. Thus, implementing combination of these different technologies is also another way preferred in grey water treatment in order to get favorable results (Pidou et al., 2007; Li et al., 2009).

2.3.1. Physicochemical Treatment Processes

Direct introduction of freshly generated grey water into an active, rich topsoil environment is the simplest and oldest well-known grey water treatment system (Al-Jayyousi, 2003). In addition, using coarse filters, membrane filters and other natural environments such as sand and mulch are known to be different physical treatment technologies followed by a disinfection step in order to remove pathogen microorganisms (Nghiem et al., 2006; Kim et al., 2007; Zuma et al., 2009). Several physicochemical processes applied for grey water treatment are presented in Table 2.6 in terms of their removal performance on selected parameters. The parameters used for expressing the grey water characteristics were, *i.* physical parameters, turbidity, suspended solids; *ii.* organic matter content in terms of TOC, COD and BOD_5; *iii.* nitrogen contents as total nitrogen; *iv.* hardness causing divalent cations, Ca^{2+} and Mg^{2+}. Bacteriological load of grey water was displayed in terms of either total coliform counts or specifically by *E.coli* as the indicator organism (Pidou et al., 2008).

Application of filtration and sedimentation followed by disinfection was applied for the treatment of grey water from bathtubs and hand-washing basins and process efficiency was expressed by turbidity, suspended solids, total nitrogen, TOC and COD (March et al, 2004). It was also reported that the treated grey water could be used for flushing the toilets. Low-load grey water was treated by coagulation and chlorination and the treatment efficiency was reported by similar parameters representing organic content (e.g. COD) as well as by hardness causing divalent cations (Friedler et al., 2008). In a recent study reported by Pidou and colleagues, grey water obtained from showers was treated by coagulation and magnetic ion exchange resin. Treatment efficiency was also expressed by the removal of coliform bacteria (Pidou et al., 2008). Moreover, Hourlier and co-workers applied direct ultrafiltration for the treatment of synthetic grey water and study concluded that direct ultrafiltration would give desirable results in terms of the removal of selected traditional wastewater parameters (e.g. COD, BOD_5, DOC and turbidity) (Hourlier et al., 2010).

However, physical treatment options (e.g. filtration and sedimentation) can only remove solid particles and have limitations on removing pollutants such as organics,

nutrients, surfactants and other micro-pollutants (e.g. xenobiotic organic compounds and metals) whose impacts can not be underestimated (Li et al., 2010).

Table 2.6. Physicochemical treatment processes for the treatment of grey water.

Sample	Treatment	Operative parameters			Reference
		Parameters	In	Out	
Grey water from bathtubs and hand-washing basins	Filtration and Sedimentation and Disinfection	Turbidity (NTU)	20	16.5	March et al., 2004
		TOC (mg OrgC L^{-1})	171	78	
		COD (mg O_2 L^{-1})	58	39.9	
		SS (mg L^{-1})	44	18.6	
		TN (mg N L^{-1})	11.4	7.6	
Low-load grey water	Coagulation and Chlorination	Turbidity (NTU)	<1	<1	Friedler et al., 2008
		Ca^{2+} (mg L^{-1})	0.2	0.1	
		Mg^{2+} (mg L^{-1})	1.1	0.7	
		TOC (mg OrgC L^{-1})	1.4	0.3	
		TN (mg N L^{-1})	0.7	0.3	
Shower grey water	Coagulation and Magnetic Ion Exchange resin	Turbidity (NTU)	46.6	3.01	Pidou et al., 2008
		COD (mg O_2 L^{-1})	791	241	
		BOD (mg O_2 L^{-1})	205	27	
		DOC (mg OrgC L^{-1})	171	78.1	
		TC (CFU 100 mL^{-1})	5.7E4	<1	
		E.coli (CFU 100 mL^{-1})	6.5E3	<1	
Synthetic Grey water	Direct Ultrafiltration	Turbidity (NTU)	4	<1	Hourlier et al., 2010
		COD (mg O_2 L^{-1})	464	77	
		BOD_5 (mg O_2 L^{-1})	63	2	
		DOC (mg OrgC L^{-1})	149	47	
		A- surfactants (mg L^{-1})	17	2	

Consequently, combination of physical and chemical treatment technologies called physicochemical processes is preferably used in grey water treatment. Physicochemical treatment processes may be as simple as two stage systems consisted of a filtration step followed by a disinfection process. On the other hand, contribution of different chemicals for coagulation and ion exchange processes are also taken into account in different physicochemical processes used for grey water treatment. According to the results obtained from Table 2.6, the most effective results in terms of removal of the selected parameters are achieved with the physicochemical treatment processes especially when using coagulation with the combination of other treatment technologies rather than applying physical treatment options alone.

2.3.2. Biological Treatment Processes

Biological treatment processes are known to be one of the most common grey water treatment technologies studied and applied throughout literature studies. Common biological treatment processes used for grey water treatment are membrane bioreactors (MBRs), rotating biological contactors (RBCs), and constructed wetlands. In this section, brief information about biological treatment processes and their application in grey water treatment through the literature studies are mentioned specifically. Several biological treatment processes including MBR and RBCs followed by UV treatment applied for grey water treatment are shown in Table 2.7.

Membrane bioreactor systems (MBR) are commonly used for grey water treatment and reuse purposes. Several studies showed that MBR technologies used for grey water treatment resulted in desirable reuse standards due to its stability and pathogen removal. Thus, different MBR technologies for grey water treatment was studied with small alterations such as with different solid retention times (SRT) and hydraulic retention times (HRTs) (Lesjean and Gnirss, 2006; Scheuman and Kraume, 2009), with submerged membrane sequencing batch reactor (SM-SBR) (Kraume et al., 2010), HUBER-MBR process (Paris and Schlapp, 2010). Rotating biological contactors also have been applied for grey water treatment in several literature studies. Many of these studies concluded that combination of RBCs with other physicochemical treatment processes such as, filtration

and disinfection makes this process more feasible and economical for medium and high load grey water treatment (Nolde, 1999; Friedler et al., 2005; Li et al., 2009; Revitt et al., 2011).

Table 2.7. Biological treatment processes applied for grey water treatment.

Sample	Treatment	Operative parameters			Reference
		Parameters	In	Out	
Mixed grey water	RBC and sedimentation and sand filtration and disinfection	Turbidity (NTU)	33	0.61	Friedler et al., 2005
		COD (mg O_2 L^{-1})	158	40	
		TSS (mg L^{-1})	43	7.9	
		BOD (mg O_2 L^{-1})	59	2.3	
		FC (CFU 100mL^{-1})	6+E5	0.1	
Low-load grey water	RBC and UV disinfection	Turbidity (NTU)	33	1.5	Gilboa and Friedler, 2008
		COD (mg O_2 L^{-1})	148	47	
		BOD (mg O_2 L^{-1})	86	45	
		TOC (mg OrgC L^{-1})	29	5.8	
		$Absorbance_{254nm}$ (cm^{-1})	0.28	0.032	
Mixed grey water	A^2O oxidation process and Microfiltration	Turbidity (NTU)	14	3	Kim et al., 2009
		COD (mg O_2 L^{-1})	44	4	
		SS (mg L^{-1})	20	5	
		E. coli (CFU 100 mL^{-1})	4,000	1,300	
High-load synthetic grey water	Flat-plate submerged membrane bioreactor	COD (mg O_2 L^{-1})	675	26.3	Huelgas and Funamizu, 2010
		TKN (mg TKN L^{-1})	25.3	12	
		NH_4-N (mg L^{-1})	0.17	0.16	
		NO_3-N (mg L^{-1})	0	9.85	
		TP (mg P L^{-1})	2.4	-	
		PO_4-P (mg L^{-1})	1.3	0.8	

Although biological treatment processes are commonly studied and applied for grey water treatment, its implementation would have some limitations in terms of removal of non-biodegradable, xenobiotic and toxic compounds that are quite resistant and have inhibitory impact on the bacterial activity of biological treatment systems (Rajeshwar and Ibanez, 1996; Marco et al., 1997). Moreover, management of waste activated sludge as the end product of biological processes is another crucial topic that has to be taken into consideration (Breithaupt et al., 2003). Up flow anaerobic sludge blanket (UASB) reactor (Elmitwalli and Otterpohl, 2007), recycled vertical flow bioreactor (Gross et al., 2007), horizontal and vertical flow constructed wetlands (Pansonato et al., 2011), reed beds (Revitt et al., 2011) are some other different biological treatment technologies investigated for grey water treatment.

2.3.3. Advanced Oxidation Processes

Although physicochemical and biological treatment processes displayed desirable results in grey water treatment, they would not be effective enough on removing several micro molecules that are considerably resistant and toxic. As a consequence, alternative treatment methods other than conventional ones should be investigated in order to treat those micro molecules. At this point, advanced oxidation processes (AOPs) may be taken into consideration in order to overcome such a problem.

Advanced oxidation processes are known to be some of the most innovative water and wastewater treatment technologies in which the main mechanism is production of highly reactive transitory oxygen species (ROS) (H_2O_2, $OH^{\bullet}$, $O_2^{\bullet-}$, O_3) that are able to degrade even the refractory organic molecules into biodegradable compounds, and eventually mineralized them to water, yielding CO_2 and inorganic anions. Among these reactive oxygen species, hydroxyl radical is the most powerful oxidizing agent. Homogeneous photolysis, heterogeneous photolysis or photocatalysis, Fenton process, photo-Fenton process, dark oxidation processes, hydrothermal oxidation, wet oxidation, radiolysis, and sonolysis are some of the advanced oxidation processes classified and studied throughout different literature studies (Chin, 2009).

2.3.3.1. Photocatalysis. Among different advanced oxidation processes, heterogeneous photocatalysis initiating semiconductor catalysts i.e. TiO_2, ZnO, Fe_2O_3, CdS, GaP and ZnS has gained specific attention due to its efficiency in degrading a wide range of equivocal resistant organics into biodegradable compounds and mineralizing to innocuous carbon dioxide and water respectively. Therefore, heterogeneous photocatalysis is accepted to be the most efficient AOPs leading to total mineralization of the parent compound and its oxidation products. Mechanisms, principles and environmental applications of semiconductor photocatalysis have been studied commonly by many researchers since 1985 (Ollis, 1985; Linsebigler et al., 1995; Fujishima et al., 2000; Malato et al., 2009).

Various materials as semiconductor photocatalysts have been investigated in terms of their performance on the photocatalytic oxidation process, however use of TiO_2 as the semiconductor photocatalyst generally gives the most desirable results because of its advantageous properties, such as good reactivity, high chemical stability, inexpensiveness, commercial availability and low toxicity (Rajeshwar, 1995). There are three main cyrstaline forms of TiO_2 exist in nature namely anatase, rutile and brookie and among them, anatase shows the greater photocatalytic activity for the most of the reactions. On the other hand, some of the studies concluded that photocatalytic reactivity of mixture of anatase and rutile forms are considerably greater than pure anatase (Malato et al., 2003; Carp et al., 2004). The most widely used TiO_2 is Degussa P-25 exhibiting mixed morphological properties composed of anatase and rutile crystal forms.

A simplified photo-induced formation mechanism occurred on TiO_2 surface is summarized and shown in Figure 2.1. When band gap energy (Ebg= 3.2 eV)of the semiconductor is exceeded or matched by a photon with an energy of (E> Ebg; λ> 300 nm) hv, promotion of an electron from the valence band, VB, into the conduction band, CB, comes out producing an electron hole-pair, e^-_{CB}/h_{vb}^+ (Reactions 2.1-2.2). Conduction band electrons in the excited state and valence band holes may go through different circumstances, such as recombination and dissipation of input energy as heat, get grasped in the metastable surface states or reacting with electron acceptors or donors adsorbed on the surface of the semiconductor (Hoffman et al., 1995).The main electron scavenger is the dissolved in aerated aqueous solutions. Through a series of reactions (2.17-2.13) hydroxyl radicals are formed and transformed into other reactive oxygen species.

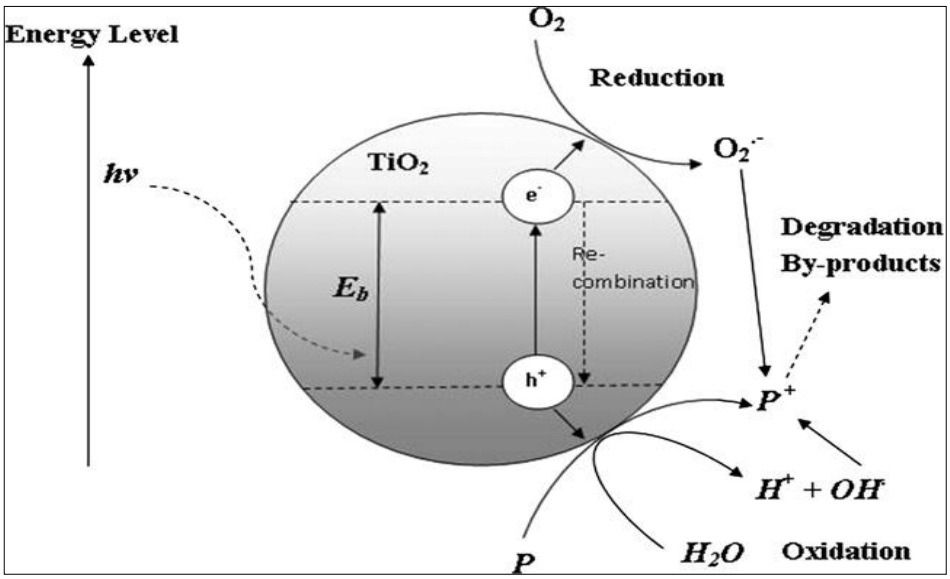

Figure 2.1. Photo-induced formation mechanism of electron hole pair in a semiconductor TiO_2 particle in the presence of water pollutant (P) (Chong et al., 2010).

Heterogeneous TiO_2 assisted photocatalysis comprises a complex sequence of reactions. The main mechanisms for the degradation of the organic matter are outlined step by step in the following equations of 2.1-2.13 respectively:

(i) Formation of redox pair through light absorption ($E_{h\nu} > E_{bg}$):

$$TiO_2 + h\nu\ (UV) \rightarrow TiO_2\ (e^-_{CB} + h^+_{VB}) \quad (2.1)$$

(ii) Direct recombination reaction leading to the inactivation of the electron hole pair:

$$TiO_2\ (e^-_{CB} + h^+_{VB}) \rightarrow TiO_2 + \text{heat} \quad (2.2)$$

(iii) Photogenerated holes (h^+_{VB}) may directly oxidize the organic substrate, P. Adsorption of H_2O molecules and OH^- by hole traps lead to formation of $OH^\bullet$ radicals which are the main reactive species with regard to their high oxidant power (E= +2.80 V) possible competing reaction leads to the formation of hydrogen peroxide.

$$h^+_{VB} + P \rightarrow P^{\bullet+} \quad (2.3)$$

$$h^+_{VB} + H_2O \rightarrow HO^\bullet + H^+ \quad (2.4)$$

$$h^+_{VB} + OH^- \rightarrow HO^\bullet \quad (2.5)$$

$$HO^{\bullet} + HO^{\bullet} \rightarrow H_2O_2 \quad (2.6)$$

(iv) On the other hand, in the presence of electron scavengers (i.e. O_2) reduction reactions may take place leading to the following sequence of the reactions:

$$e^-_{CB} + O_2 \rightarrow O_2^{\bullet -} \quad (2.7)$$

$$e^-_{CB} + H_2O_2 \rightarrow OH^- + HO^{\bullet} \quad (2.8)$$

$$O_2^{\bullet -} + H^+ \rightarrow HO_2^{\bullet} \quad (2.9)$$

$$O_2^{\bullet -} + HO_2^{\bullet} \rightarrow HO_2^- + O_2 \quad (2.10)$$

$$HO_2^{\bullet} + HO_2^{\bullet} \rightarrow O_2 + H_2O_2 \quad (2.11)$$

$$H_2O_2 \leftrightarrow HO_2^- + H^+ \qquad pK_a=11.6 \quad (2.12)$$

$$HO^{\bullet} + HO_2^{\bullet} \rightarrow H_2O + O_2 \quad (2.13)$$

Similar to other treatment processes, performance of photocatalytic oxidation systems depend on several crucial operational parameters, such as photocatalyst loading, pH, temperature, dissolved oxygen, solution matrix, light intensity and so on. All of these parameters have been investigated whether they cause enhancement or inhibition of photocatalytic oxidation reactivity. Thus, influence of those parameters on the efficiency of photocatalytic oxidation system has been explored in detail (Gaya and Abdullah, 2008; Godinez and Darnault, 2011; Rodrìguez et al., 2011).

Semiconductor photocatalysis comprise a wide range of research area from water purification and air cleaning to cancer treatment (Fujishima et al., 2000). On the other hand, it has gained a great importance and interest in water and wastewater treatment more specifically due to its several advantageous properties mentioned before. Photocatalytic oxidation for the treatment of several industrial wastewaters (Hu and Xu, 2004; Banu et al., 2008; Ghaly et al., 2011; Pablos et al., 2012), domestic wastewaters and drinking waters (Ollis and Turchi, 1990; Murray and Parsons, 2004; Uyguner and Bekbolet, 2007) are known to be some of the most studied topics with regard to environmental applications of photocatalytic oxidation processes in particular. Some of the advanced oxidation processes studied on grey water treatment applied either to real grey water samples or biologically pretreated grey water are presented in Table 2.8.

Table 2.8. Advanced oxidation processes applied for the treatment of different grey water compositions.

Sample	Process	Operative parameters			Reference
		Parameters	In	Out	
Grey water from shower	Membrane Chemical Reactor (MCR)	Turbidity (NTU)	18.7	3.57	Rivero et al., 2006
		COD (mg O_2 L^{-1})	324	72	
		BOD (mg O_2 L^{-1})	135	17	
Grey water from shower, laundry, and teeth-brushing	UVC/H_2O_2	COD (mg O_2 L^{-1})	191	23	Chin et al., 2009
		BOD_5 (mg O_2 L^{-1})	42	13	
		COD/BOD_5	0.22	0.58	
Biologically pretreated grey water	Solar photocatalytic oxidation and activated carbon	TOC (mg OrgC L^{-1})	5.5	<2	Gulyas et al., 2009
Laundry grey water	Photocatalytic oxidation	DOC (mg OrgC L^{-1})	29.3	10.3	Sanchez et al., 2010
		A-surfactants (mg L^{-1})	1.84	0.1	

Evaluation of photocatalytic reactor configurations has also gained a great deal of interest for further improvement in water and wastewater treatment purposes. As a consequence, photocatalytic membrane reactors, double-skin sheet reactors, have been studied in water and wastewater treatment in terms of their characterization, classification

and possible application particularly (Gulyas et al., 2004; Rivero et al., 2006; Chong et al., 2010; Mozia, 2010; Xiao et al., 2010; Zhang et al., 2012). It can be inferred from Table 2.8 that implementation of advanced oxidation technologies for grey water treatment gives satisfactory results especially for the removal of chemical parameters, such as COD, BOD_5 TOC and DOC content constituting the main organic fraction of grey water pollutants. However, no distinct role of detergents was assessed although grey water samples were taken from batroom/laundry facilities.

2.3.4. Summary of the Previous Studies Performed for the Assessment of Photocatalytic Treatment of Grey Water

Although advanced oxidation processes (AOPs) are commonly used for the treatment of drinking water, domestic wastewater and industrial wastewater, its application in grey water treatment is limited to particular systems such as photocatalytic oxidation and photo-Fenton processes. Moreover, compared to real grey water samples, synthetic grey water compositions are preferably used in photocatalytic oxidation studies of grey water treatment (Zhu et al., 2008; Ludwick et al., Pidou et al., 2009). This section focuses on the literature studies paying attention to application and evaluation of photocatalytic treatment of grey water concisely.

Rivero and co-workers studied a grey water treatment system consisted of a membrane chemical reactor and a microfiltration unit (Rivero et al., 2006). Shower grey water was subjected to photocatalysis in photocatalytic oxidation reactor in which 125W UVC lambs used as light source and Hombikat UV-100 TiO_2 used as photocatalyst with the dosages of 5 mg L^{-1} and 10 mg L^{-1} followed by a microfiltration unit in order to separate TiO_2 from sample. It was concluded that desirable effluent quality of several parameters, such as BOD, turbidity and TC could be achieved by applying membrane chemical reactor for the treatment of grey water.

Zhu et al. (2008) studied photocatalytic oxidation of aqueous ammonia in model grey waters. A synthetic grey water composed of anionic, cationic, and nonionic surfactants and monosaccharides was subjected to photocatalytic degradation in presence of Degussa TiO_2

Aeroxide® P-25 (Akron, OH) without purification as photocatalyst. It was concluded that although surfactants and monosaccharides slowed down photocatalytic degradation rates of ammonia due to their •OH scavenging mechanism, desired removal of those three different compounds was achieved showing that carbonaceous biochemical oxygen demand (CBOD) and nitrogenous biochemical oxygen demand (NBOD) could be removed effectively by this process. Gulyas and co-workers investigated a combined system composed of photocatalytic oxidation and activated carbon adsorption for the treatment of biologically pretreated grey water (Gulyas et al., 2009). Effluent of a constructed wetland treating separately collected grey water and TiO_2 P-25 (Degussa-Huels) were used for photocataltytic degradation experiments. In addition, powdered activated carbon (PAC) was also used in some of experiments in order to see its influence on photocatalytic degradation process. It was concluded that combination of photocatalytic oxidation and powdered activated carbon (PAC) with adequate UV-A fluence reduced total organic carbon concentration to below 2 mg L^{-1}. The major role of PAC could be attributed to the enlarged surface area exposed to the target compounds.

Sanchez and co-workers studied photocatalytic oxidation of grey water over titanium dioxide suspensions (Sanchez et al, 2010). Two different grey water sources, a hotel grey water and a household grey water with two different organic matter loading characteristics as high-load and low-load were used. It was concluded that with low dissolved organic carbon (DOC) concentrations, photocatalytic oxidation was a suitable treatment option for low strength grey water treatment and reuse. In addition, complete removal of anionic surfactants was achieved by photocatalytic oxidation of low strength grey waters. Ludwick and colleagues studied performance of silica-titania carbon composites for photocatalytic degradation of grey water (Ludwick et al., 2011). Synthetic grey water composition was created with the contribution of NASA Johnson Space Center (JSC). TiO_2 Degussa P-25 as the photocatalyst and SiO_2 as photocatalyst support were used for the photocatalytic degradation experiments. It was found that SiO_2 and TiO_2 composites were applicable for the removal of TOC concentration from 3,000 ppb to desired value of 500 ppb in photocatalytic degradation processes.

3. MATERIALS AND METHODS

3.1. Materials

3.1.1. Preparation and Compositional Properties of Synthetic Grey Water

Performance of several treatment technologies have been evaluated by preparing synthetic solutions of water and wastewater samples (Jefferson et al., 2001; Toifl et al., 2006; Henkel et al., 2009; Pidou et al., 2009). In the current study photocatalytic treatment of synthetic grey water was assessed in terms of the performance of the treatment system on removal of organic matter and bacterial content intentionally. Thus, synthetic grey water was composed of particular materials instead of mixture of various compounds. Two main mechanisms of the photocatalytc oxidation process were assessed in this study, the first one is the effective degradation of organic matter content and the second one is the photocatalytic bactericidal activity of TiO_2.

Two grey water compositions were taken into account for all experiments according to their organic matter loading. First one is defined as ‘’high load grey water’’ that contains high concentration of organic matter meeting with DOC content of grey water samples in previous studies, and second one is defined as ‘’low load grey water’’ containing comparatively lower concentrations of organic matter. Commercial humic acid with specified concentrations was prepared and used in synthetic grey water compositions as representative of DOC content of grey water (Oschman et al., 2005). In addition, photocatalytically oxidized fractions of humic acid solutions were also used in synthetic grey water preparation for breaking down the refractory structure of humic acid solution having considerably higher DOC concentrations and monitoring the impact of oxidized molecules on photocatalytic oxidation process. Consequently, Aldrich Humic Acid (150 mg L^{-1}) was subjected to photocatalytic oxidation for several irradiation times of 0, 20, 40, 60, 90 and 180 minutes in the presence of 0.5 mg mL^{-1} TiO_2 as the photocatalyst. All these samples were mixed up with untreated humic acid solution (150 mg L^{-1}) in appropriate ratios to prepare the corresponding DOC concentration of high load grey water sample (Table 3.1).

Table 3.1. Composition of grey water constituents representing organic matter, low and high anion contents.

Constituents	Concentration Range ($mg\ L^{-1}$)		
	Low	High	
Organic matter (DOC)	6.4-6.6	12.9-14.5	
	Stock Solution	Low	High
Anions			
F^-	20	0.04	0.34
Cl^-	100	0.40	2.14
NO_2^-	100	0.53	6.36
NO_3^-	100	0.21	2.14
Br^-	100	0.98	9.56
SO_4^{2-}	100	0.29	2.08
PO_4^{3-}	200	0.40	3.95

Solution matrix is one of the most important operational parameters affecting the performance of photocatalytic oxidation process. As a consequence, impact of solution matrix on the photocatalytic oxidation of grey water was investigated in terms of ionic strength specifically. To this end, two different specified ranges of the concentrations of the anions defined as ‘’high load anion content’’ and ‘’low load anion content’’ were prepared and added to synthetic grey water samples. Stock solution containing seven different anions (F^-, Cl^-, Br^-, NO_2^-, NO_3^-, PO_4^{3-} and SO_4^{2-}) was used in synthetic grey water compositions with appropriate dilution to get specified ranges of the concentrations mentioned previously. Concentrations of the specified ranges of anions exist in stock solution and in grey water compositions are displayed in Table 3.1.

Another component of the synthetic grey water was its bacteriological composition that could exist in real grey waters naturally with a diverse range of quantity and quality. For this purpose, a mixed culture consisted of Total Coliform (TC), Faecal Coliform (FC)

and Faecal Streptococci (FS) bacteria were chosen and inoculated to low load and high load synthetic grey water samples referring to the bacterial content of grey water samples studied in the literature previously (Eriksson et al., 2002). Besides the presence of organic loadings and low anion contents, mixed bacterial consortium of low load and high load grey water samples were displayed in Table 3.2.

Table 3.2. Microbiological constitutes of low load and high load grey water samples.

Synthetic grey water type	Bacterial Content (CFU 100 mL^{-1})		
	Total Coliform	Faecal Colifrom	Faecal Streptococci
High Load Grey Water	$7.2x10^4$	$5.4x10^4$	$1.8x10^4$
Low Load Grey Water	$5.4x10^4$	$3.8x10^4$	$1.6x10^4$

3.1.2. Humic Acid

Commercial humic acid was supplied from Aldrich (Aldrich Co. Ltd., USA).Stock humic acid solution with a concentration of 1000 mg L^{-1} was prepared by adding 1g humic acid into 1L of ultra pure water and dissolved using the ultrasonic sonication in order to get homogenous solution. Humic acid solution used for the experiments was prepared from the stock solution by appropriate dilution (50 mg L^{-1} and 150 mg L^{-1}). Ultra pure water was prepared by using Millipore Milli-Q system and used in the preparation of all aqueous solutions. Conductivity values of the ultra pure water were in the range of 0.2-0.3 μScm^{-1}.

3.1.3. Titanium Dioxide

Commercial Degussa P25-TiO_2 was supplied from Degussa-tvorikaverage particle size of 20-30 nm and BET surface area of 50 ± 15 m^2 g^{-1} was used in the experiment. The crystal form of TiO_2 is composed of 70% anatase and 30% rutile.The loading of the photocatalyst was kept constant as 0.25 mg mL^{-1} for humic acid and its molecular size

fractions and for low load grey water samples and 0.5 mg mL^{-1} for high load grey water samples.

3.2. Methodology

3.2.1. Photocatalytic Oxidation of Grey Water

3.2.1.1. Experimental Set-Up. Experimental system consisted of a cylindrical Pyrex reaction vessel with a diameter of 7.5 cm and height of 3.5 cm and a working volume of 50 mL as the photo reactor. In order to maximize the light intensity and to provide surface reflection, the photoreactor was enclosed by a mirror casing and internal walls were covered with Al foil. A 125W black light fluorescent lamp (BLF) emitting radiation between 300 and 420 nm with a maximum intensity at 365nm was used as the light source. Potassium ferrioxalate actinometer (Hatchard and Parker, 1956) was used in order to measure intensity of incident light a value of $2.85x10^{16}$ quanta sec^{-1}.

3.2.1.2. Experimental Procedure. TiO_2 Degussa P-25 as the photocatalyst between the concentration ranges of 0.1–1.0 mg mL^{-1} was used in all the experiments. For low load grey water samples photocatalyst dose was chosen as 0.25 mg mL^{-1} and for high load grey water samples photocatalyst dose was chosen as 0.5 mg mL^{-1}. 50 mL of synthetic grey water sample was measured and poured directly to the reaction vessel. Then weighted TiO_2 was added to the vessel and sonicated for three minutes to provide a homogenous mixture of grey water and photocatalyst. After that, reaction vessel placed on a magnetic stirrer to be exposed to irradiation for certain reaction periods (0, 10, 20, 30, 40, 60 and 90 minutes for low load grey water and 0, 60, 90, 120, 150 and 180 minutes for high load grey water). Ultra pure water was used for volume corrections caused by evaporation loss of water at longer irradiation periods. 0.45 μm membrane filters were used to separate particulate TiO_2 from aqueous suspension at the end of photocatalytic degradation processes samples taken for microbiological analysis according to the methods outlined in 3.2.3.4 section.

3.2.2. Molecular Size Fractionation with Ultrafiltration

Humic acid solutions used in synthetic grey water composition were separated into two different molecular size fractions (100 kDa and 30 kDa) by using a 50 mL Amicon Model 8050 ultrafiltration cell in order to get different organic matter concentrations for different grey water compositions. The system consisted of an ultrafiltration cell with a magnetic stirrer, a nitrogen gas tube and a pressure control valve for pressurizing cell (P= 5atm) properly. As a preliminary step, humic acid solutions were filtered through 0.45µm Millipore cellulose acetate filters. Then Millipore YM series cellulose membrane filters with 25 mm diameter and with nominal molecular weight cutoffs as 100 kDa and 30 kDa were used for sequential fractionation of humic acid solutions. YM membranes were rinsed with deionized water for 15 minutes in order to remove ethanol and at the beginning of the ultrafiltration process, 50 mL deionized water was filtered through membrane. Schematic diagram of stirred cell ultrafiltration unit is presented in Figure 3.1.

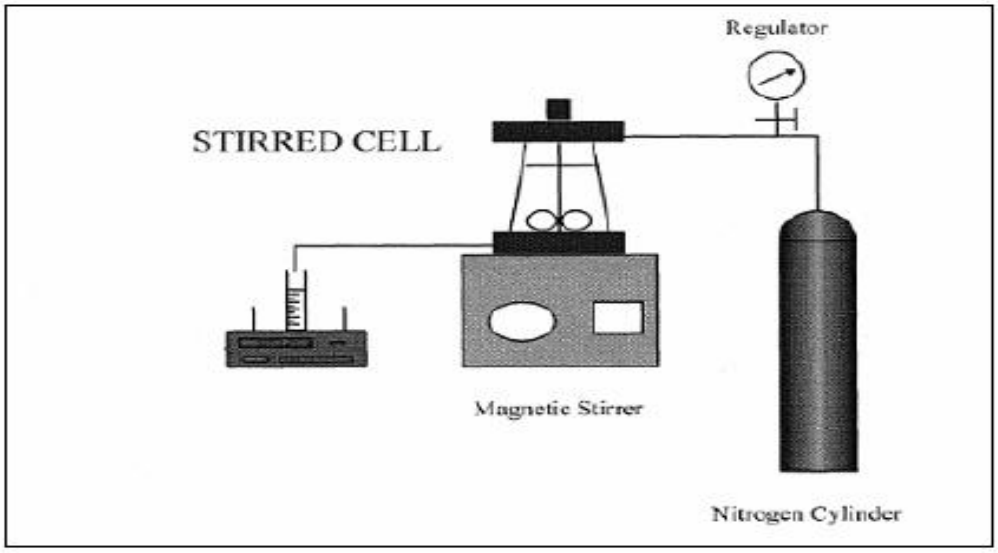

Figure 3.1. Schematic diagram of stirred cell ultrafiltration unit (Aykac, 2011).

At the end of ultrafiltration, membrane was rinsed with 0.1M NaOH for 30 minutes followed by through flushing with deionized water. For storage, membranes were kept in 10% ethanol-water solution at +4°C.

3.2.3. Analytical Methods

3.2.3.1. UV-vis Spectroscopic Measurements. A Perkin Elmer Lamda 35 UV-vis double beam spectrophotometer with Hellma quartz cuvettes of 1.0 cm optical path length was used to record UV-vis absorption spectra. Organic matter content and color forming components present in synthetic grey water were characterized by recording absorbance values at 436 nm ($Color_{436}$), 365 nm (UV_{365}), 280 nm (UV_{280}), and 254 nm (UV_{254}) by UV-vis spectra. Representative of these parameters are explained as follows:

$Color_{436}$: Color forming moieties, absorbance at 436 nm, m^{-1}
UV_{365} : Organic matter content, absorbance at 365 nm, m^{-1}
UV_{280} : Organic matter content, absorbance at 280 nm, m^{-1}
UV_{254} : Organic matter content, absorbance at 254 nm, m^{-1}

3.2.3.2. Fluorescence Measurements. A Perkin Elmer LS 55 Luminescence Spectrometer equipped with a 150W Xenon arc lamp and a red sensitive photomultiplier tube was used for the fluorescence measurements of samples in the emission scan and synchronous scan modes. Quartz cells with 1-cm pathlength were used for the placement of samples in the instrument. A scan speed of 400 nm min^{-1} with a slit width opening of 10 nm was set and used for all measurements. While synchronous scan spectra of samples were recorded in the excitation wavelength range of 200-600 nm with the bandwidth of $\Delta\lambda$=18 nm between the excitation and emission monochromators, emission scan spectra were recorded between the wavlength range of 360-600 nm at excitation wavelength of 350 nm.

3.2.3.3. Total Organic Carbon (TOC) Measurements. A Shimadzu TOC Vwp Total Organic Carbon Analyzer was used for Total Organic Carbon (TOC, mg OrgC L^{-1}) as Dissolved Organic Carbon (DOC) measurements of samples. Potassium hydrogen phthalate in the concentration range of 0-25 mg C L^{-1} was used for the calibration of instrument.

3.2.3.4. Specific parameters. Normalization of absorbance values of specified UV-vis parameters (UV_{254}, UV_{280}, UV_{365} and $Color_{436}$) to DOC contents gives specific UV-vis parameters as $SUVA_{254}$, $SUVA_{280}$, $SUVA_{365}$ and $SCoA_{436}$. In addition, normalization of

fluorescence intensities (FI_{emis} and FI_{sync}) in terms of emission scan and synchronous scan modes give specific fluorescence parameters. Normalization of maximum fluorescence intensities at 450 nm for emission scan mode and at 470 nm for synchronous scan mode to DOC concentrations revealed specific fluorescence parameters of SFI_{emis} and SFI_{sync}. All these specific parameters were determined and employed in many different studies to get information about the composition and properties of organic matter and its fractions elaborately. In addition, change observed of specific parameters with respect to photocatalytic oxidation contributed further evaluation of the process as well as mechanisms and interactions occurring within the system.

3.2.3.5. Microbiological Analyses. Enumaration of total colifrom (TC), faecal coliform (FC) and faecal streptococci (FS) bacteria was conducted according to Standard Methods for the Examination of Water and Watewater (APHA, AWWA, WPCF, 1999). Membrane filter technique as one of the methods for enumeration of individual bacteria was taken into account due to its environmental application in enumeration and identification of coliform (total and faecal) and faecal streptococci bacteria specifically. A pre-sterilized absorbent pad was placed into petri dish using dispenser and 2 mL of culture media was pipetted onto the pad. Culture media containing the nutrients necessary for the growth of the specific target bacteria was prepared for total colifrom (MF-Endo Broth), faecal colifrom (M-FC Broth) and faecal streptococci (KF Agar) particularly according to methodology given in Standard Methods. After a sterile membrane filter centered on the filter support, the funnel top is attached and a well-shaken sample with a volume of 100 mL was filtered through the membrane followed by rinsing the sides of the funnel with 20-30 mL ultra pure water. Then membrane filter was removed from the filter base by sterile foreceps and rolled onto the pad to avoid the formation of bubbles. Enumaration of bacterial cultures were done after petri dishes were stayed in the incubator for 22-24 hours. A low power microscope with daylight was used to count colonies. For the determination of total colifrom bacteria, a shiny greenish-gold surface was examined on the filter whereas faecal coliform bacteria exhibited light or dark blue color specifically. On the other hand, examination of carmine red or pink color indicated the presence of faecal streptococci bacteria.

4. RESULTS AND DISCUSSION

This study aimed to investigate the photocatalytic oxidation process for the treatment of compositionally different grey water samples in detail. To this end, several experimental studies conducted according to the instructions given in the Materials and Methods section. Consequently, detailed information about all experimental results and discussions were given separately for every different stages respectively.

In material specification part, characterization of different compositional humic acid solutions and their molecular size fractions were achieved in order to get specific information about organic content of synthetic grey water samples. Spectroscopic properties of samples in terms of UV-vis and fluorescence spectral parameters and normalization of those parameters to DOC content of samples defined as specific UV-vis and fluorescence parameters were specifically taken into consideration for the characterization of samples in this section and also in the following three sections respectively.

In the second part, photocatalytic oxidation of different molecular size fractions of humic acid was investigated in order to observe the performance of photocatalytic oxidation process in the presence of sole organic matter content of synthetic grey water. For this purposes, 0.45 μm filtered fraction of humic acid, 100 kDa fraction of humic acid and 30 kDa fraction of humic acid were subjected to photocatalytic oxidation in the presence of TiO_2 as photocatalyst for several irradiation times. Followed by the second part, photocatalytic oxidation of different synthetic grey water compositions classified as ‘’low load grey water’’ and ‘’high load grey water’’ according to their organic matter content were explored in the third and fourth part. Effect of solution matrix on the photocatalytic oxidation process was also taken into consideration by making compositional changes in grey water contents in terms of organic matter loading, ionic strength (low anion content and high anion content) and bacterial content (total colifroms, faecal coliforms and faecal streptococci) in these sections separately.

In the fifth part, performance of the photocatalytic oxidation process treating grey water was evaluated by determining the removal efficiencies of the specific and specified parameters in order to view the experimental results from a different perspective for further interpretation. To achieve this goal, removal efficiencies of the selected UV-vis parameters, DOC contents and bacterial contents of the synthetically prepared low load and high load grey water samples were discussed in a comparative style in this section.

In the last section, kinetic modelling of the photocatalytic degradation profiles of all grey water samples using the specified UV-vis parameters as well as DOC was presented. In addition, kinetic consideration of photocatalytic inactivation of bacterial consortium *i.e.* total coliforms, faecal coliforms and faecel streptococci present in the low load and high load grey water samples were assessed in terms of the individual bacterial inactivation rate constants and half life values.

4.1. Material Specification

Humic acid solutions and their molecular size fractions were used in synthetic grey water compositions as a representative of dissolved organic matter content present in real grey water samples (Table 2.3). Different humic acid solutions *i.e.* sole humic acid and photocatalytically treated humic acid composed of different molecular size fractions were prepared according to instructions mentioned in Materials and Methods section. Evaluation and specification of humic materials were presented by the specified and specific UV-vis and fluorescence spectroscopic properties. Up to now, characterization of humic substances under various conditions for the assessment of the treatment efficiencies have been studied widely in terms of spectroscopic properties especially in terms of UV-vis and fluorescence properties (Milori et al., 2002; Goslan et al., 2004; Uyguner Demirel and Bekbolet, 2011). Taking into account these findings, in a comparative manner, characterization of the properties of the prepared humic acid solution and its molecular size fractions (0.45 μm filtered fraction, 100 kDa fraction and 30 kDa fraction) were assessed by determination and evaluation of the UV-vis and fluorescence spectroscopic properties as well as DOC contents of those samples in the following sections.

4.1.1. Dissolved Organic Carbon Contents of the Sole Humic Acid, Mixed Humic Acid and Their Molecular Size Fractions

Dissolved orgnic carbon contents of the prepared humic acid solutions were determined according to the method outlined in the materials and methods section. Sole humic acid in the concentration of 50 mg L^{-1} expressed 14.92 mg OrgC L^{-1} DOC. Following the application of ultrafiltration the obtained molecular size fractions displayed a decreasing trend of DOC as 13.2 mg OrgC L^{-1} for 0.45 mm filtered fraction, 6.4 mg OrgC $L^{-1}$for 100 kDa fraction and 2.6 mg OrgC L^{-1} for 30 kDa fraction. Decreasing molecular size fractionation resulted in a substantial decrease of DOC content (80%) of the humic acid fractions.

Mixed humic acid as prepared according to the procedure outlined in Materials and Methods section (Section 3.1.1) primarily expressed an initial DOC content of 14.9 mg OrgC L^{-1}. In a similar manner, following ultrafiltration, the obtained molecular size fractions displayed a decreasing trend of DOC as 14.5 mg OrgC L^{-1} for 0.45 μm filtered fraction, 11.2 mg OrgC L^{-1} for 100 kDa fraction and 6.60 mg OrgC L^{-1} for 30 kDa fraction respectively. As expected, filtration through 0.45 μm membrane filter did not alter the DOC content significantly (< 5%). Decreasing molecular size fractionation resulted in a substantial decrease of DOC content (54%) of the humic acid fractions. Since the mixed humic acid solution contained both native humic acid (150 mg L^{-1}= 82 mg OrgC L^{-1}) and photocatalytically treated thereby partially oxidized humic acid fractions (76 mg OrgC L^{-1}), the resulting DOC was accepted as representative organic carbon content of high load grey water. On the other hand, 100 kDa fraction of sole humic acid (50 mg L^{-1}=10.8 mg OrgC L^{-1}) was used as the representative organic carbon content of low load grey water.

Since the specified UV-vis and fluorescence parameters could also be expressed in terms of DOC normalized specific parameters ($SUVA_{254}$, $SUVA_{280}$, $SUVA_{365}$, $SCoA_{436}$, SFI_{emis} and SFI_{sync}), the UV-vis and fluorescence data were further evaluated by using the above indicated DOC data and presented in the respective tables that were given in the following sections.

4.1.2. Spectroscopic Analysis of Humic Acid Solution and its Molecular Size Fractions

UV-vis absorption spectra of samples were measured between the wavelength range of 200-600 nm and specifically absorbance values at 436 nm, 365 nm, 280 nm and 254 nm were recorded for determination of spectral parameters of $Color_{436}$, UV_{365}, UV_{280} and UV_{254}. The change observed of absorbance values of humic acid and its molecular size fractions were presented in Figure 4.1. Previous studies about molecular size distribution of humic substances concluded that a general declining trend from high molecular size fraction to the lower molecular size fractions obtained irrespective of the origin and source of the organic matter (Alberts et al., 2002). A decreasing trend in absorbance values measured in UV-vis region of 200-600 nm of humic acid and its molecular size fractions were obtained due to decreasing molecular size fractions in the order of 0.45 μm filtered fraction> 100 kDa fraction> 30 kDa fraction that showed compatibility with previous studies throughout the literature (Aykac, 2011; Degirmenci Ilhan, 2011). For comparative evaluation purposes, change in UV_{254} and $Color_{436}$parameters specifically selected in terms of characterization of the humic acid and its molecular size fractions. Absorbance values of UV_{254} were obtained as 117.07 m^{-1} for 0.45 μm filtered fraction> 54.92 m^{-1} for 100 kDa fraction> 21.52 m^{-1} for 30 kDa fraction and absorbance values of $Color_{436}$ were obtained as 22.31 m^{-1} for 0.45 μm filtered fraction> 8.65 m^{-1} for 100 kDa fraction> 2.57 m^{-1} for 30 kDa fraction.

Fluorescence intensities of humic acid and its molecular size fractions were presented in Figure 4.2A in the emission scan mode and in Figure 4.2B in the synchronous scan mode. Fluorescence intensities of humic acid and its molecular size fractions displayed a decreasing trend with decreasing molecular size fractions as recorded in the emission scan mode. Moreover, all molecular size fractions had the characteristic peak at emission wavelength of 450 nm. For longer wavelengths e.g. 540 nm, fluorescence intensities of 0.45 μm filtered fraction of humic acid and 100 kDa fraction of humic acid displayed an overlapping trend. Synchronous scan fluorescence spectra of humic acid and its molecular size fractions expressed a general decreasing trend in fluorescence intensity with respect to decreasing molecular size fractions at emission wavelength of 470 nm where a predominant characteristic sharp peak also occurred.

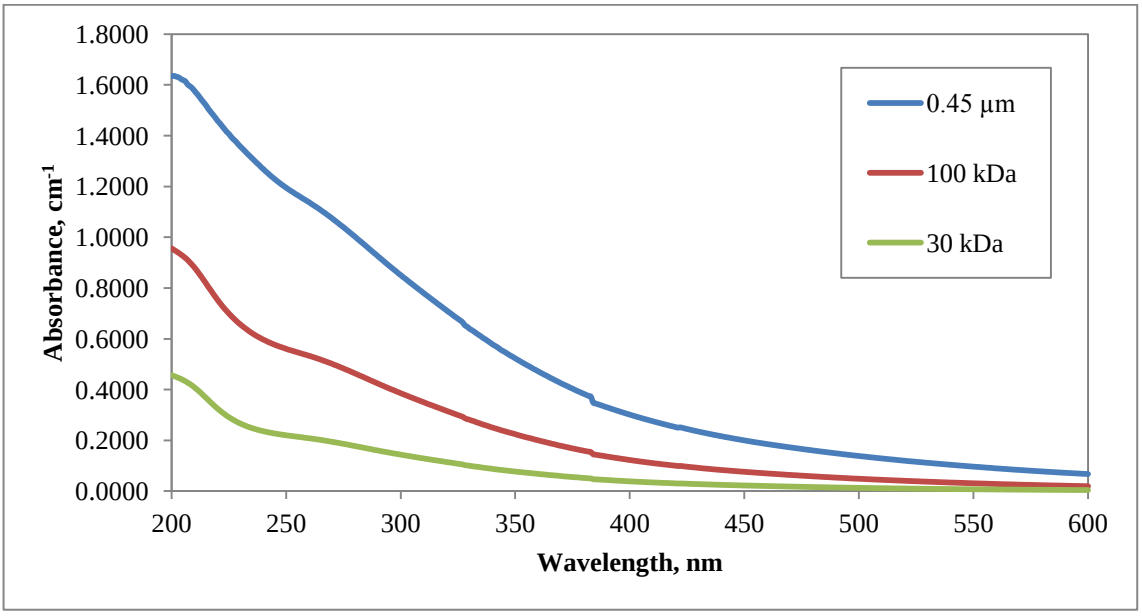

Figure 4.1. UV-vis scan spectra of humic acid and its molecular size fractions.

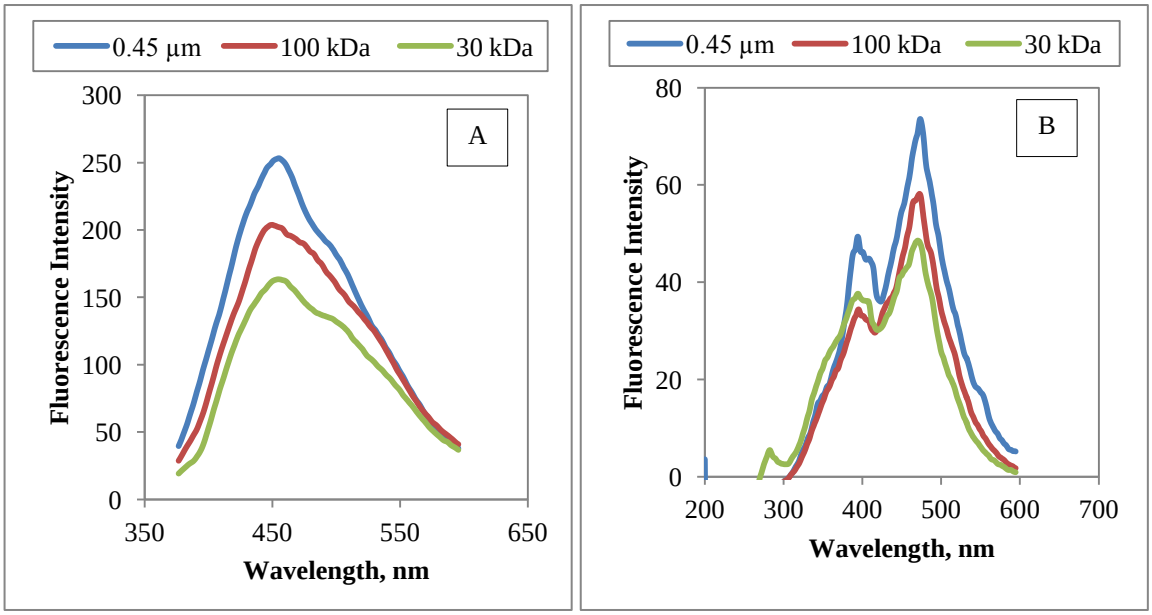

Figure 4.2. Fluorescence intensities of humic acid and its molecular size fractions in the emission scan mode (2A) and in the synchronous scan mode (2B).

Spectral and specific parameters of humic acid and its molecular size fractions were all displayed in Table 4.1. While decreasing molecular size fractions caused a rapid fall in DOC content of samples, UV-vis absorbance values and fluorescence intensities of samples decreased rather slowly, thus some of the specific UV-vis and fluorescence parameters gave either insignificant or increasing trends instead of giving decreasing trend as molecular size fractions getting smaller.

Table 4.1. Spectral and specific parameters observed of humic acid and its molecular size fractions.

	UV-vis Properties (m^{-1})				Fluorescence Properties (cm^{-1})	
	UV_{254}	UV_{280}	UV_{365}	$Color_{436}$	FI_{emis}	FI_{sync}
0.45 µm ff**	117.07	100.23	30.11	22.31	176.77	70.62
100 kDa f*	54.92	46.37	12.26	8.65	159.13	57.60
30 kDa f*	21.52	17.75	3.83	2.57	134.65	48.54
	Specific UV-vis Parameters (m^{-1} $mg^{-1}L$)				Specific Fluorescence Parameters (cm^{-1} $mg^{-1}L$)	
	$SUVA_{254}$	$SUVA_{280}$	$SUVA_{365}$	$SCoA_{436}$	SFI_{emis}	SFI_{syn}
0.45 µm ff**	7.85	6.72	3.00	1.50	11.85	14.12
100 kDa f*	8.54	7.21	2.94	1.35	24.74	8.96
30 kDa f*	8.40	6.93	2.46	1.00	52.53	18.94

*fraction

**filtered fraction

As a result, $SUVA_{254}$, $SUVA_{280}$ and SFI_{sync} parameters of humic acid and its molecular size fractions displayed an increasing trend in the following order; 0.45 µm filtered fraction< 30 kDa fraction< 100 kDa fraction.and SFI_{emis} parameters displayed increasing trend with the order of 0.45 µm filtered fraction< 30 kDa fraction< 100 kDa fraction. On the other hand, $SUVA_{365}$ and $SCoA_{436}$ exhibited typical declining trend as molecular size fractions decreased due to the fact that both the $Color_{436}$ and UV_{365} parameters decreased more significantly with respect to DOC.

4.1.3. Spectroscopic Analysis of Mixed Humic Acid solution and its Molecular Size Fractions

Mixed humic acid solution was composed of 150 mg L^{-1} humic acid solution and photocatalytically oxidized fractions of 150 mg L^{-1} humic acid solutions in order to prepare high load organic matter that was one of the components of high load grey water. Characterization of this solution was conducted similarly with the characterization of sole humic acid solution (50 mg L^{-1}) by separation of humic acid solution into different molecular size fractions of 100 kDa fraction and 30 kDa fraction. In this section, spectroscopic analyses of mixed humic acid solution and its molecular size fractions were evaluated in terms of UV-vis and fluorescence properties and specified parameters concomitantly.

UV-vis scan spectra of mixed humic acid solution and its molecular size fractions were displayed in Figure 4.3. A gradual decrease in absorbance values of UV_{254} were obtained in the following order; 127.96 m^{-1} for 0.45 μm filtered fraction> 105.54 m^{-1} for 100 kDa fraction> 60.16 m^{-1} for 30 kDa fraction. In addition, absorbance values of $Color_{436}$ gave the similar decreasing trend observed of UV_{254} with the same order as 21.36 m^{-1} for 0.45 μm filtered fraction> 17.02 m^{-1} for 100 kDa fraction> 7.91 m^{-1} for 30 kDa fraction. Compared to humic acid solution and its molecular size fractions, mixed humic acid solution and its molecular size fractions gave significantly higher absorbance values for UV_{254} and $Color_{436}$ parameters on account of having both oxidized fractions and raw untreated humic material in one composition.

Fluorescence intensities of mixed humic acid solution and its molecular size fractions displayed similar decreasing order with respect to decreasing molecular size fractions in both emission scan mode and synchronous scan mode as displayed in figures 4.4A and 4.4B. On the other hand, all fractions had the characteristic sharp peak at 450 nm for emission scan mode and another characteristic sharp peak at 470 nm and a moderate peak at 400 nm for synchronous scan mode specifically as expected in comparison to the fluorescence spectra attained for sole humic acid and its molecular size fractions (Figure 4.2A and 4.2B).

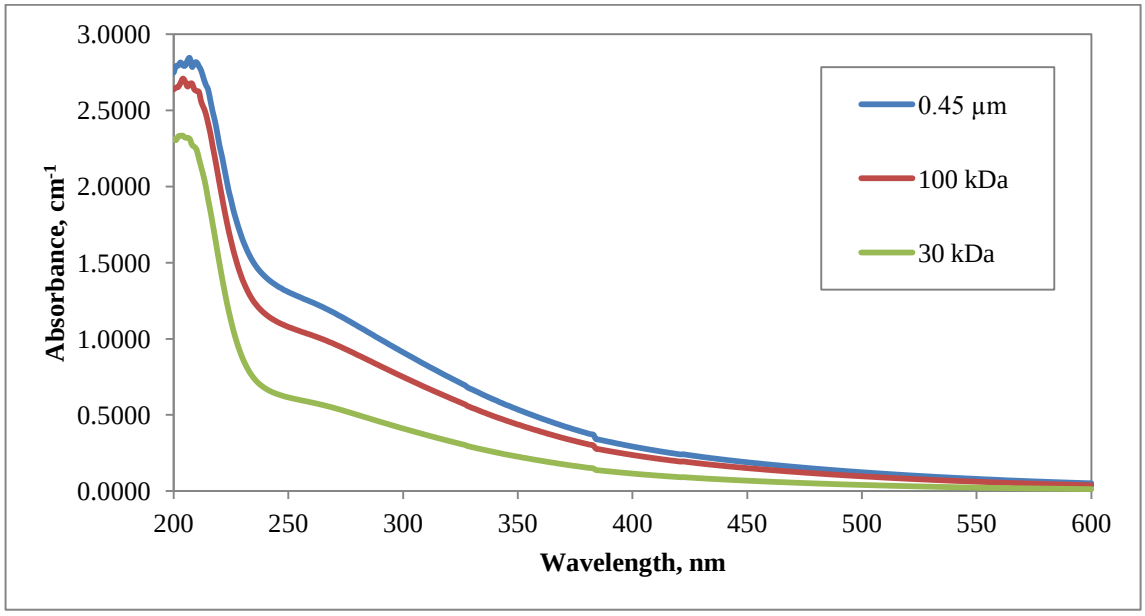

Figure 4.3. UV-vis scan spectra of mixed humic acid solution and its molecular size fractions.

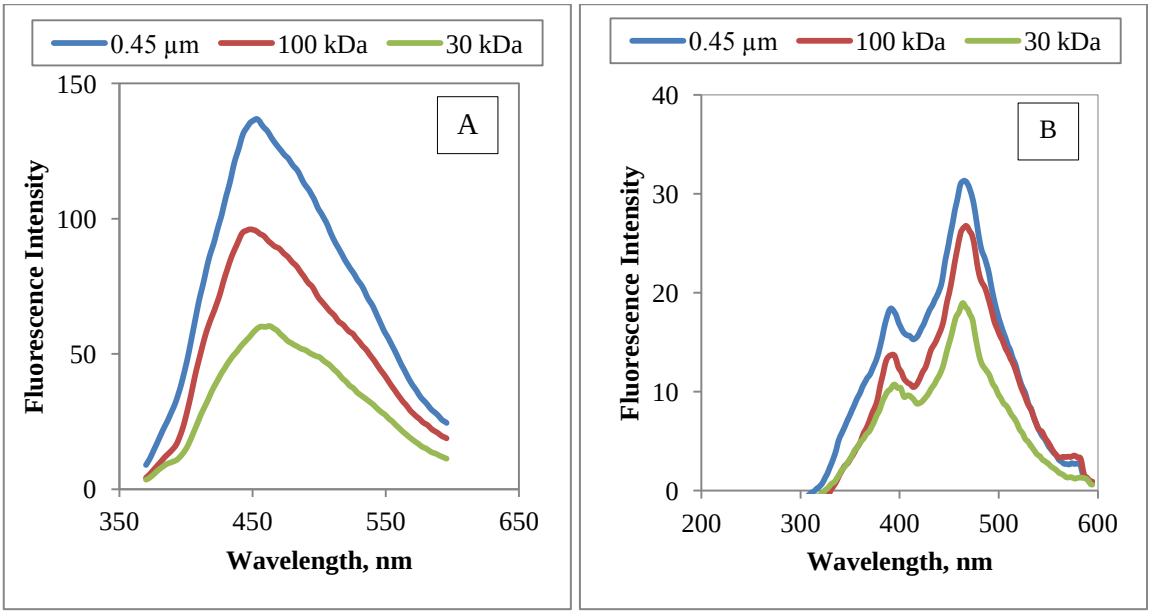

Figure 4.4. Fluorescence intensities of mixed humic acid solution and its molecular size fractions in the emission scan mode (4A) and in the synchronous scan mode (4B).

Specified UV-vis and fluorescence parameters displayed an insignificant trend different from gradual decrease. $SUVA_{254}$ and $SUVA_{280}$ parameters decreased in the following order 100 kDa fraction> 30 kDa fraction> 0.45 μm filtered fraction while $SUVA_{365}$ and $SCoA_{436}$ parameters of samples showed a decreasing trend in the following order of 100 kDa fraction> 0.45 μm filtered fraction> 30 kDa fraction. SFI_{emis} changed in the order of 0.45 μm filtered fraction> 30 kDa fraction> 100 kDa fraction independently.

Table 4.2. Spectral and specific parameters observed of mixed humic acid solution and its molecular size fractions.

	UV-vis Properties (m^{-1})				Fluorescence Properties Fluorescence Intensity (cm^{-1})	
	UV_{254}	UV_{280}	UV_{365}	$Color_{436}$	FI_{emis}	FI_{sync}
0.45 μm ff**	127.96	108.48	45.22	21.36	136.09	30.61
100 kDa f*	105.54	89.44	36.79	17.02	95.91	26.28
30 kDa f*	60.16	50.12	18.74	7.91	57.67	17.93
	Specific UV-vis Parameters (m^{-1} $mg^{-1}L$)				Specific Fluorescence Parameters (cm^{-1} $mg^{-1}L$)	
	$SUVA_{254}$	$SUVA_{280}$	$SUVA_{365}$	$SCoA_{436}$	SFI_{emis}	SFI_{syn}
0.45 μm ff**	8.82	7.48	3.12	1.47	9.39	2.11
100 kDa f*	9.36	7.93	3.26	1.51	8.50	2.33
30 kDa f*	9.12	7.59	2.84	1.20	8.74	2.72

*fraction
**filtered fraction

Moreover, $SUVA_{254}$ values (8.82-9.12) obtained for mixed humic acid solution and its molecular size fractions were 11% higher for 0.45 μm filtered fraction, 9% higher for 100 kDa fraction and 8% higher for 30 kDa fraction compared to $SUVA_{254}$ values obtained for humic acid solution and its molecular size fractions. In addition, $SCoA_{436}$ values of samples were found to be 2%, 11% and 17% higher than results obtained for humic acid solution and its molecular size fractions (Table 4.1).

4.2. Photocatalytic Oxidation of Humic Acid and its Molecular Size Fractions

For comparative purposes, raw humic acid and its molecular size fractions were also subjected to photocatalytic oxidation prior to photocatalytic oxidation of grey water samples. Evaluation of data obtained for photocatalytic oxidation of humic acid and its molecular size fractions were achieved by monitoring parameters in terms of UV-vis spectroscopic parameters, fluorescence spectroscopic parameters and specific parameters.

4.2.1. Photocatalytic Oxidation of 0.45 µm Filtered Fraction of Humic Acid

UV-vis spectral changes observed of absorbance values of 0.45 µm filtered fraction of humic acid during photocatalytic oxidation was presented in Figure 4.5. Degradation of larger molecules into smaller ones contributed a monotonous decreasing trend in absorbance values of samples with respect to increasing irradiation time. The effect of initial adsorption mechanism could be observed at t=0 that caused pronounced reduction of absorbance value in the UV-vis scan spectra. On the other hand, photocatalytic oxidation of 0.45 µm filtered fraction of humic acid for 20 minutes and 40 minutes did not make a significant reduction in absorbance values and displayed a very slight decreasing trend until after photocatalytic irradiation time of 60 minutes. After irradiation time of 60 minutes, UV_{254} absorbance value decreased from 117.07 m^{-1} to 67.16 m^{-1} and $Color_{436}$ absorbance value decreased from 22.31 m^{-1} to 8.96 m^{-1}. Fluorescence spectra of samples were scanned in terms of emission scan and synchronous scan modes respectively.

The changes observed of fluorescence intensities of 0.45 µm filtered fraction of humic acid during photocatalytic oxidation were displayed in Figure 4.6A and Figure 4.6B in the emission scan mode and in the synchronous scan mode. A decreasing fluorescence intensity trend with increasing photocatalytic irradiation time was observed for 0.45 µm filtered fraction of humic acid in the emission scan mode. Parallel to emission scan mode, fluorescence intensities of synchronous scan mode also showed a slight decreasing trend with increasing irradiation time. In addition, all samples had the characteristic peak at 470 nm that gradually decreased with increasing irradiation time and a moderate peak at 400 nm that changed insignificantly with increasing irradiation time.

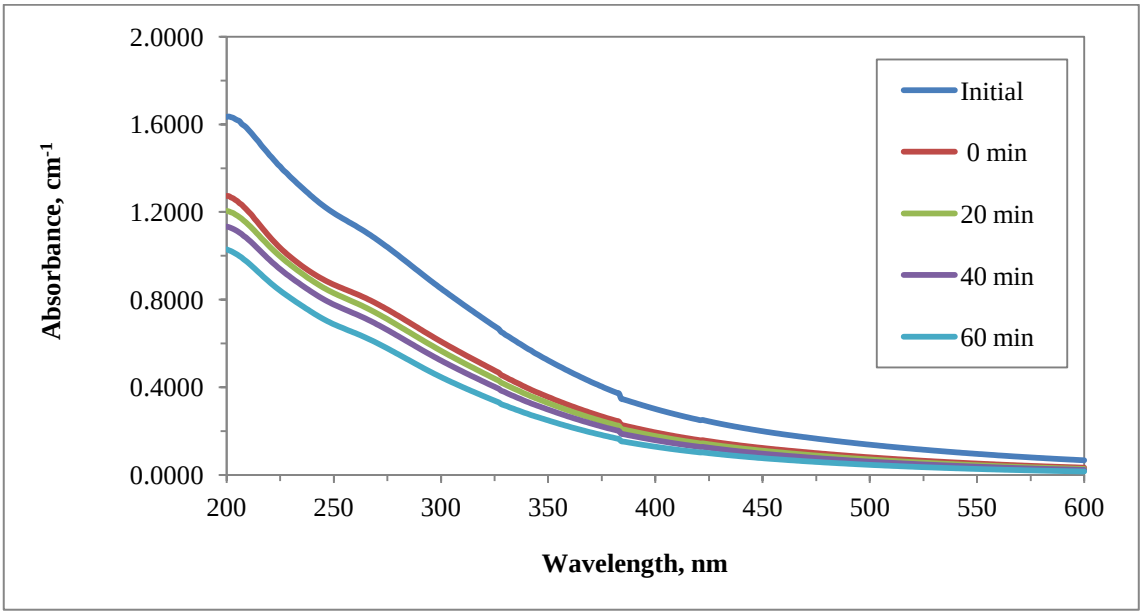

Figure 4.5. UV-vis scan spectra of 0.45 µm filtered fraction of humic acid during photocatalytic oxidation.

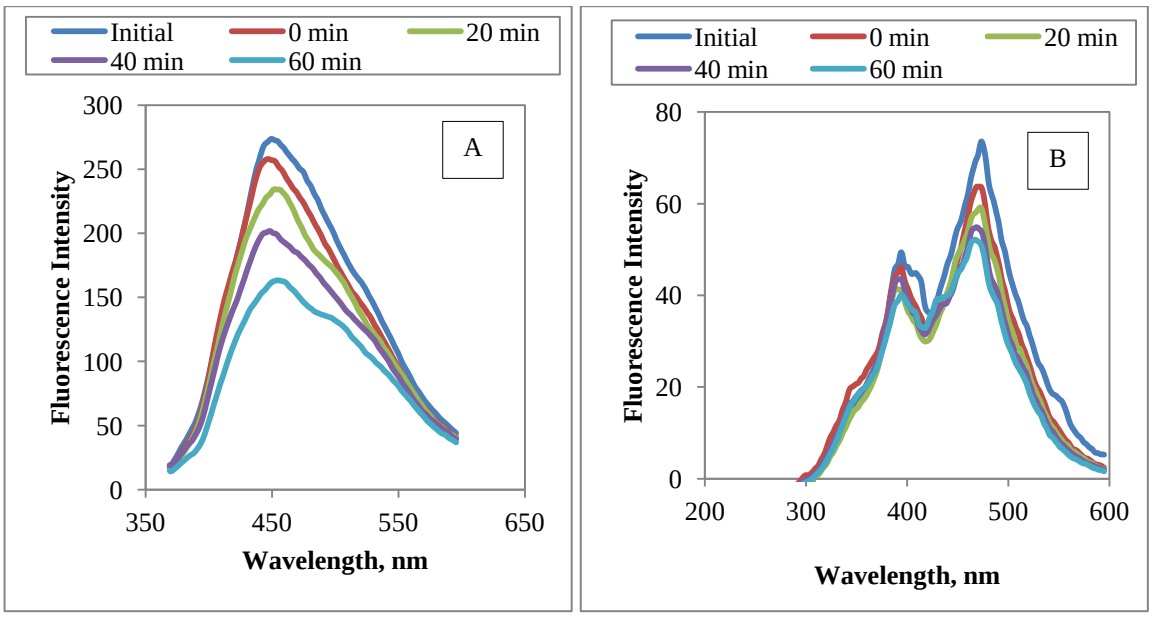

Figure 4.6. Fluorescence intensities of 0.45 µm filtered fraction of humic acid in the emission scan mode (6A) and in the synchronous scan mode (6B) during photocatalytic oxidation.

All specified UV-vis parameters gradually decreased with increasing irradiation time that caused reduction in UV-vis spectral parameters and in DOC content of samples during photocatalytic oxidation (Table 4.3).

Table 4.3. Spectral and specific parameters observed of 0.45 µm filtered fraction of humic acid during photocatalytic oxidation.

	UV-vis Properties (m^{-1})				Fluorescence Properties Fluorescence Intensity (cm^{-1})	
	UV_{254}	UV_{280}	UV_{365}	$Color_{436}$	$FI_{emis\ 350}$	FI_{syn}
Initial	117.07	100.23	44.76	22.31	273.65	70.62
0	85.10	72.69	30.00	13.95	256.89	63.74
20	81.25	68.20	27.64	12.64	232.93	58.71
40	76.07	63.42	25.02	11.18	200.51	54.74
60	67.16	55.14	20.76	8.96	161.95	51.80
	Specific UV-vis Parameters (m^{-1} $mg^{-1}L$)				Specific Fluorescence Parameters (cm^{-1} $mg^{-1}L$)	
	$SUVA_{254}$	$SUVA_{280}$	$SUVA_{365}$	$SCoA_{436}$	SFI_{emis}	SFI_{syn}
Initial	7.85	6.72	3.00	1.50	18.34	4.73
0	8.11	6.93	2.86	1.33	24.49	6.08
20	7.75	6.50	2.64	1.21	22.21	5.60
40	7.53	6.28	2.45	1.11	19.85	5.42
60	7.41	6.08	2.29	0.99	17.86	5.71

However, increasing fluorescence intensities in the emission scan mode with increasing irradiation time contributed increasing trend in SFI_{emis} and slow degradation of DOC content lead to increasing trend in SFI_{sync} parameter although their fluorescence intensities decreased with increasing irradiation time. While 6% reduction in $SUVA_{254}$, 10% reduction in $SUVA_{280}$, 24% reduction in $SUVA_{365}$ and 34% reduction in $SCoA_{436}$.were obtained for the specific UV-vis parameters, 3% decrease in SFI_{emis} and 17% increase in SFI_{sync} were obtained for the specific fluorescence parameters.

4.2.2. Photocatalytic Oxidation of 100 kDa Fraction of Humic Acid

A broad declining trend of UV-vis absorbance values with respect to photocatalytic irradiation time was obtained for photocatalytic oxidation of 100 kDa fraction of humic acid as displayed in Figure 4.7. The pronounced effect of initial adsorption mechanism at t=0 could also be noticed from the UV-vis scan spectra of samples. Significant changes in the absorptivity of samples were achieved upon irradiation time of 60 minutes. Prior to photocatalytic oxidation, initial adsorption at t=0 caused a reduction in UV_{254} from 54.92 m^{-1} to 36.55 $m^{-1}$and in $Color_{436}$ from 8.65 m^{-1} to 5.07 m^{-1} UV-vis spectra displayed a considerably insignificant difference upon exposure to light for 20 and 40 minutes followed by a rapid decrease in all absorbance values recorded in the 200-350 nm region. However, in the visible region no discrimination could be observed due to the removal of color forming moieties by photocatalysis. Photocatalytic oxidation of 100 kDa fraction of humic acid for 60 minutes resulted in reductions in UV_{254} from 54.92 $m^{-1}$to 20.07 m^{-1} and in $Color_{436}$ from 8.65 m^{-1} to 1.73 cm^{-1}.

Fluorescence intensities of all samples had the characteristic sharp peak at 450 nm giving a decreasing trend with respect to increasing photocatalytic irradiation time in the emission scan mode (Figure 4.8A). When considering photocatalytic oxidation of 100 kDa fraction of humic acid, the most significant changes observed in fluorescence intensities were recorded at 450 nm since beyond this wavelength, overlapping patterns were displayed leading to difficulties to distinguish samples from each other specifically. In case of fluorescence synchronous scan mode, the most pronounced reduction in fluorescence intensities of samples was observed after irradiation times of 20 minutes as shown in Figure 4.8B. For longer irradiation periods, the characteristic sharp peak observed at emission wavelength of 470 nm was disappeared. Although another moderate peak at emission wavelength of 400 nm was observed for all samples, the fluorescence spectral features changed insignificantly with respect to photocatalytic irradiation time. A distinctive peak emerged at around emission wavelength of 275 nm expressing an irradiation time dependent variations in fluorescence intensities being comparatively higher for the humic sub-fraction upon irradiation period of 60 minutes.

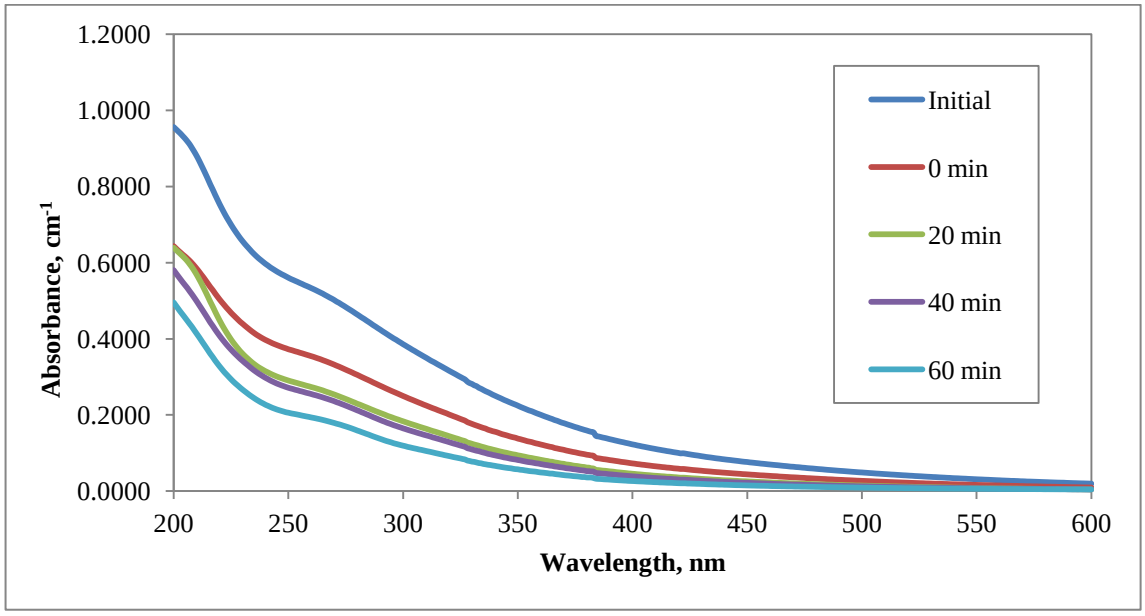

Figure 4.7. UV-vis scan spectra of 100 kDa fraction of humic acid during photocatalytic oxidation.

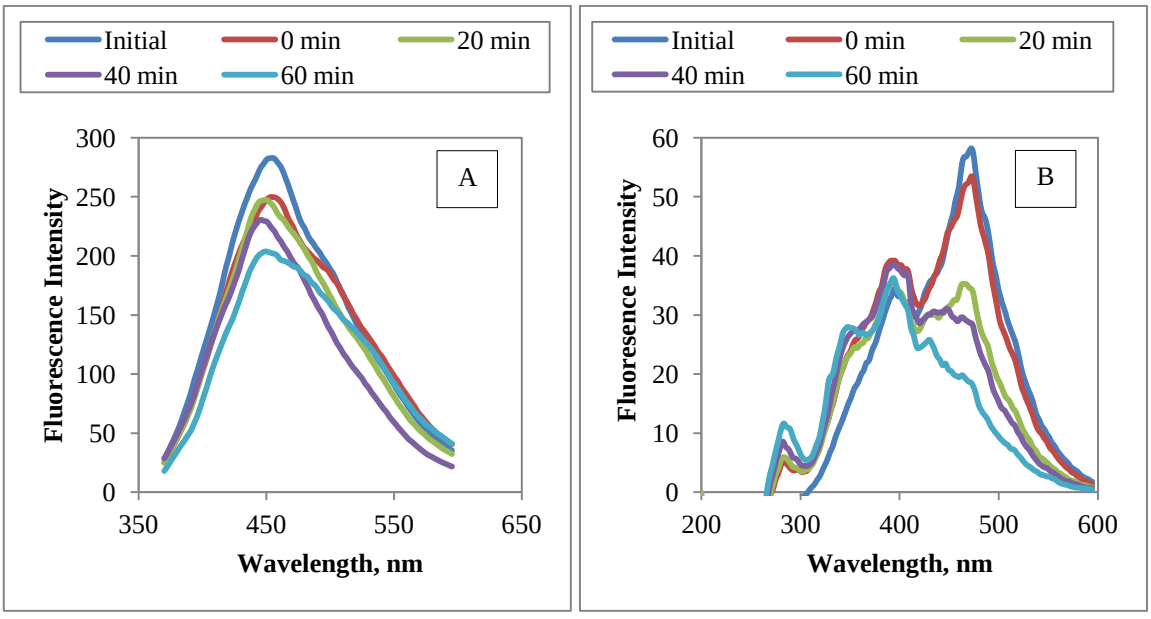

Figure 4.8. Fluorescence intensities of 100 kDa fraction of humic acid in the emission scan mode (8A) and in the synchronous scan mode (8B) during photocatalytic oxidation.

The changes observed for spectral and specific parameters of 100 kDa fraction of humic acid were displayed in Table 4.4. Photocatalytic oxidation of 100 kDa fraction of humic acid for 60 minutes revealed the following results in terms of the removal efficiencies of specific parameters; 16% reduction of $SUVA_{254}$, 21% reduction of $SUVA_{280}$, 44% reduction of $SUVA_{365}$ and 54% reduction of $SCoA_{436}$ respectively.

Table 4.4. Spectral and specific parameters observed of 100 kDa fraction of humic acid during photocatalytic oxidation.

	UV-vis Properties (m^{-1})				Fluorescence Properties Fluorescence Intensity (cm^{-1})	
	UV_{254}	UV_{280}	UV_{365}	$Color_{436}$	$FI_{emis\ 350}$	FI_{syn}
Initial	54.92	46.37	18.92	8.65	281.07	57.60
0	36.55	30.55	11.58	5.07	247.35	52.58
20	28.36	22.96	7.73	3.02	247.27	34.72
40	26.50	21.23	6.65	2.56	229.04	28.75
60	20.07	15.88	4.57	1.73	203.88	18.71
	Specific UV-vis Parameters (m^{-1} $mg^{-1}L$)				Specific Fluorescence Parameters (cm^{-1} $mg^{-1}L$)	
	$SUVA_{254}$	$SUVA_{280}$	$SUVA_{365}$	$SCoA_{436}$	SFI_{emis}	SFI_{syn}
Initial	8.54	7.21	2.94	1.35	43.71	8.96
0	8.55	7.15	2.71	1.19	57.89	12.30
20	7.86	6.37	2.14	0.84	68.55	9.63
40	8.26	6.62	2.07	0.80	71.40	8.96
60	7.20	5.70	1.64	0.62	73.18	6.72

Although reduction in fluorescence intensities and DOC contents of samples were obtained during photocatalytic oxidation, slight reduction of fluorescence intensities of samples and broad reduction of DOC content of samples ended up increasing the ratio of $FI_{emis\ 350}$ to DOC, thus 67% increase of SFI_{emis} was achieved after photocatalytic oxidation of 100 kDa fraction of humic acid for 60 minutes.

4.2.3. Photocatalytic Oxidation of 30 kDa Fraction of Humic Acid

Photocatalytic oxidation of 30 kDa fraction of humic acid was assessed in order to get elaborate understanding of mechanisms and interactions occurring during and after the process while molecular size fractions of samples changed. Moreover, having characterization of photocatalytic oxidation of 30 kDa fraction of humic acid would give further information about the behavior of 100 kDa fraction of humic acid during photocatalytic oxidation.

Photocatalytic oxidation of 30 kDa fraction of humic acid caused changes in terms of UV-vis scan spectra as presented in Figure 4.9. UV-vis absorptivity of samples displayed declining trend with respect to photocatalytic irradiation time in the Uv-vis region. Initial adsorption of humic fractions onto oxide surface slightly altered the spectra in the UV region (λ<220nm). Effect of smaller molecular size fraction on the photocatalytic oxidation process could be clearly observed in this section in terms of UV-vis absorbance values that almost reached to zero after 350 nm. Among three different molecular size fractions of humic acid, the most pronounced reduction in absorbance values of UV_{254} , from 21.52 m^{-1} to 2.57 m^{-1}, and $Color_{436}$, from 2.69 m^{-1} to 0.40 m^{-1}, were achieved by photocatalytic oxidation of 30 kDa fraction of humic acid.

Fluorescence spectra in the emission scan and synchronous scan mode were acquired for 30 kDa fraction of humic acid during photocatalytic oxidation and displayed in Figure 4.10A and Figure 4.10B. Fluorescence intensities in synchronous scan mode and emission scan mode both showed a decreasing trend with respect to photocatalytic irradiation time for photocatalytic oxidation of 30 kDa fraction of humic acid as expected. For the emission scan mode, the characteristic sharp peak at 450 nm became broad after irradiation time of 40 minutes and disappeared after irradiation time of 60 minutes respectively. In addition, the characteristic sharp peak at 470 nm was disappeared after irradiation time of 20 minutes for synchronous scan mode and a moderate peak at 400 nm decreased gradually with increasing photocatalytic irradiation time. Consequently, among all molecular size fractions of humic acid solution, the most substantial decrease in terms of fluorescence intensities in the emission scan and synchronous scan mode was achieved by photocatalytic oxidation of 30 kDa farction of humic acid.

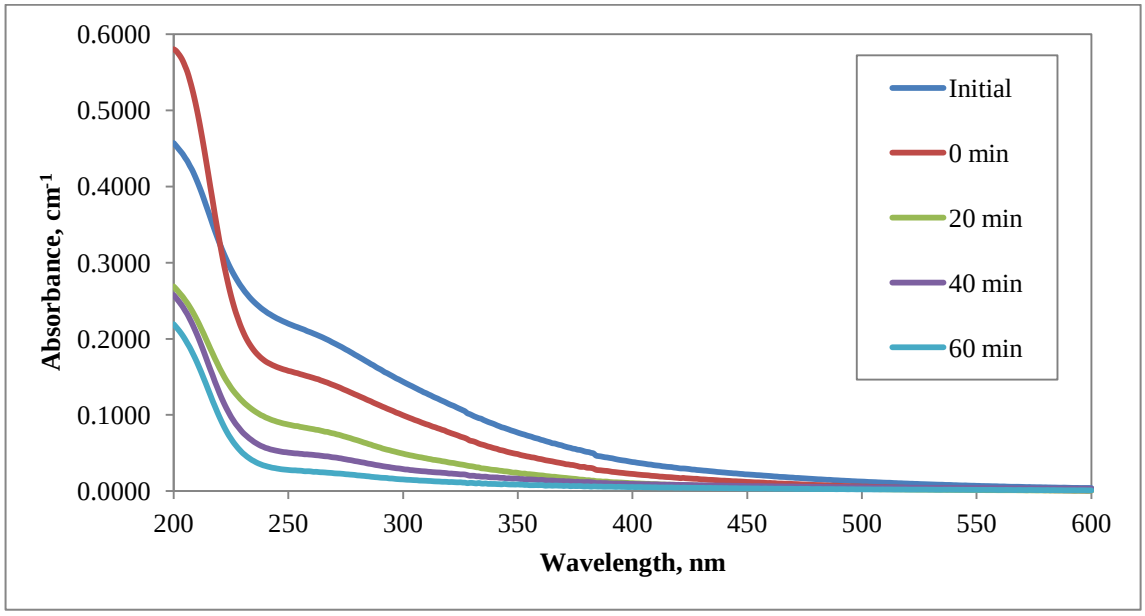

Figure 4.9. UV-vis scan spectra of 30 kDa fraction of humic acid during photocatalytic oxidation.

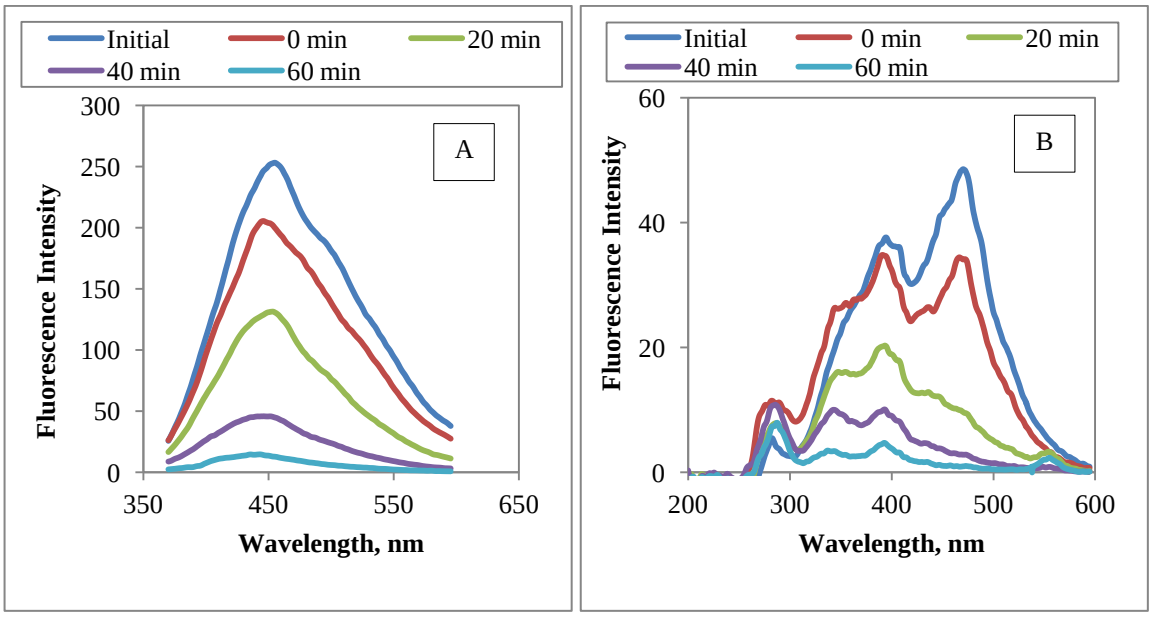

Figure 4.10. Fluorescence intensities of 30 kDa fraction of humic acid in the emission scan mode (10A) and in the synchronous scan mode (10B) during photocatalytic oxidation.

The changes attained for the UV-vis parameters and fluorescence intensities of samples as well as the specific UV-vis and fluorescence parameters were displayed in Table 4.5. After irradiation time of 60 minutes, 57% reduction in $SUVA_{254}$, 60% reduction in $SUVA_{280}$, 62% reduction in $SUVA_{365}$ and 46% reduction in $SCoA_{436}$ were achieved for the photocatalytic oxidation of 30 kDa fraction of humic acid.

Table 4.5. Spectral and specific parameters observed of 30 kDa fraction of humic acid during photocatalytic oxidation.

	UV-vis Properties (m^{-1})				Fluorescence Properties Fluorescence Intensity (cm^{-1})	
	UV_{254}	UV_{280}	UV_{365}	$Color_{436}$	$FI_{emis\ 350}$	FI_{syn}
Initial	21.52	17.75	6.30	2.57	250.64	48.54
0	15.48	12.58	3.91	1.45	204.04	34.11
20	8.55	6.69	1.90	0.66	130.94	9.68
40	4.95	3.91	1.40	0.75	45.84	2.83
60	2.69	2.06	0.70	0.40	13.62	0.98
	Specific UV-vis Parameters (m^{-1} $mg^{-1}L$)				Specific Fluorescence Parameters (cm^{-1} $mg^{-1}L$)	
	$SUVA_{254}$	$SUVA_{280}$	$SUVA_{365}$	$SCoA_{436}$	SFI_{emis}	SFI_{syn}
Initial	8.40	6.93	2.46	1.00	97.79	18.94
0	8.49	6.90	2.15	0.80	111.93	18.71
20	6.01	4.70	1.34	0.46	92.02	6.80
40	4.80	3.79	1.36	0.73	44.46	2.75
60	3.60	2.76	0.94	0.54	18.23	1.32

Removal efficiencies of $SUVA_{254}$, $SUVA_{280}$ and $SUVA_{365}$ reached their highest values by photocatalytic oxidation of 30 kDa fraction of humic acid. In addition, photocatalytic oxidation of 30 kDa fraction of humic acid gave 81% decrease of SFI_{emis} and 96% decrease of SFI_{sync} as the highest removal efficiencies through the results obtained for other molecular size fractions of humic acid.

4.3. Photocatalytic Oxidation of Low Load Grey Water

Photocatalytic oxidation of three different compositions of low load grey water samples namely as ‘’low load grey water with low anion content’’, ‘’low load grey water with high anion content’’ and ‘’ low load grey water with microorganism and low anion content were evaluated elaborately according to the specific and specified parameters considered previously.

4.3.1. Photocatalytic Oxidation of Low Load Grey Water with Low Anion Content

Response of samples to the photocatalytic oxidation of low load grey water with low anion content in terms of UV-vis scan spectra was displayed in Figure 4.11. A monotonous declining trend of UV-vis scan spectra with increasing photocatalytic irradiation time was observed. This could be attributed breaking of bonds between organic molecules supervened by degradation of those organic molecules into smaller ones. In addition, removal of aromatic organic moities and polyphenolic groups also contributed to a reduction in UV-vis absorptivity (Uyguner and Bekbolet, 2007). Initial adsorption at t=0 caused UV_{254} reduction from 56.38 m^{-1} to 39.47 m^{-1} and $Color_{436}$ reduction from 9.02 m^{-1} to 5.62 m^{-1}.

It could be obtained from Figure 4.12A that although all samples had the characteristic sharp peak at 450 nm, pronounced reduction in the fluorescence intensities of samples were observed after photocatalytic irradiation time of 40 minutes in the emission scan mode. Considering the synchronous scan spectra of low load grey water with low anion content as shown in Figure 4.12B, the characteristic sharp peak at 470 nm decayed in intensity with increasing photocatalytic irradiation time and disappeared after irradiation time of 60 minutes. In addition, a moderate peak at 400 nm with an insignificant change and another peak at 290 nm that increased in intensity with increasing photocatalytic irradiation time were also observed indicating the formation and/or degradation of new species during photocatalytic oxidation.that were more fluorescent.

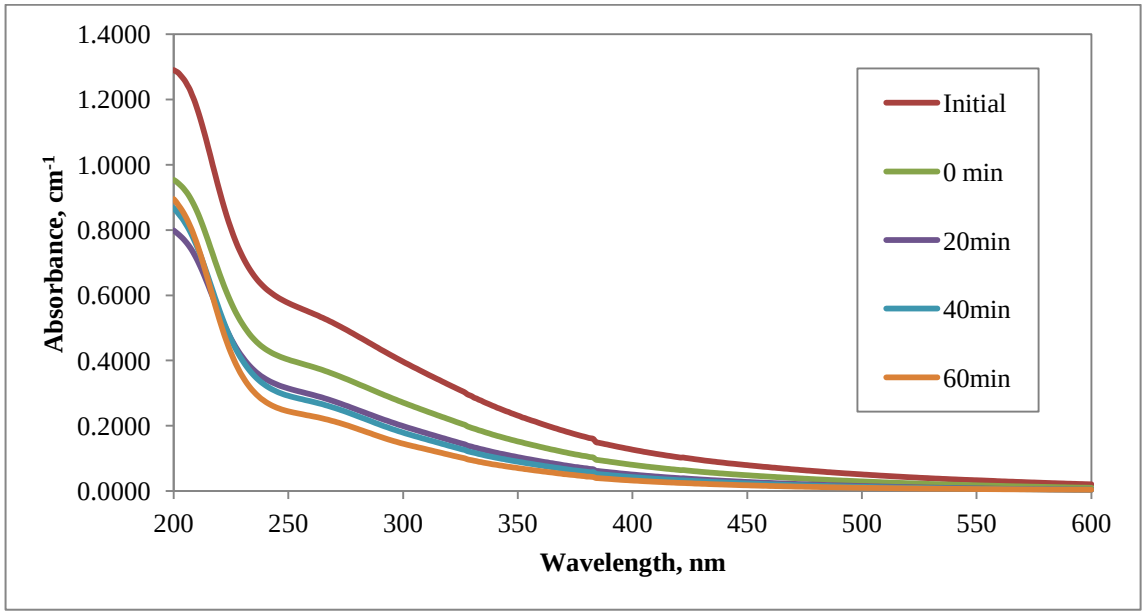

Figure 4.11. UV-vis scan spectra of low load grey water with low anion content during photocatalytic oxidation.

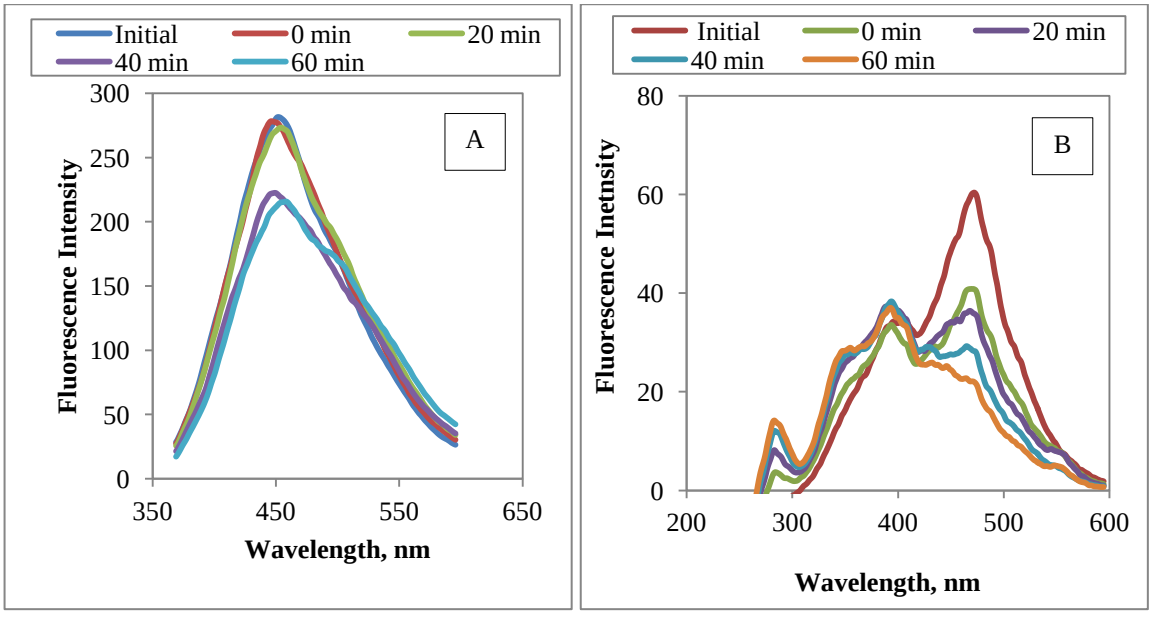

Figure 4.12. Fluorescence intensities of low load grey water with low anion content in the emission scan mode (12A) and in the synchronous scan mode (12B) during photocatalytic oxidation.

Photocatalytic oxidation of low load grey water with low anion content lead to changes in terms of UV-vis and fluorescence properties and DOC contents of samples as well as specific UV-vis and fluorescence parameters that were all displayed in Table 4.6.

Table 4.6. Spectral and specific parameters observed of low load grey water with low anion content during photocatalytic oxidation.

	UV-vis Properties (m^{-1})				Fluorescence Properties Fluorescence Intensity (cm^{-1})	
	UV_{254}	UV_{280}	UV_{365}	$Color_{436}$	$FI_{emis\ 350}$	FI_{sync}
Initial	56.38	47.54	19.56	9.02	280.19	60.16
0	39.47	32.97	12.76	5.61	277.30	40.89
20	30.68	24.92	8.58	3.34	270.66	36.14
40	28.47	23.01	7.35	2.80	222.26	28.47
60	23.82	19.09	5.68	2.08	211.53	22.10
	Specific UV-vis Parameters (m^{-1} $mg^{-1}L$)				Specific Fluorescence Parameters (cm^{-1} $mg^{-1}L$)	
	$SUVA_{254}$	$SUVA_{280}$	$SUVA_{365}$	$SCoA_{436}$	SFI_{emis}	SFI_{syn}
Initial	8.48	7.15	2.94	1.36	42.13	9.05
0	8.34	6.97	2.70	1.19	58.61	8.64
20	7.94	6.45	2.22	0.86	70.01	9.35
40	7.82	6.32	2.02	0.77	61.04	7.82
60	7.84	6.28	1.87	0.69	69.63	7.28

While all UV-vis and fluorescence parameters decreased effectively after irradiation time of 60 minutes, slow degradation of DOC parameter limited removal efficiencies of specific parameters, thus approximately only 8% decrease of $SUVA_{254}$, 12% decrease of $SUVA_{280}$, 36% decrease of $SUVA_{365}$, 49% decrease of $SCoA_{436}$ and 20% decrease of SFI_{sync} were achieved On the other hand, change in the fluorescence intensities of samples in the emission scan mode were comparatively slower than the change observed of DOC content of samples that ended up giving 65% increase of SFI_{emis}.

4.3.2. Photocatalytic Oxidation of Low Load Grey Water with High Anion Content

Photocatalytic oxidation and characterization of low load grey water samples with high anion content were conducted under the same conditions mentioned in photocatalytic oxidation of low load grey water with low anion content section. On the other hand, compositional difference of low load grey water with high anion content in terms of ionic strength contributed comparative evaluation of mechanisms occurred during and after photocatalytic oxidation of two different grey water samples.

UV-vis spectra of low load grey water with high anion content during photocatalytic oxidation were presented in Figure 4.13. An initial adsorption was observed for low load grey water with high anion content when it was first introduced to TiO_2 at time 0 by which removal of more than half of the UV-vis parameters were achieved. On the other hand, an insignificant decreasing trend with different irradiation times were obtained for the absorbance values of samples after irradiation time of 20 minutes. That could be attributed to hydroxyl radical scavenging tendency of high anion concentration that prevented hydroxyl radicals from attacking organic matter existed in sample. In addition, for longer wavelengths e.g. 450 nm absorbance values of samples were overlapped and significance of difference between absorbance values was disappeared. UV_{254} was found to be 54.74 m^{-1} for initial, 20.95 m^{-1} for t= 0 condition and 13.35 m^{-1} for t= 60 minutes and $Color_{436}$ were obtained as 8.61 m^{-1} for initial, 2.45 m^{-1} for t= 0 condition and 1.52 m^{-1} for t= 60 minutes of irradiation period as an indicator of less effective impact of photocatalytic oxidation compared to initial adsorption mechanism.

Fluorescence intensities in terms of emission scan and synchronous scan modes were displayed in Figure 4.14A and Figure 4.14B. A monotonously decreasing trend with increasing irradiation time was observed for emission scan spectra of samples until irradiation time of 40 minutes. As observed in UV-vis spectra, no significant difference between t= 40 minutes and t= 60 minutes was observed. Perceptible differences between the fluorescence intensities of samples in the synchronous scan mode were obtained after initial adsorption revealed at t= 0 and after photocatalytic irradiation time of 60 minutes.

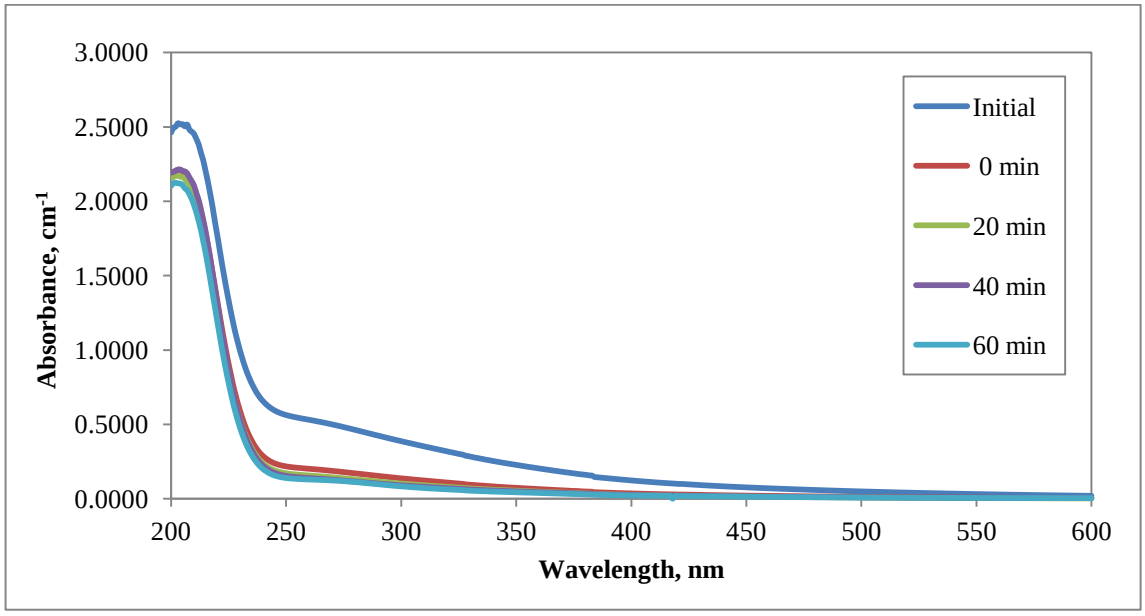

Figure 4.13. UV-vis scan spectra of low load grey water with high anion content during photocatalytic oxidation.

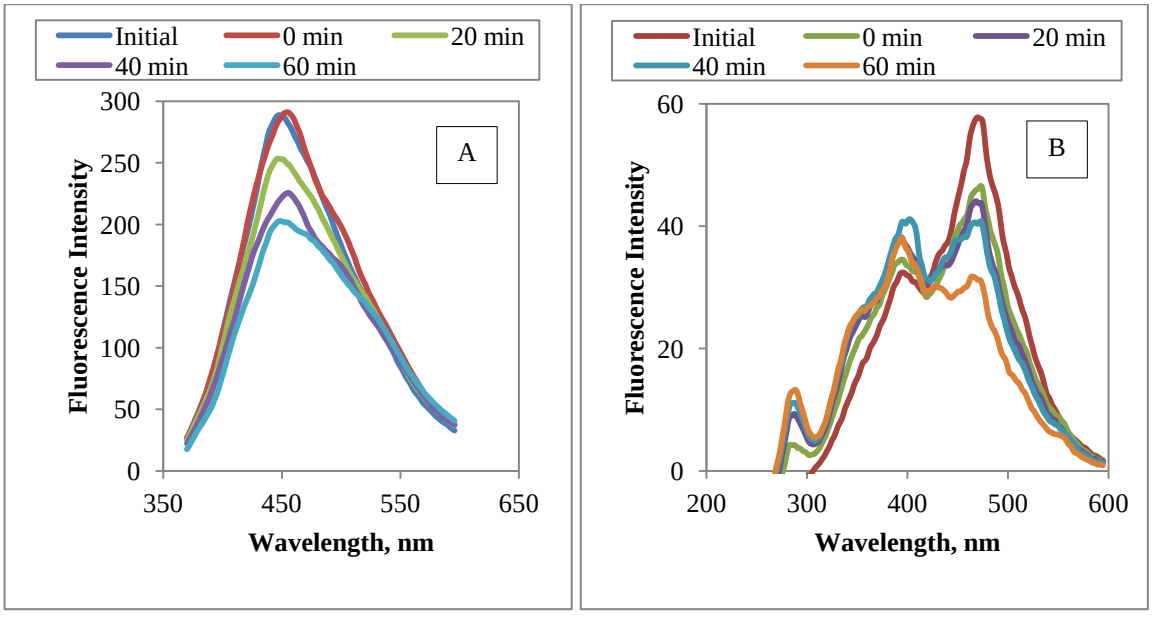

Figure 4.14. Fluorescence intensities of low load grey water with high anion content in the emission scan mode (14A) and in the synchronous scan mode (14B) during photocatalytic oxidation.

Photocatalytic oxidation of low load grey water with high anion content gave the following results for specified UV-vis parameters after irradiation time of 60 minutes; 11% decrease for $SUVA_{254}$, 12% decrease for $SUVA_{280}$, 32% for $SUVA_{365}$ and 36% for $SCoA_{436}$ that were comparatively lower than reduction in specified UV-vis parameters obtained for photocatalytic oxidation of low load grey water with low anion content (Table 4.7). It should also be stated that the $SUVA_{254}$ value reached at 60 minutes of irradiation period still reflected aromatic properties of the organic fraction.

Table 4.7. Spectral and specific parameters observed of low load grey water with high anion content during photocatalytic oxidation.

	UV-vis Properties (m^{-1})				Fluorescence Properties Fluorescence Intensity (cm^{-1})	
	UV_{254}	UV_{280}	UV_{365}	$Color_{436}$	$FI_{emis\ 350}$	FI_{sync}
Initial	54.74	46.21	19.15	8.61	288.05	57.83
0	20.95	17.08	6.08	2.45	288.00	39.39
20	16.40	13.05	4.49	1.75	253.11	36.87
40	14.58	11.52	4.16	1.80	221.91	37.74
60	13.35	11.15	3.60	1.52	202.56	31.26
	Specific UV-vis Parameters (m^{-1} $mg^{-1}L$)				Specific Fluorescence Parameters (cm^{-1} $mg^{-1}L$)	
	$SUVA_{254}$	$SUVA_{280}$	$SUVA_{365}$	$SCoA_{436}$	SFI_{emis}	SFI_{syn}
Initial	8.56	7.23	3.00	1.35	45.06	9.05
0	8.65	7.05	2.51	1.01	118.91	8.44
20	7.17	5.70	1.96	0.77	110.58	8.97
40	7.54	5.98	2.16	0.94	115.22	9.07
60	7.59	6.34	2.05	0.87	115.22	7.64

In addition, a substantial increase in SFI_{emis} and 16% decrease for SFI_{sync} were achieved after irradiation time of 60 minutes that were also comparatively lower than data obtained for photocatalytic oxidation of low load grey water with low anion content as presented in Table 4.6.

4.3.3. Photocatalytic Oxidation of Low Load Grey Water with Microorganism and Low Anion Content

In this section grey water composition was selected and prepared in the presence of humic acid, low range anion content and bacterial cultures and then subjected to photocatalytic oxidation with the aim of investigating degradation of organic matter and disinfection tendency of the process simultaneously. It was concluded from previous sections that high concentrations of anions caused inhibitory effect on the photocatalytic oxidation process, thus anion concentration of grey water composition was chosen in the low range.

Photocatalytic oxidation of low load grey water with microorganism and low anion content revealed the UV-vis scan spectra displayed in Figure 4.15. A monotonously decreasing trend with respect to increasing photocatalytic irradiation time was observed. Although, a slight increase in absorbance values was appeared after irradiation time of 40 minutes, the most pronounced decrease of UV-vis spectra of samples was achieved after irradiation time of 60 minutes. UV-vis absorptivity almost reached to zero measured at wavelength of 350 nm, by photocatalytic oxidation of low load grey water with microorganism and low anion content followed by the irradiation period of 90 minutes displaying almost complete removal of organic moities.

The variations attained in fluorescence intensities by photocatalytic oxidation of low load grey water with microorganism and low anion content were displayed in Figure 4.16A and Figure 4.16B in terms of emission and synchronous scan spectra. Fluorescence intensities of samples in the emission scan mode and synchronous scan mode both showed gradual decreasing trend with respect to increasing photocatalytic irradiation time. Moreover, the characteristic sharp peak at emission wavelength of 450 nm was observed until after irradiation time of 40 minutes and after that time, trend of fluorescence intensities of samples became widened. After an irradiation period of 90 minutes, fluorescence intensity of low load grey water sample with microorganism and low anion content only showed a peak at 290 nm in the synchronous scan mode.

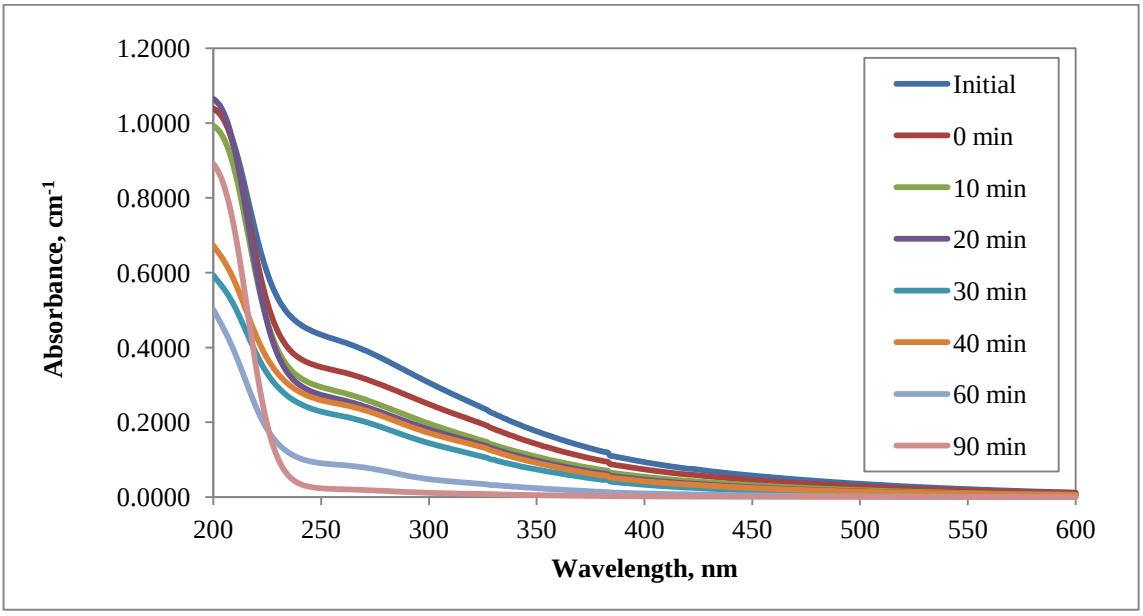

Figure 4.15. UV-vis scan spectra of low load grey water with microorganism and low anion content during photocatalytic oxidation.

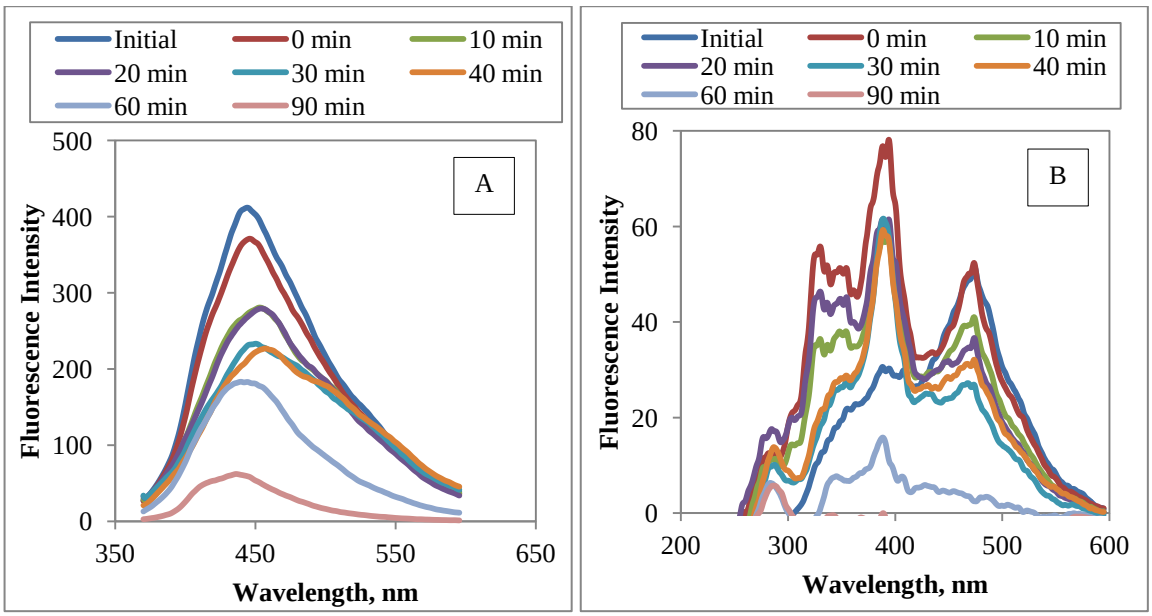

Figure 4.16. Fluorescence Intensities of low load grey water with microorganism and low anion content in the emission scan mode (16A) and in the synchronous scan mode (16B) during photocatalytic oxidation.

Fluorescence intensity of the samples measured at 300 nm in the synchronous scan mode were disappeared which was an indicator of almost complete degradation of organic matter into carbon dioxide and water. Table 4.8 gave the spectral and specific parameters obtained for low load grey water with microorganism and low anion content during photocatalytic oxidation.

Table 4.8. Spectral and specific parameters observed of low load grey water with microorganism and low anion content during photocatalytic oxidation.

	UV-vis Properties (m^{-1})				Fluorescence Properties Fluorescence Intensity (cm^{-1})	
	UV_{254}	UV_{280}	UV_{365}	$Color_{436}$	$FI_{emis\ 350}$	FI_{sync}
Initial	42.60	36.55	14.68	6.60	402.77	48.96
0	34.20	29.54	11.75	5.20	366.36	50.09
10	28.80	24.04	8.84	3.70	278.40	39.44
20	26.80	22.26	7.91	3.10	276.90	34.51
30	22.30	18.27	5.83	2.00	233.24	26.59
40	25.40	21.27	7.29	2.80	222.08	30.77
60	8.80	6.89	1.84	0.60	180.80	3.34
90	2.20	1.64	0.39	0.10	53.56	2.73
	Specific UV-vis Parameters (m^{-1} $mg^{-1}L$)				Specific FluorescenceParameters (cm^{-1} $mg^{-1}L$)	
	$SUVA_{254}$	$SUVA_{280}$	$SUVA_{365}$	$SCoA_{436}$	SFI_{emis}	SFI_{syn}
Initial	3.93	3.38	1.36	0.61	37.19	4.52
0	3.41	2.95	1.17	0.52	36.53	4.99
10	2.95	2.46	0.90	0.38	28.48	4.03
20	3.09	2.57	0.91	0.36	31.91	3.98
30	2.68	2.19	0.70	0.24	28.01	3.19
40	3.12	2.61	0.90	0.34	27.27	3.78
60	1.37	1.08	0.29	0.09	28.22	0.52
90	0.44	0.33	0.08	0.02	10.63	0.54

89% decrease for $SUVA_{254}$, 80% decrease for $SUVA_{280}$, 94% decrease for $SUVA_{365}$, 97% decrease for $SCoA_{436}$ and 71% decrease for SFI_{emis} and 88% decrease in SFI_{sync} were achieved after irradiation time of 90 minutes.

4.4. Photocatalytic Oxidation of High Load Grey Water

Effect of organic matter loading on the performance of photocatalytic oxidation process was evaluated by using high load organic matter in synthetic grey water composition. In this section, photocatalytic oxidation of high load grey water samples with different compositions were taken into consideration in terms of UV-vis and fluorescence properties and specified parameters that were also functions of UV-vis, fluorescence and DOC properties.

4.4.1. Photocatalytic Oxidation of High Load Grey Water with Low Anion Content

The changes observed in the UV-vis scan spectra of samples were presented in Figure 4.17. Although ionic strength of high load grey water sample chosen in the specified low range, higher organic matter loading made it difficult to degrade those large molecules into simpler ones, thus a broad declining trend of UV-vis spectra was obtained for the photocatalytic oxidation of high load grey water with low anion content. The most pronounced change in the UV-vis absorptivity was obtained at t=0 when sample was firstly introduced to TiO_2 and the initial adsorption mechanism occurred.

Spectral changes in terms of emission scan mode and synchronous scan mode were displayed in Figure 4.18A and Figure 4.18B. Emission scan spectra of high load grey water with low anion content had the characteristic sharp peak at 450 nm decayed in fluorescence intensity gradually with respect to increasing photocatalytic irradiation time. Fluorescence intensities of samples displayed a monotonous and featureless declining trend with respect to increasing photocatalytic irradiation time in the synchronous scan mode. Moreover, another moderate peak at 400 nm was also attained with an increasing trend parallel to increasing photocatalytic irradiation time on account of emerging of new compounds due to degradation of larger molecules into smaller but more fluorescent ones (Uyguner and Bekbolet, 2005a).

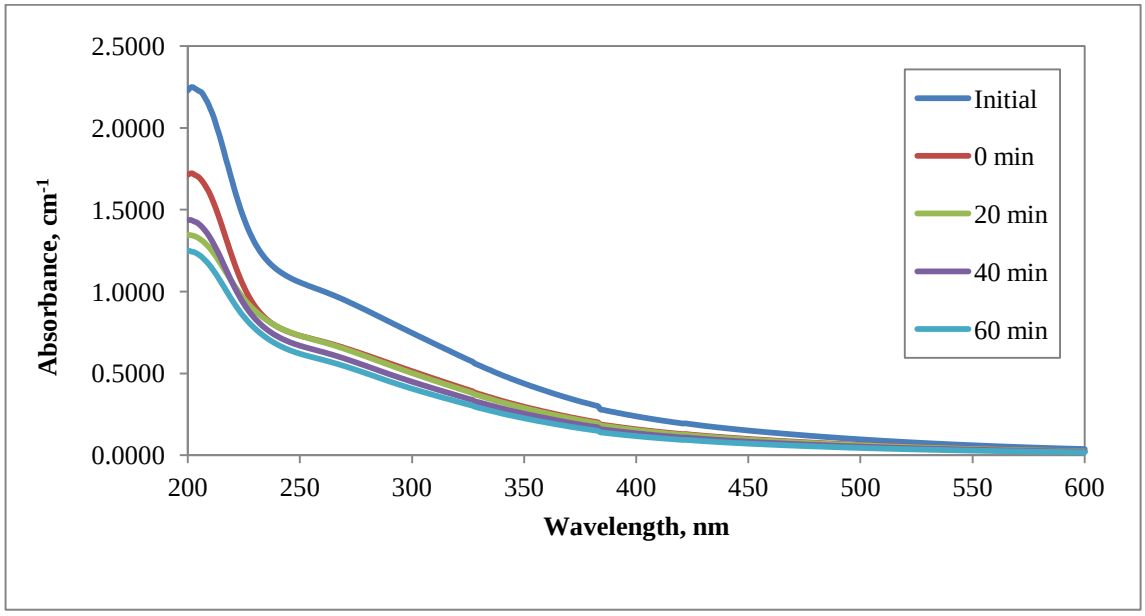

Figure 4.17. UV-vis scan spectra of high load grey water with low anion content during photocatalytic oxidation.

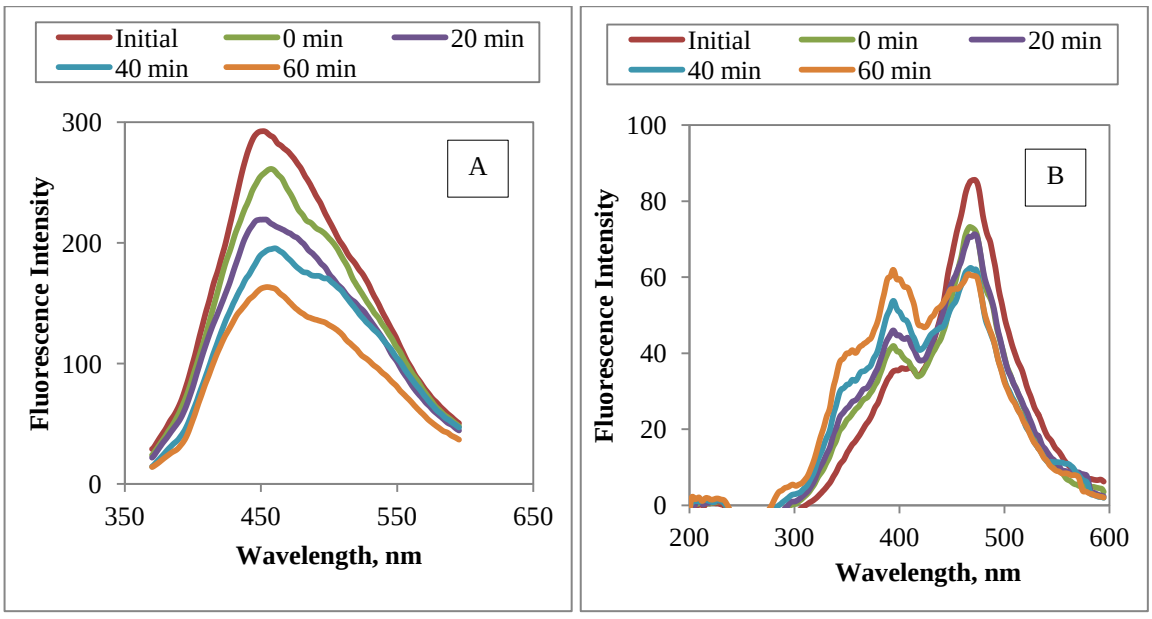

Figure 4.18. Fluorescence intensities of high load grey water with low anion content in the emission scan mode (18A) and in the synchronous scan mode (18B) during photocatalytic oxidation.

The UV-vis and fluorescence spectral as well as the specific parameters of high load grey water with low anion content with respect to photocatalytic irradiation time were displayed in Table 4.9.

Table 4.9. Spectral and specific parameters observed of high load grey water with low anion content during photocatalytic oxidation.

	UV-vis Properties (m^{-1})				Fluorescence Properties Fluorescence Intensity (cm^{-1})	
	UV_{254}	UV_{280}	UV_{365}	$Color_{436}$	$FI_{emis\ 350}$	FI_{sync}
Initial	103.50	88.39	37.02	17.18	340.48	85.61
0	71.64	61.04	24.97	11.41	292.48	72.89
20	71.47	60.10	24.14	10.89	255.31	70.93
40	65.37	54.32	21.16	9.38	219.21	61.96
60	60.48	49.82	18.75	8.11	189.96	60.38
	Specific UV-vis Parameters (m^{-1} $mg^{-1}L$)				Specific Fluorescence Parameters (cm^{-1} $mg^{-1}L$)	
	$SUVA_{254}$	$SUVA_{280}$	$SUVA_{365}$	$SCoA_{436}$	SFI_{emis}	SFI_{syn}
Initial	7.93	6.77	2.84	1.32	26.10	6.56
0	8.57	7.30	2.99	1.37	34.98	8.72
20	8.28	6.96	2.80	1.26	29.57	8.22
40	7.98	6.63	2.58	1.15	76.76	7.56
60	7.45	6.15	2.31	1.00	23.43	7.45

UV-vis parameters of high load grey water with low anion content, ended up with 6% decrease of $SUVA_{254}$, 9% decrease of $SUVA_{280}$, 18% decrease of $SUVA_{365}$ and 24% decrease of $SCoA_{436}$ by photocatalytic oxidation for 60 minutes. It could also be stated that $SUVA_{254}$ (7.93-7.45) expressed the presence of the aromatic character (SUVA> 4) as expected. Parallel to specific UV-vis parameters, undistinguished declining trend of fluorescence intensities of samples caused only 10% decrease of SFI_{emis} and 14% increase of SFI_{sync}.

4.4.2. Photocatalytic Oxidation of High Load Grey Water with High Anion Content

Influence of anion strength on the performance of photocatalytic oxidation of grey water were evaluated by increasing the anion concentration of high load grey water composition studied in previous section and subjecting this new composition to photocatalytic oxidation respectively. All samples were characterized according to the parameters taken into account in previous sections.

High load grey water with high anion content displayed an insignificant monotonously decreasing trend with respect to increasing photocatalytic irradiation in terms of UV-vis scan spectra as shown in Figure 4.20. This could be attributed to high concentrations of organic matter and anions together. Due to their tendency of hydroxyl radical scavenging mechanism, high concentrations of anions captured those hydroxyl radicals before reaching organic matter for the degradation of larger organic molecules into smaller and simpler ones. After irradiation time of 60 minutes, UV_{254} decreased from 102.58 m^{-1} to 74.12 m^{-1} and $Color_{436}$ decreased from 17.16 m^{-1} to 10.56 m^{-1} that were slightly higher than UV_{254} and $Color_{436}$ reduction of high load grey water with low anion content.

Fluorescence properties of high load grey water with high anion content were assessed in terms of emission scan spectra and synchronous scan spectra as presented in Figure 4.21A and Figure 4.21B separately. Emission scan spectra of high load grey water with high anion content displayed a monotonous broad declining trend with increasing photocatalytic irradiation time. The most significant reduction in fluorescence intensity of samples was attained after photocatalytic irradiation time of 40 minutes in the emission scan mode and after that time extended photocatalytic irradiation time did not affect the declining of fluorescence intensity appreciably. Although all samples exhibited the characteristic sharp peak at 470 nm, fluorescence intensities of samples displayed an undistinguished but slightly declining trend with respect to increasing photocatalytic irradiation time in terms of synchronous scan mode indicating that degradation of organic matter was mitigated by means of large organic molecules and high concentrations of anions.

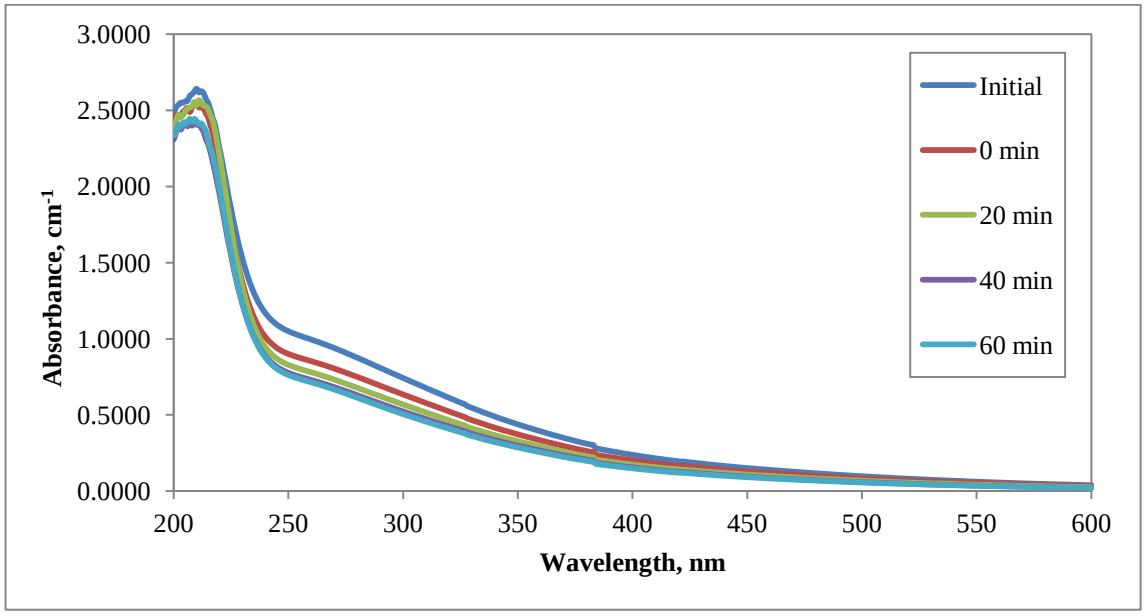

Figure 4.19. UV-vis scan spectra of high load grey water with high anion content during photocatalytic oxidation.

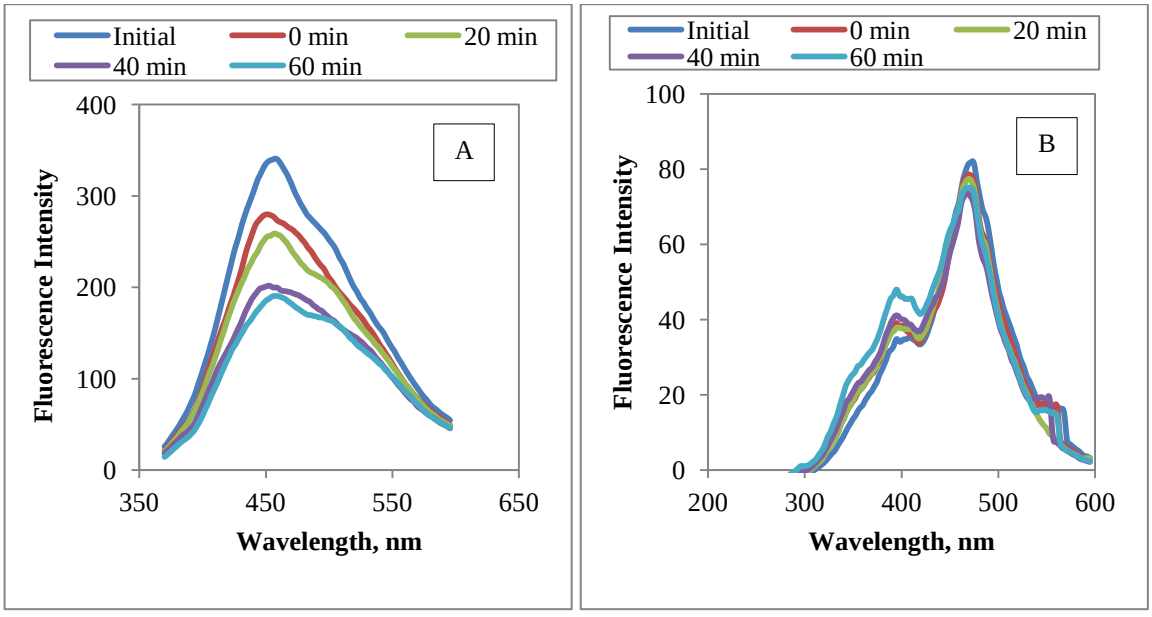

Figure 4.20. Fluorescence intensities of high load grey water with high anion content in the emission scan mode (20A) and in the synchronous scan mode (20B) during photocatalytic oxidation.

Influence of photocatalytic oxidation on the UV-vis and fluorescence spectral as well as the specific parameters of high load grey water with high anion content were shown in Table 4.10.

Table 4.10. Spectral and specific parameters observed of high load grey water with high anion content during photocatalytic oxidation.

	UV-vis Properties (m^{-1})				Fluorescence Properties Fluorescence Intensity (cm^{-1})	
	UV_{254}	UV_{280}	UV_{365}	$Color_{436}$	$FI_{emis\ 350}$	FI_{sync}
Initial	102.58	87.62	37.08	17.16	335.07	81.55
0	87.83	74.93	31.34	14.46	279.50	78.56
20	80.77	67.93	27.62	12.43	254.14	77.38
40	75.60	63.06	25.07	11.00	200.78	73.07
60	74.12	61.37	24.06	10.56	185.46	75.08
	Specific UV-vis Parameters (m^{-1} $mg^{-1}L$)				Specific Fluorescence Parameters (cm^{-1} $mg^{-1}L$)	
	$SUVA_{254}$	$SUVA_{280}$	$SUVA_{365}$	$SCoA_{436}$	SFI_{emis}	SFI_{syn}
Initial	7.97	6.81	2.88	1.33	26.02	6.33
0	8.82	7.52	3.15	1.45	28.06	7.89
20	8.98	7.55	3.07	1.38	28.26	8.60
40	8.96	7.47	2.97	1.30	23.79	8.66
60	9.94	8.23	3.23	1.42	24.87	10.07

25% increase of $SUVA_{254}$, 21% increase of $SUVA_{280}$, 12% increase of $SUVA_{365}$, 7% increase of $SCoA_{436}$ and 59% increase of SFI_{sync} were attained after photocatalytic oxidation of high load grey water with high anion content for 60 minutes. In contrast to results obtained for high load grey water with high anion content, only 4% decrease of SFI_{emis} was achieved.in terms of specific fluorescence parameters.

4.4.3. Photocatalytic Oxidation of High Load Grey Water with Microorganism and Low Anion Content

UV-vis scan spectra of high load grey water in the presence of microorganism and low anion content during photocatalytic oxidation were displayed in Figure 4.21. A significant declining trend in UV-vis absorptivity was attained for the photocatalytic oxidation of high load grey water with microorganism and low anion content with respect to increasing phtocatalytic irradiation period. Considering the unavoidable filtration step to eliminate the photocatalyst particles through 0.45 mm membrane filters, the suspended bacteria were also successfully removed. The UV-vis spectra clearly displayed the featureless spectral features of oxidized humic fractions leading to the possible evaluation of the specified and specific parameters. After irradiation time of 180 minutes, UV_{254} decreased from 126.98 m^{-1} to 36.81 m^{-1} and $Color_{436}$ decreased from 21.48 m^{-1} to 2.47 m^{-1} obtained as the lowest value among all of the other high load grey water samples. Besides the attained efficient decolorization, from a general perspective, slow degradation of organic matter could be attributed to the prevailing competitive conditions occurring among organic matter, anions and microorganisms as hydroxyl radical scavengers.

Change in fluorescence properties of high load grey water with microorganism and low anion content during photocatalytic oxidation was presented in Figure 4.22A in the emission scan mode and in Figure 4.22B in the synchronous scan mode. Fluorescence intensities of samples displayed the similar decreasing trend with increasing irradiation time as observed for previous experiments. More specifically, instead of the characteristic sharp peak observed emission wavelength of 450 nm, the sharpest peak for synchronous scan mode was obtained emission wavelength of 400 nm increasing with increasing irradiation time until a reaction period of 150 minutes. Following this period, fluorescence intensities decreased with increasing irradiation time that could be attributed to production of intermediates with higher fluorescence intensities during photocatalytic oxidation. In addition, formation of new species exhibiting a significant absorption revealed moderate twin peaks at 330 nm and at 350 nm that were also observed for synchronous scan spectra of low load grey water with microorganism and low anion content during photocatalytic oxidation (Figure 4.16B).

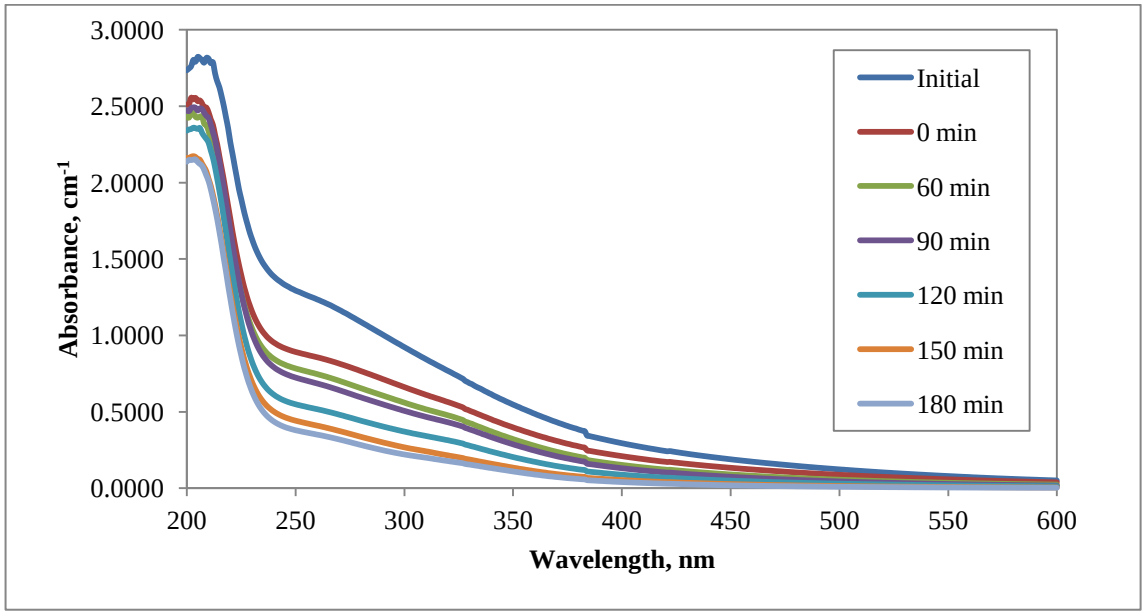

Figure 4.21. UV-vis scan spectra of high load grey water with microorganism and low anion content during photocatalytic oxidation.

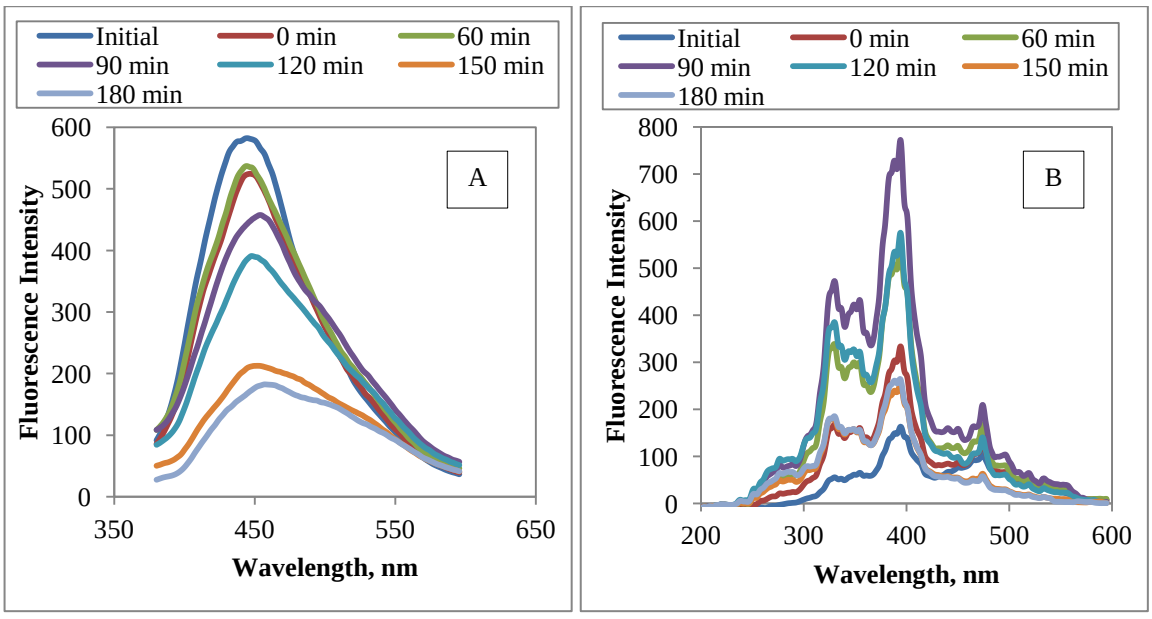

Figure 4.22. Fluorescence intensities of high load grey water with microorganism and low anion content in the emission scan mode (22A) and in the synchronous scan mode (22B) during photocatalytic oxidation.

While 20% decrease for $SUVA_{254}$, 28% decrease for $SUVA_{280}$, 51% decrease for $SUVA_{365}$ and 68% decrease for $SCoA_{436}$ were achieved, up to 16% decrease for SFI_{emis} and 41% increase for SFI_{sync} were achieved for the specified fluorescence parameters of high load grey water with microorganism and low anion content.

Table 4.11. Spectral and specific parameters observed of high load grey water with microorganism and low anion content during photocatalytic oxidation.

	UV-vis Properties (m^{-1})				Fluorescence Properties Fluorescence Intensity (cm^{-1})	
	UV_{254}	UV_{280}	UV_{365}	$Color_{436}$	$FI_{emis\ 350}$	FI_{sync}
Initial	126.98	108.84	45.97	21.48	578.71	93.28
0	87.67	76.60	32.94	15.07	528.82	108.17
60	76.91	65.52	25.77	10.49	522.03	135.50
90	70.83	59.52	22.72	8.77	453.75	166.41
120	53.54	44.16	15.76	5.75	389.46	109.60
150	42.80	33.64	10.18	3.25	212.57	52.99
180	36.81	28.38	8.21	2.47	176.80	47.75
	Specific UV-vis Parameters (m^{-1} $mg^{-1}L$)				Specific Fluorescence Parameters (cm^{-1} $mg^{-1}L$)	
	$SUVA_{254}$	$SUVA_{280}$	$SUVA_{365}$	$SCoA_{436}$	SFI_{emis}	SFI_{syn}
Initial	9.62	8.25	3.48	1.63	43.84	7.07
0	10.56	9.23	3.97	1.82	63.71	13.03
60	10.54	8.98	3.53	1.44	71.51	18.56
90	10.42	8.75	3.34	1.29	66.73	24.47
120	9.07	7.48	2.67	0.97	66.01	18.58
150	9.22	7.25	2.19	0.70	45.81	11.42
180	7.68	5.92	1.71	0.52	36.91	9.97

Among all different high load grey water samples, highest removal efficiencies for the specified UV-vis and fluorescence parameters were achieved by photocatalytic oxidation of high load grey water sample with microorganism and low anion content (Tables 4.9,

4.10 and 4.11). The reason could be mainly attributed to the low ionic strength exerted by the presence of low anionic solution matrix (Uyguner and Bekbolet, 2009).

4.5. Comparative Evaluation of Photocatalytic Oxidation of Different Grey Water Samples in Terms of Removal Efficiencies of Selected Parameters

Photocatalytic oxidation and characterization of compositionally different grey water samples were investigated in terms of the changes observed in reduction of UV-vis and fluorescence parameters and as well as the specific parameters as reported separately in previous sections. On the other hand, circumstantial assessment of the attained results could be presented by taking different aspects of experimental results into consideration in detail. For this purpose, performance of photocatalytic oxidation process was evaluated in terms of removal efficiencies of selected parameters particularly. In addition, impact of solution matrix and interactions between the components of grey water samples could be observed and discussed. The abbreviations used in order to define different grey water compositions were listed in Table 4.12.

Table 4.12. Abbreviations used for grey water compositions.

Abbreviation	Explanation
LLOM	Low load organic matter used for the preparation of low load grey water
HLOM	High load organic matter used for preparation of high load grey water
LLGWLIC	Low load grey water with low anion content
LLGWHIC	Low load grey water with high anion content
LLGW	Low load grey water with microorganism and low anion content
HLGWLIC	High load grey water with low anion content
HLGWHIC	High load grey water with high anion content
HLGW	High load grey water with microorganism and low anion content

In this section, removal efficiencies of selected UV-vis parameters, DOC content and bacterial content of different compositions of grey water samples were assessed separately with respect to photocatalytic oxidation process.

4.5.1. Comparative Evaluation of UV-vis Parameters of Different Grey Water Samples During Photocatalytic Oxidation

Comparative evaluation of UV-vis parameters of different grey water samples (LLGWLIC, LLGWHIC, LLGW, HLGWLIC, HLGWHIC and HLGW) and organic matter contents used in grey water compositions (LLOM and HLOM) during photocatalytic degradation were evaluated by pesenting the changes in $Color_{436}$, UV_{365}, UV_{280} and UV_{254} parameters attained for t=0 condition as well as followed by the irradiation period of 60 minutes. The following figures 4.23-4.26 represented the removals of the UV-vis parameters attained under the specified conditions.

Decolorization efficiency as expressed by $Color_{436}$ removal of different grey water samples were displayed in Figure 4.23. After irradiation time of 60 minutes, $Color_{436}$ removal efficiencies of low load grey water samples were obtained as 91% for LLGW> 82% for LLGWHIC> 77% for LLGWLIC> 66% for LLOM. Prior to photocatalytic oxidation, all samples came under the influence of initial adsorption at t=0 and removed some of $Color_{436}$, but made the effect of photocatalytic oxidation insignificant for the treatment of low load grey water with low anion content that resulted in only 10% removal of $Color_{436}$ specifically.

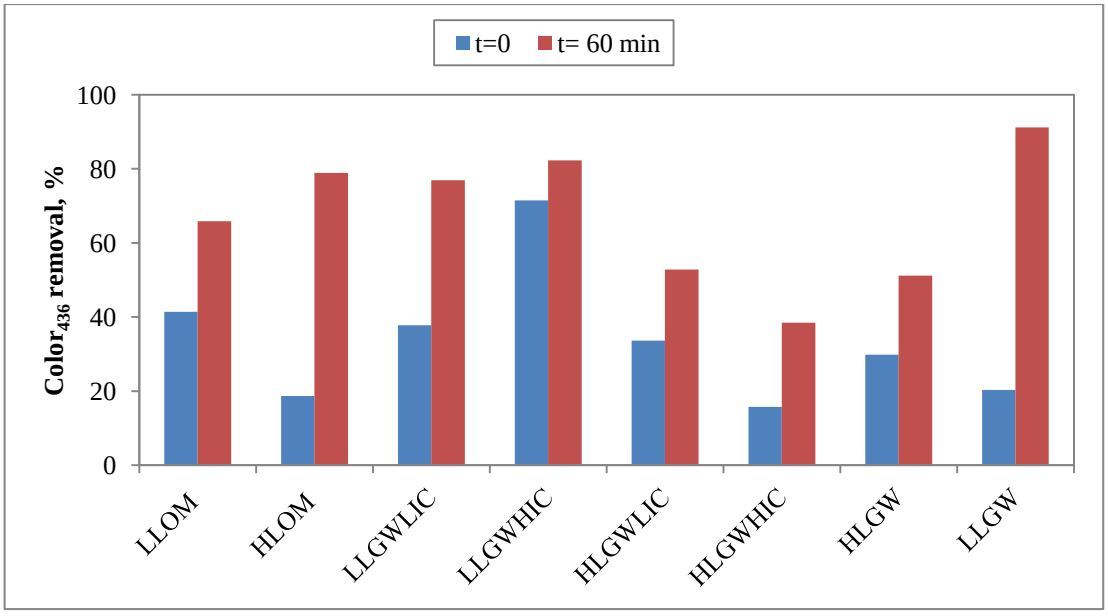

Figure 4.23. Comparative evaluation of $Color_{436}$ removal of different grey water samples.

$Color_{436}$ removal efficiencies of high load grey water samples were displayed a decreasing trend in the order of 79% for HLOM> 53% for HLGWLIC>51% for HLGW>28%for HLGWHIC after irradiation time of 60 minutes. When considering all grey water samples in terms of $Color_{436}$ removal, the most desirable result was attained for the photocatalytic oxidation of low load grey water with microorganism and low anion content ended up with 91% percent removal of $Color_{436}$. Inhibitory effect of solution matrixes on the decolourisation of high load grey water samples observed from figure in which highest $Color_{436}$ removal percentage was achieved for the photocatalytic oxidation of high load organic matter containing nothing except the organic component of high load grey water composition.

Removal efficiencies of species having absorptivity at 365 nm (UV_{365}) with respect to photocatalytic irradiation time were presented in Figure 4.24 for different grey water compositions particularly. After photocatalytic irradiation time of 60 minutes, low load grey water samples gave the following order of UV_{365} removal as 88% for LLGW> 81% for LLGWHIC> 76% for LLOM> 71% for LLGWLIC that were significantly higher than UV_{365} removal of high load grey water samples that reached up to 73% for HLOM> 49% for HLGWLIC> 44% for HLGW> 35% for HLGWHIC respectively.

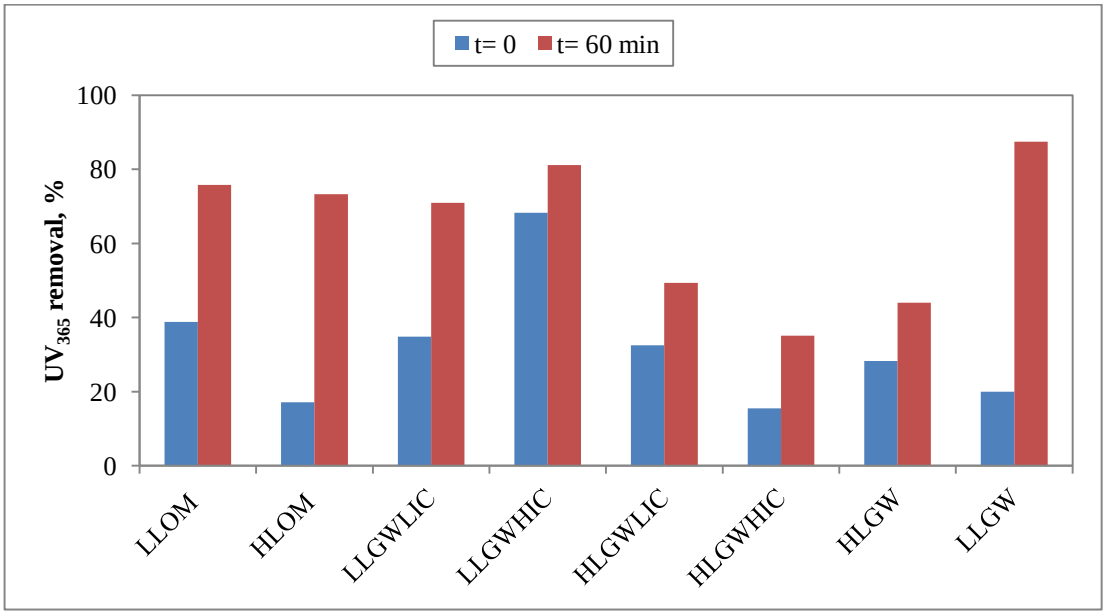

Figure 4.24. Comparative evaluation of UV_{365} removal of different grey water samples.

Parallel to results obtained for removal percentages of UV-vis parameters previously, the highest UV_{365} removal efficiency was achieved by the photocatalytic oxidation of low load grey water with microorganism and low anion for 60 minutes.

Compositional differences of grey water samples expressed varying removal percentages of UV_{280} with regard to photocatalytic oxidation as presented in Figure 4.25. Approximately 81%, 76%, 71%, 48% removal of UV_{280} were attained for LLGW, LLGWHIC, LLGWLIC and LLOM respectively after photocatalytic oxidation for 60 minutes that were comparatively lower than the removal efficiencies attained for $Color_{436}$ and UV_{365} as expected (Uyguner and Bekbolet, 2005b). Photocatalytic oxidation of high load grey water samples displayed the following trend in terms of UV_{280} removal as 62% for HLOM> 44% for HLGWLIC> 40% for HLGW> 28% for HLGW. Although UV_{280} removal expressed 76% for LLGWHIC, 63% removal of UV_{280} had already been achieved at t=0 by initial adsorption mechanism indicating an efficient surface coverage for photocatalytic oxidation process. Regarding the aromaticity of humic substances as expressed by UV_{280}, the extent of surface coverage could not be correlated well to the photocatalytic removal efficiencies of UV_{280} attained for an irradiation period of 60 minutes.

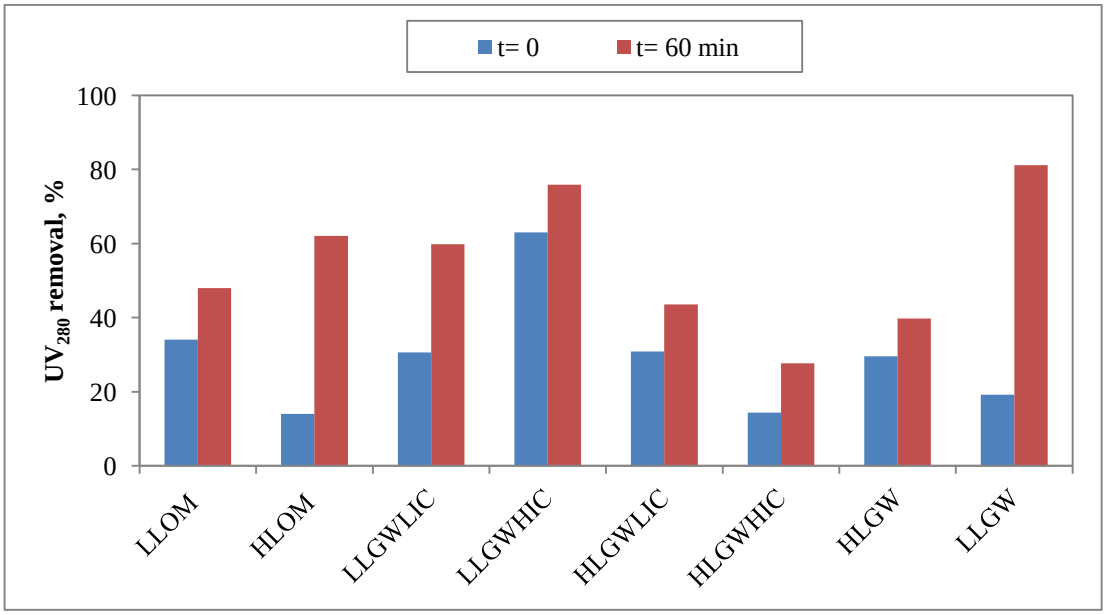

Figure 4.25. Comparative evaluation of UV_{280} removal of different grey water samples.

Contribution of solution complexity to the photocatalytic oxidation process was again proven in terms of UV_{280} removal that gave the highest value for LLGW. On the other hand, same conditions caused inhibitory effect on the performance of photocatalytic oxidation treating high load grey water samples by giving the lowest UV_{280} removal percentages.

Comparative UV_{254} removal efficiencies with respect to photocatalytic irradiation time were displayed in Figure 4.26. UV_{254} removal efficiencies of low load grey water samples decreased in the following order of 79% for LLGW> 76% for LLGWHIC> 66% for LLOM> 58% for LLGWLIC. The overall UV_{254} removal tendency followed 42% for HLGWLIC> 39% for HLGW> 28% for HLGWHIC> 26% for HLOM trend for high load grey water samples that were comparatively lower than removal efficiencies obtained for low load grey water samples.

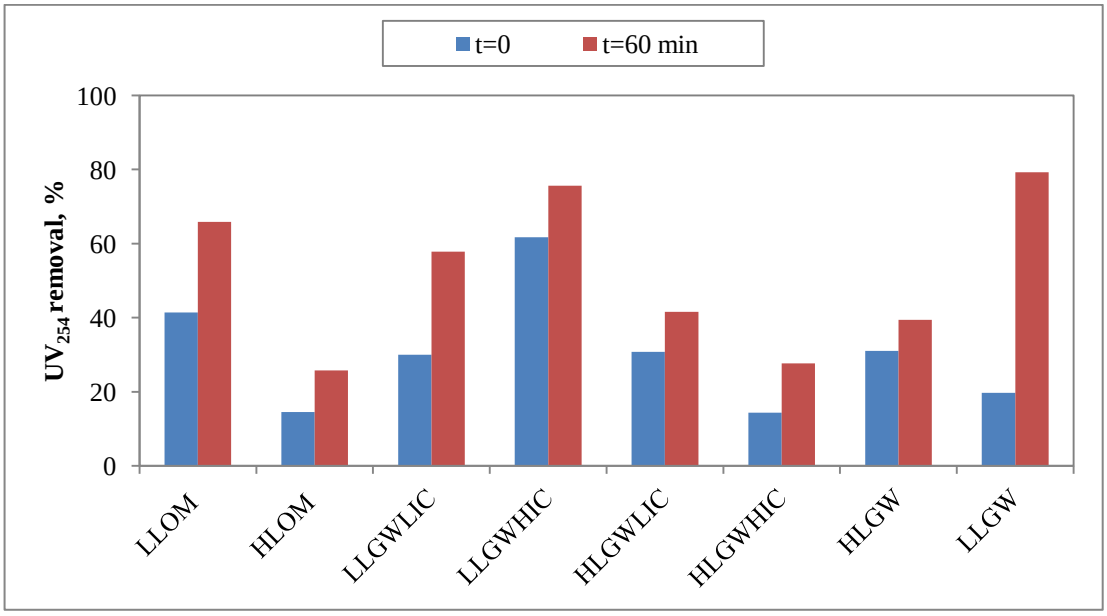

Figure 4.26. Comparative evaluation of UV_{254} removal of different grey water samples.

Among all different grey water compositions, the highest removal efficiency of UV_{254} was obtained as 79% for the photocatalytic oxidation of low load grey water composition in the presence of microorganism and low anion content indicating that solution matrix and presence of smaller organic molecules enhanced the performance of photocatalytic oxidation process effectively. On the other hand, increasing ionic strength due to the

presence of anions (F^-, Cl^-, NO_2^-, NO_3^-, Br^-, SO_4^{2-} and PO_4^{3-}) caused inhibitory effect on the performance of photocatalytic oxidation process, thus considerable amount of UV_{254} removal of both high load and low load grey water samples with high anion content were achieved via initial adsorption at t=0 prior to photocatalytic oxidation.

4.5.2. Comparative Evaluation of DOC Removal of Different Grey Water Samples During Photocatalytic Oxidation

The mineralization efficiency as represented by calculated DOC removals of different grey water compositions as a result of photocatalytic oxidation were all shown in Figure 4.27. Following an irradiation time of 60 minutes, DOC removal tendencies were 57%, 54%, 36% and 36% for LLOM, LLGWLIC, LLGW and LLGWHIC respectively. On the other hand, DOC removal of different high load grey water samples during photocatalytic oxidation gave 45%, 38%, 42% and 27% removal of HLGW, HLGWLIC, HLGWHIC and HLOM respectively.

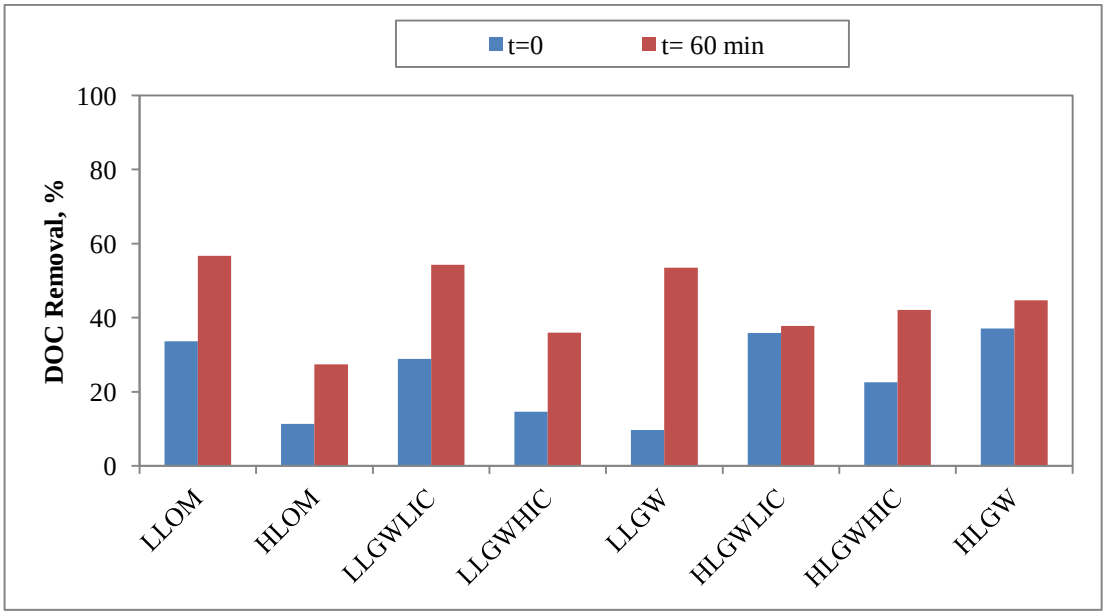

Figure 4.27. Comparative evaluation of DOC removal of different grey water samples.

Although, UV_{254} used as surrogate parameters instead of TOC and/or DOC content in terms of performance of photocatalytic oxidation processes, their removal efficiencies

displayed different results. This could be attributed to adsorption and/or photocatalytic oxidation of organic matter compounds of grey water samples having absorptivity at 254 nm (Huang et al., 2008). Another possibility of those results could be the transformation of some of the organic matters from unsaturated structure to saturated structure significantly by photocatalytic oxidation (Jin-hui, 2012).

4.5.3. Comparative Evaluation of Bacterial Removal of Different Grey Water Samples During Photocatalytic Oxidation

Removal of microorganisms from grey water was considered as one of the most important topics in terms of public health concerns related to grey water reuse. For this purpose, photocatalytic oxidation of two different synthetic grey water samples with different organic matter content were investigated in terms of removal of three different species of microorganisms ‘’Total Coliforms’’, ‘’Faecal Coliforms’’ and ‘’Faecal Streptococci’’ that could be encountered in real grey water samples. A comparative evaluation of removal efficiencies of those microorganisms from two different grey water samples were displayed in Figure 4.28. While TC, FC and FS were used as abbreviations stood for ‘’ Total Coliform’’, ‘’Faecal Coliform’’ and ‘’Faecal Streptococci’’, L and H were used as abbreviations for representing ‘’ Low Load Grey water’’ and ‘’High Load Grey Water’’.

The highest removal efficiencies for three types of bacteria, complete removal of total coliform and faecal coliform and 85% removal of faecal streptococci, were achieved by photocatalytic degradation of low load grey water composition. Removal efficiencies of bacterial content of high load grey water were found to be 45% for total colifrom and 30% removal for faecal streptococci which were considerably lower than results obtained for low load grey water except removal of faecal colifrom bacteria that reached up to 93%. This could be attributed to organic matter structure of high load grey water in which presence of higher organic molecules created a shielding effect on bacteria and prevented them from exposing to UV radiation and to hydroxyl radicals.

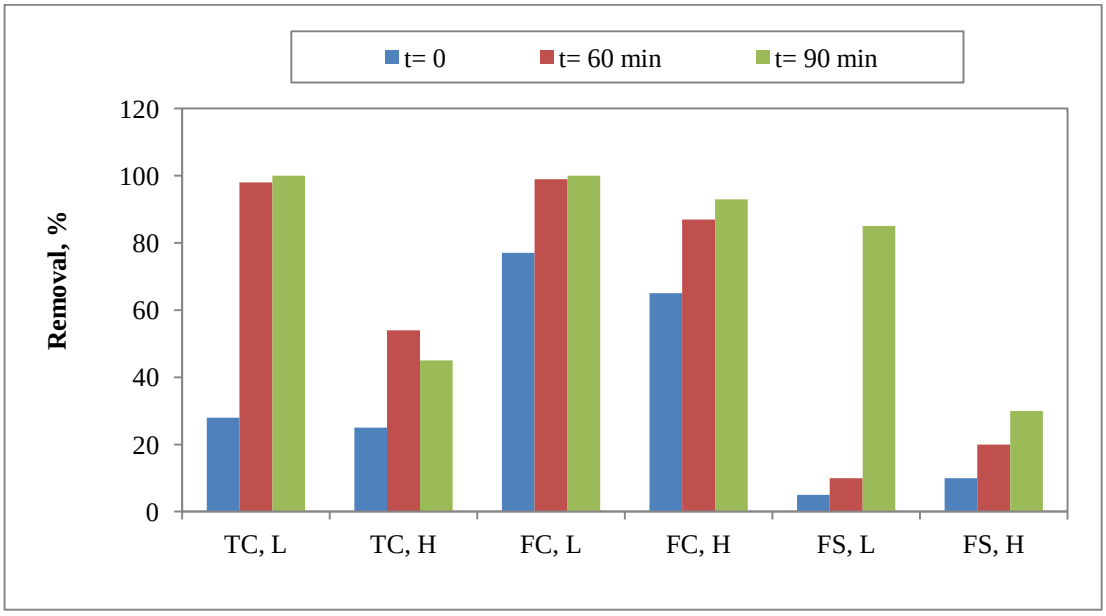

Figure 4.28. Comparative evaluation of two different synthetic grey water compositions in terms of bacterial inactivation.

Three different species of bacteria i.e. TC, FC and FS representing indicator organisms in grey water responded differently to the photocatalytic oxidation process by exhibiting different removal efficiencies under the specified experimental conditions (Figure 4.28). While an initial adsorption mechanism should be considered as important prior to the initiation of photocatalysis (as explained by t=0 condition at which attachment of bacteria to the oxide surface upon an instanteneous introduction of TiO_2), the inactivation rates achieved upon irradiation of 90 minutes could not be correlated to the observed adsorptive removal trend as expressed by the decreasing order of FC,L>FC,H>TC,L>TC,H>FS,H>FS,L. Based on the above presented results, the photocatalytic inactivation mechanism could be explained by Eley-Rideal mechanism rather than surface oriented Langmuir-Hinshelwood mechanism (Bekbolet and Araz, 1996; Bekbolet, 1997, Bekbolet, 2006). It should also be stated that the presence of varying amounts of organic fractions as well as anions could possibly interfere with the pH dependent electrostatic interactions prevailing between the negatively charged bacterial species, partially negatively charged humic moieties due to the deprotonation of the carboxylic groups (pKa 3-5), anions and the negatively/positively charged TiO_2 surface (pH_{zpc}=6.3) (Christl and Kretzschmar, 2001; Carp et al, 2004).

4.6. Kinetic Evaluation

Several kinetic models have been studied and proposed in order to express the mechanisms occur during photocatalytic oxidation reactions. Photocatalytic degradation of organic matter displays a basic declining logarithmic trend with respect to photocatalytic irradiation time in terms of UV-vis absorptivity (Bekbolet et al., 2002; Kerc et al., 2003a.b; Uyguner and Bekbolet, 2004; Rizzo et al., 2008). Due to the observed trend in the irradiation time dependent degradation profiles of all samples displaying the same basic declining logarithmic trend, photocatalytic oxidation data could be modeled by pseudo first-order kinetic equation using the specified UV-vis parameters as well as DOC. The pseudo first-order kinetic model is expressed by the following equation:

$$\text{Rate} = R = -dC/dt = k\,C \qquad (4.1)$$

R: Pseudo first-order rate ($m^{-1}min^{-1}$ in terms of UV-vis parameters or mg $L^{-1}min^{-1}$ in terms of DOC removal)

C: Specified UV-vis parameters of samples (m^{-1}) or DOC concentration of samples (mg Org C L^{-1})

t: Irradiation time (min)

k: pseudo first-order reaction rate constant (min^{-1})

The related half-life, ($t_{1/2}$) values could be assessed by the following equation;

$$t_{1/2} = 0.693/k \qquad (4.2)$$

In this section, kinetic evaluation of the specified UV-vis parameters ($Color_{436}$, UV_{365}, UV_{280} and UV_{254}), DOC content and bacterial content (TC, FC and FS) of the studied grey water samples were taken into consideration in terms of their removals elaborately. In this respect calculation and evaluation of pseudo first order reaction rate parameters as rate constants, half-life values and reaction rates were presented.

4.6.1. Kinetic Evaluation of the Removal of UV-vis Parameters

4.5.1.1. Kinetic Evaluation of Photocatalytic Oxidation of Humic Acid and Its Molecular Size Fractions. Pseudo first-order kinetic model parameters determined for the photocatalytic oxidation of humic acid and its molecular size fractions were all shown in Table 4.13 in detail. While degradation rate constants (k, min^{-1}) for UV_{254} decreased in the order of $3.39x10^{-2}$ min^{-1} for 30 kDa fraction> $1.07x10^{-2}$ min^{-1} for 0.45 μm filtered fraction> $0.93x10^{-2}$ min^{-1} for 100 kDa fraction, degradation rates were found to be 1.253 $m^{-1}min^{-1}$ for 0.45 μm filtered fraction> 0.730 $m^{-1}min^{-1}$ for 30 kDa fraction> 0.511 $m^{-1}min^{-1}$ for 100 kDa fraction respectively. Pseudo first-order degradation rate constants for UV_{280} removal were found to be $3.50x10^{-2}$ min^{-1}, $1.14x10^{-2}$ min^{-1} and $1.02x10^{-2}$ min^{-1} for 30 kDa fraction, 0.45 μm filtered fraction and for 100 kDa fraction. On the other hand, degradation rates for UV_{280} removal followed the order of 1.143 m^{-1} min^{-1} for 0.45 μm filtered fraction> 0.621 m^{-1} min^{-1} for 30 kDa fraction> 0.473 m^{-1} min^{-1} for 100 kDa fraction of humic acid. UV_{365} removal of humic acid and its molecular size fractions revealed the following degradation rate constants as $3.45x10^{-2}$ min^{-1}, $2.21x10^{-2}$ min^{-1} and $1.46x10^{-2}$ min^{-1} for 30 kDa fraction, 100 kDa fraction and 0.45 μm filtered fraction of humic acid respectively and gave the degradation rates 0.653 m^{-1} min^{-1}, 0.418 m^{-1} min^{-1} and 0.218 m^{-1} min^{-1} for 0.45 μm filtered fraction, 100 kDa fraction and 30 kDa fraction of humic acid.

Considering the decolourisation of humic acid and its molecular size fractions via photocatalysis, pseudo first order degradation rate constants for $Color_{436}$ removal were found to be $2.76x10^{-2}$ min^{-1}, $1.70x10^{-2}$ min^{-1} and $1.65x10^{-2}$ min^{-1} for 30 kDa fraction, 100 kDa fraction and 0.45μm filtered fraction of humic acid respectively as expected (Bebolet et al., 2002; Kerc et al., 2003; Uyguner and Bekbolet, 2010). On the other hand, photocatalytic degradation rates of $Color_{436}$ displayed the following order 0.368 m^{-1} $min^{-1}$for 0.45 μm filtered fraction of humic acid> 0.147 m^{-1} $min^{-1}$for 100 kDa fraction of humic acid> 0.047 m^{-1} min^{-1} for 30 kDa fraction of humic acid The reverse order attained in $Color_{436}$ removal rates should be attributed to the initial $Color_{436}$ values (22.31 m^{-1} for 0.45 μm filtered fraction of humic acid, 8.65 m^{-1} for 100 kDa fraction of humic acid and 2.57 m^{-1} for 30 kDa fraction of humic acid) rather than any operational factor during photocatalytic treatment as presented in Table 4.1.

Table 4.13. Pseudo-first-order kinetic model parameters of photocatalytic oxidation of different molecular size fractions of humic acid in terms of removal of UV-vis parameters.

	Absorbance (m^{-1})	k (min^{-1})	$t_{1/2}$ (min)	R (m^{-1} min^{-1})
UV_{254}				
0.45 μm ff*	117.07	$1.07x10^{-2}$	65	1.253
100 kDa fraction	54.92	$0.93x10^{-2}$	75	0.511
30 kDa fraction	21.52	$3.39x10^{-2}$	20	0.730
UV_{280}				
0.45 μm ff*	100.23	$1.14x10^{-2}$	61	1.143
100 kDa fraction	46.37	$1.02x10^{-2}$	68	0.473
30 kDa fraction	17.75	$3.50x10^{-2}$	20	0.621
UV_{365}				
0.45 μm ff*	44.76	$1.46x10^{-2}$	47	0.653
100 kDa fraction	18.92	$2.21x10^{-2}$	31	0.418
30 kDa fraction	6.3	$3.45x10^{-2}$	20	0.217
$Color_{436}$				
0.45 μm ff*	22.31	$1.65x10^{-2}$	42	0.368
100 kDa fraction	8.65	$1.70x10^{-2}$	41	0.147
30 kDa fraction	2.57	$2.76x10^{-2}$	25	0.071

*filtered fraction

Photocatalytic degradation rate constants could also be expressed by the half-life values varying from 20 to 75 minutes for UV_{254}, from 20 to 68 minutes for UV_{280}, from 20 to 47 minutes for UV_{365} and from 25 to 42 minutes for $Color_{436}$. Corresponding half-life values for the removal of all UV-vis parameters gave almost the same results (20 minutes) for the photocatalytic oxidation of 30 kDa fraction of humic acid (Table 4.13).

While degradation rates for UV_{254} and UV_{280} removal followed the insignificant order of 0.45 μm filtered fraction> 30 kDa fraction> 100 kDa fraction, UV_{356} and $Color_{436}$ removal rates displayed a decreasing order parallel to decreasing molecular size fractions as 0.45 μm filtered fraction> 100 kDa fraction> 30 kDa fraction.

Pseudo first-order kinetic parameters of $Color_{436}$ removal for photocatalytic oxidation of low load and high load grey water samples were calculated and displayed in Table 4.14. Photocatalytic oxidation of low load grey water samples gave the following trend of pseudo first-order reaction rate constants as $4.36x10^{-2}$ min^{-1} for LLGW> $2.59x10^{-2}$ min^{-1} for LLGWHIC> $2.29x10^{-2}$ min^{-1} for LLGWLIC. Parallel to reaction rate constants, .photocatalytic degradation rates gave the following decreasing order of 0.286 m^{-1} min^{-1} for LLGW> 0.223 m^{-1} min^{-1} for LLGWHIC> 0.207 m^{-1} min^{-1} for LLGWLIC. On the other hand, photocatalytic degradation rates of $Color_{436}$ were found to be 0.206 m^{-1} min^{-1} for HLGWLIC> 0.202 m^{-1} min^{-1} for HLGW> 0.135 m^{-1} min^{-1} for HLGWHIC. The corresponding half-life values were obtained in the range of 16-30 minutes for low load grey water samples and in the range of 58-88 minutes for high load grey water samples indicating that removal of 50% of $Color_{436}$ was considerably slower for the photocatalytic oxidation of high load grey water samples.

Table 4.14. Pseudo first-order kinetic model parameters of photocatalytic oxidation of different grey water compositions in terms of $Color_{436}$ removal.

	$Color_{436}$ (m^{-1})	k (min^{-1})	$t_{1/2}$ (min)	R (m^{-1} min^{-1})
LLGWLIC	9.02	$2.29x10^{-2}$	30	0.207
LLGWHIC	8.61	$2.59x10^{-2}$	27	0.223
LLGW	6.56	$4.36x10^{-2}$	16	0.286
HLGWLIC	17.18	$1.20x10^{-2}$	58	0.206
HLGWHIC	17.16	$7.89x10^{-3}$	88	0.135
HLGW	21.48	$9.42x10^{-3}$	74	0.202

Considering the photocatalytic decolourisation of different grey water samples composed of varying organic matter contents in terms pseudo first-order kinetic model parameters, the highest degradation rate obtained for low load grey water with low anion and microorganism content (LLGW) while the lowest photocatalytic degradation rate was attained for high load grey water with high anion content (HLGWHIC). It should also be emphasized that the respective initial $Color_{436}$ values were 6.56 m^{-1} and 17.16 m^{-1} for LLGW and HLGW respectively.

Comparative evaluation of pseudo first order kinetic model parameters of different grey water compositions were shown in Table 4.15 elaborately in terms of UV_{365} removal. The pseudo first order kinetics revealed rate constants as $3.85x10^{-2}$ min^{-1}, $2.55x10^{-2}min^{-1}$ and $3.85x10^{-2}$ min^{-1} for LLGW, LLGWHIC and LLGWLIC respectively. Following the same decreasing trend, photocatalytic degradation rates for the removal of UV_{365} were calculated as 0.565 m^{-1} min^{-1} for LLGW> 0.490 $m^{-}1$ min^{-1} for LLGWHIC> 0.378 $m^{-}1$ min^{-1} for LLGWLIC. Pseudo first-order reaction rate constants of high load grey water samples differed from data obtained for low load grey water samples by giving the following order of $1.09x10^{-2}$ min^{-1} for HLGWLIC> $7.54x10^{-3}$ min^{-1} for HLGW> $6.97x10^{-3}$ min^{-1} for HLGWHIC, thus photocatalytic reaction rates of UV_{365} revealed the same decreasing order of 0.404 m^{-1} min^{-1} for HLGWLIC> 0.347 m^{-1} min^{-1} for HLGW> 0.258 m^{-1} min^{-1} for HLGWHIC respectively. The related half life values were found to be in the range of 18-36 minutes for low load grey water samples and 64-99 minutes for high load grey water samples indicating that high load grey water samples needed to expose to photocatalytic irradiation two or three times longer than time needed for low load grey water samples for 50% removal of UV_{365}.

Table 4.15. Pseudo first-order kinetic model parameters of photocatalytic oxidation of different grey water compositions in terms of UV_{365} removal.

	UV_{365} (m^{-1})	k (min^{-1})	$t_{1/2}$ (min)	R (m^{-1} min^{-1})
LLGWLIC	19.6	$1.93x10^{-2}$	36	0.378
LLGWHIC	19.2	$2.55x10^{-2}$	27	0.490
LLGW	14.68	$3.85x10^{-2}$	18	0.565
HLGWLIC	37.02	$1.09x10^{-2}$	64	0.404
HLGWHIC	37.08	$6.97x10^{-3}$	99	0.258
HLGW	45.97	$7.54x10^{-3}$	92	0.347

Considering the kinetic evaluation of different grey water compositions in terms of UV_{365} removal, the highest degradation rate constants and degradation rates were achieved for the photocatalytic oxidation of low load grey water samples that showed consistency with the results obtained for kinetic evaluation of $Color_{436}$ removal previously.

Kinetic evaluation of different grey water samples for UV_{280} removal were presented in Table 4.16. Pseudo first-order reaction rate constants were determined as $3.27x10^{-2}$ min^{-1} for LLGW, $2.20x10^{-2}$ min^{-1} for LLGWLIC and $1.37x10^{-2}$ min^{-1} for LLGWHIC respectively. Following the same decreasing trend, photocatalytic degradation rates were found to be 1.195 m^{-1} min^{-1} for LLGW> 1.017 m^{-1} min^{-1} for LLGWHIC> 0.651 m^{-1} min^{-1} for LLGWLIC. Pseudo first-order reaction rate constants of high load grey water samples were found to be in the order of $9.11x10^{-3}$ min^{-1} for HLGWLIC> $5.96x10^{-3}$ min^{-1} for HLGW> $5.71x10^{-3}$ min^{-1} for HLGWHIC that were considerably lower than results obtained for low load grey water samples. Photocatalytic degradation rates of UV_{280} removal were found to be 0.805 m^{-1} min^{-1} for HLGWHIC> 0.649 m^{-1} min^{-1} for HLGW> 0.500 m^{-1} min^{-1} for HLGWHIC respectively. Half life values for UV_{280} were found to be in the range of 21-51 minutes for low load grey water samples and 76-121 minutes for high load grey water samples.

Table 4.16. Pseudo first-order kinetic model parameters of photocatalytic oxidation of different grey water compositions in terms of UV_{280} removal.

	UV_{280} (m^{-1})	k (min^{-1})	$t_{1/2}$ (min)	R (m^{-1} min^{-1})
LLGWLIC	47.54	$1.37x10^{-2}$	51	0.651
LLGWHIC	46.21	$2.20x10^{-2}$	32	1.017
LLGW	36.55	$3.27x10^{-2}$	21	1.195
HLGWLIC	88.39	$9.11x10^{-3}$	76	0.805
HLGWHIC	87.62	$5.71x10^{-3}$	121	0.500
HLGW	108.84	$5.96x10^{-3}$	116	0.649

It should also be indicated that for all of the grey water samples composed of varying contents of organic sub-fractions and anion contents, $Color_{436}$ and UV_{365} parameters followed a comparatively faster regime of degradation with respect to the photocatalytic removal of UV_{280}.. The reason could be explained by the reactivity of the aromatic core of humic moities represented by UV_{280} rather than the reactivity of color forming groups *i.e.* conjugated double bond systems and hetero atoms containing lone pair of electrons ($Color_{436}$ and UV_{365}) towards hydroxyl radical during photocatalysis.

Change in UV_{254} were determined and discussed separately in previous sections for several purposes. As a representative of organic matter content, evaluation of UV_{254} data from different perspectives comprised a great importance in order to elaborate results for further assessment. For these purposes, kinetic evaluation of photocatalytic oxidation of different grey water compositions were taken into consideration in terms of UV_{254} specifically.

Pseudo first-order kinetic model parameters of photocatalytic oxidation of different grey water compositions were presented in Table 4.17. UV_{254} degradation rate constants were found to be $3.12x10^{-2}$ min^{-1}, $2.18x10^{-2}$ min^{-1} and $1.29x10^{-2}$ min^{-1} for LLGW, LLGWHIC and LLGWLIC respectively. Decreasing trend of UV_{254} did not make any change in the order of photocatalytic degradation rates as followed 1.329 m^{-1} min^{-1} for LLGW> 1.193 m^{-1} min^{-1} for LLGWHIC> 0.727 m^{-1} min^{-1} for LLGWLIC. Compared to low load grey water samples, high load grey water samples exhibited rather smaller pseudo first-order reaction rate constants in the order of $8.50x10^{-3}$ min^{-1} for HLGWLIC> $5.54x10^{-3}$ min^{-1} for HLGW> $5.21x10^{-3}$ for HLGWHIC. On the other hand, high values of UV-vis parameters employed in determination of photocatalytic reaction rates caused enhancement of photocatalytic degradation rates of high load grey water samples.

Table 4.17. Pseudo first-order kinetic model parameters of photocatalytic oxidation of different grey water compositions in terms of UV_{254}.

	UV_{254} (m^{-1})	k (min^{-1})	$t_{1/2}$ (min)	R (m^{-1} min^{-1})
LLGWLIC	56.38	$1.29x10^{-2}$	54	0.727
LLGWHIC	54.74	$2.18x10^{-2}$	32	1.193
LLGW	42.59	$3.12x10^{-2}$	22	1.329
HLGWLIC	103.5	$8.50x10^{-3}$	82	0.880
HLGWHIC	102.58	$5.21x10^{-3}$	133	0.534
HLGW	126.98	$5.54x10^{-3}$	125	0.703

Photocatalytic removal rates obtained according to the first-order kinetic model showed that photocatalytic oxidation of low load grey water with microorganism and low

anion content gave the most effective results in terms of removal of UV_{254} parameter. Although similar conditions existed for LLGW and HLGW except organic matter content, degradation rate of LLGW obtained as two times higher than degradation rate of HLWG that could be attributed to presence of larger molecules in anions and bacteria together HLGW composition, thus hydroxyl radicals became inadequate for the degradation of those large molecules due to competitive conditions occurred among grey water components. Similar to conditions occurred for LLGW and HLGW, photocatalytic degradation rate constants of LLGWHIC and HLGWHIC were noticeably different from each other On the other hand, although their organic matter content were different from each other, photocatalytic degradation rate constants of LLGWLIC and HLGWLIC expressed closer results indicating that presence of specific anion concentration in the low range caused enhancement of photocatalytic oxidation process whether organic molecules were large or small.

4.6.2. Kinetic Evaluation of DOC Removal

Although UV_{254} is interchangeably measured with TOC/DOC as surrogate parameter to represent the natural organic matter in waters, it gives limited information about organic constitutes of water and wastewater samples that have UV absorptivity at 254 nm (Uyguner Demirel and Bekbolet, 2011). In addition, abundance and diversity of organic matter make characterization of the synthetic grey water samples more complicated and inadequate. Thus, UV-vis and fluorescence spectroscopic parameters representing the chemical and structural properties of organic matter content could also be used in accordance with DOC removals during photocatalytic oxidation process.

Kinetic evaluation of different grey water compositions in terms of DOC removal was presented in Table 4.18. Pseudo first order degradation rate constants (k, min^{-1}) were found to be $8.3x10^{-3}$ min^{-1} for LLGW, $1.2x10^{-2}$ min^{-1} for LLGWLIC and $7.15x10^{-3}$ min^{-1} for LLGWHIC in terms of DOC removal of samples. Although pseudo first order degradation rate constants displayed the decreasing order of LLGWLIC> LLGWHIC> LLGW, initial DOC concentrations of samples changed the order of photocatalytic degradation rates as 0.090 mg L^{-1} min^{-1} for LLGW> 0.080 mg L^{-1} min^{-1} for LLGWLIC> 0.046 mg L^{-1} min^{-1} for

LLGWHIC. On the other hand, k values calculated for high load grey water samples displayed the following order of $8.51x10^{-3}$ min^{-1} for HLGWHIC> $7.40x10^{-3}$ min^{-1} for HLGWLIC> $5.70x10^{-3}$ for HLGW which were in parallel with pseudo first-order reaction rates of high load grey water samples obtained as 0.110 mg L^{-1} min^{-1} for HLGWHIC> 0.097 mg L^{-1} min^{-1} for HLGWLIC> 0.075 mg L^{-1} min^{-1} for HLGW. The corresponding half life values were obtained in the range of 57-97 minutes for low load grey water samples and 12-94 minutes for high load grey water samples.

Table 4.18. Comparative evaluation of pseudo-first-order kinetic model parameters of different grey water samples during photocatalytic oxidation in terms of DOC removal.

	DOC (mg L^{-1})	k (min^{-1})	$t_{1/2}$ (min)	R (mg L^{-1} min^{-1})
LLOM	6.9	$1.31x10^{-2}$	53	0.090
LLGW	10.83	$8.30x10^{-3}$	83	0.090
LLGWLIC	6.65	$1.21x10^{-2}$	57	0.080
LLGWHIC	6.39	$7.15x10^{-3}$	97	0.046
HLOM	14.9	$5.53x10^{-3}$	125	0.082
HLGW	13.20	$5.70x10^{-3}$	122	0.075
HLGWLIC	13.05	$7.40x10^{-3}$	94	0.097
HLGWHIC	12.88	$8.51x10^{-3}$	81	0.110

Effect of solution matrix complexity on the pseudo-first order kinetic model parameters were observed and discussed by monitoring differences among different grey water samples in terms of removal of organic matter content expressed by DOC. Variety of components caused enhancing impact on the kinetic evaluation of low load grey water samples while high load grey water with microorganism and low anion content displayed the lowest results for pseudo first-order kinetic parameters. It should also be mentioned that low load grey water samples contained 100 kDa fraction of untreated humic acid whereas high load grey water samples contained partially oxidized humic fractions prior to the addition of bacterial species as well as anions.

4.6.3. Kinetic Evaluation of Bacterial Inactivation

Among other advanced oxidation technologies, advantageous properties of photocatalytic oxidation process have been mentioned in detail previously. One of the most important aspects of photocatalytic oxidation is its useful application in photocatalytic bactericidal action on bacteria and viruses effectively. Kinetic considerations of photocatalytic inactivation of bacteria have been widely studied by many researchers in detail (Matsunaga et al., 1985; Bekbolet and Araz, 1996; Bekbolet, 1997; Bekbolet, 2006; Chen et al., 2009; Malato et al., 2009, Chong et al., 2010). The basis of methods estimating the destruction of microorganisms was mainly introduced by Chick (1908) who postulated the close similarity between microbial inactivation by chemical disinfectants and chemical reactions. The related law rate could be expressed in the following equation:

$$\text{Rate, } r = -kN \tag{4.3}$$

r: The inactivation rate (organism killed/volume-time)

N: Concentration of microorganisms (Number of microorganisms/volume)

An exponential decay in microorganism count was obtained in batch systems, representing the inactivation kinetic model with reaction rate constant k as constant. Therefore, photocatalytic inactivation kinetics of microorganisms could also be evaluated by the application of the pseudo first order kinetic model.

Comparative evaluation of the bacterial inactivation profiles of different grey water samples were presented in Figure 4.29A for low load grey water and in Figure 4.29B for high load grey water particularly. While removal of TC and FC gave the basic exponential declining trend with respect to irradiation time, resistance of FS bacteria against photocatalytic oxidation displayed considerably different removal trend. FS bacteria expressed an initial resistance to photocatalytic oxidation in the presence of both solution matrix components and other bacterial consortium. For an irradiation period of 30 minutes a slight deviation was attained in the removal of FS for low loaded grey water. A logarithmic declining trend could be observed up to 70 minutes of irradiation conditions. A

rapid removal was evident after 70 minutes and total elimination of FS bacteria could be reached upon irradiation period of 80 minutes. For an irradiation period of 90 minutes, in the presence of high organic content and low anion medium, no significant removal of FS (5%) was observed. A substantial drop (72%) was attained upon further irradiation conditions of 150 minutes and 75% removal was attained after 180 minutes of irradiation time. The reason could be attributed both the presence of organic loading as well as competitive interaction of TC and FC bacteria.

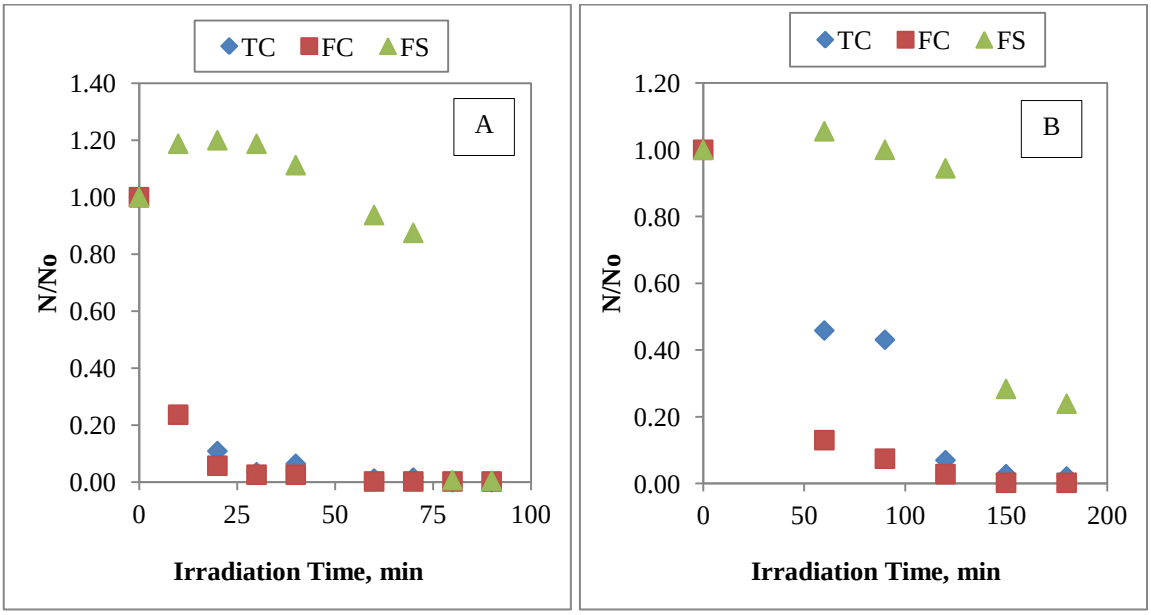

Figure 4.29. Normalized bacterial concentration profiles for low load grey water (29A) and for high load grey water (29B) with respect to photocatalytic irradiation time.

Pseudo first-order kinetic parameters calculated for different grey water compositions were displayed in Table 4.19 in terms of removal of total coliforms (TC) and faecal coliforms (FC) specifically. While photocatalytic inactivation rate constants of low load grey water sample were found to be 8.84×10^{-2} min for TC and 6.54×10^{-2} min^{-1} for FC, high load grey water revealed comparatively lower photocatalytic inactivation rate constants as 2.26×10^{-2} min^{-1} for TC and 3.23×10^{-2} min^{-1} for FC. The insignificant trend attained for FS removal could not be fitted into pseudo first-order kinetic modeling, thus determination of pseudo first-order kinetic parameters was not accessed for FS. Corresponding half-life values for the inactivation of TC found to be 8 and 30 minutes for LLGW and for HLGW indicating that 50% removal of TC took four times longer for HLGW than time required

for 50% removal of TC present in LLGW. In addition, bactericidal activity of photocatalytic oxidation process revealed the following half-life values for the removal of FC as 11 minutes for LLGW and 21 minutes for HLGW showing that time requirement for 50% removal of FC was almost two times higher for HLGW than LLGW. All of the results could be attributed to the impact of organic matter loading of grey water samples that photocatalytic inactivation of bacteria enhanced in the presence of smaller molecules while degradation of larger molecules consumed more hydroxyl radicals and made them deficient for the effective removal of bacteria.

Table 4.19. Kinetic evaluation of bacterial inactivation of low load and high load grey water compositions.

	Total Coliform, TC			Faecal Coliform, FC		
	k (min^{-1})	$t_{1/2}$ (min)	r (CFU min^{-1})	k (min^{-1})	$t_{1/2}$ (min)	r (CFU min^{-1})
LLGW	$8.84x10^{-2}$	8	$6.4x10^{3}$	$6.54x10^{-2}$	11	$3.5x10^{3}$
HLGW	$2.26x10^{-2}$	30	$1.2x10^{3}$	$3.23x10^{-2}$	21	$1.2x10^{3}$

The reactivity of hydroxyl radical towards organic matter was found to be more significant than the bacterial inactivation rate. Under similar irradiation conditions (60 minutes) for LLGW, the removal of organic matter was 36% whereas almost complete removals of TC and FC (100%) and a very minor elimination of FS (6%) were attained. On the other hand, for HLGW, comparatively higher DOC removal (45%) was attained following by considerably lower removals of TC (54%) and FC (87%) and almost no inactivation of FS. The removal rate of TC in LLGW was found to be considerably higher than the rate attained for the removal of TC in HLGW. The difference observed in the inactivation rates of TC and FC could be accepted as related to the initial bacterial load in these two different grey water samples. In a similar fashion, FC inactivation rates were also found to be different under different grey water compositions. The same rate of inactivation attained for TC and FC for HLGW could also be explained by the reaction mechanism in relation to the initial bacterial load effect.

5. CONCLUSIONS

Photocatalytic oxidation of grey water has been investigated from several perspectives with the aim of assessing the performance of the system in case of compositional changes occurred. To this end, diversified synthetic grey water samples were prepared and classified according to their compositions prior to photocatalytic oxidation. Consequently, efficiency of photocatalytic oxidation on grey water treatment was evaluated by monitoring and determining selected parameters and their fluctuations over time. UV-vis and fluorescence spectroscopic properties, DOC contents and functions of these parameters defined as specific parameters were taken into consideration to observe the changes in organic fraction of grey water samples. Moreover, potential disinfection mechanism of photocatalytic oxidation process was examined by determination of bacterial inactivation of grey water samples in terms of removal percentages and kinetic considerations.

Photocatalytic oxidation profiles of all samples including humic acid solutions and thier molecular size fractions and different synthetic grey water compositions exhibited general monotonous declining trend in terms of UV-vis and fluorescence propoerties as well as DOC contents with respect to increasing photocatalytic irradiation time. The changes observed in selected parameters via photocatalysis fluctuated with regard to varying solution matrix conditions. A general decreasing order of 0.45 μm filtered fraction> 100 kDa fraction> 30 kDa fraction was attained with respect to UV-vis and fluorescence spectral parameters. Compositional differences of grey waters revealed following order of selected UV-vis parameters after they were subjected to photocatalysis for the same irradiation times as HLGW> HLGWHIC> HLGWLIC> LLGWLIC> LLGWHIC> LLGW respectively. DOC normalized UV-vis and fluorescence parameters also gave crucial information about nature and mechanisms of organic matter and color forming moieties of all samples specifically. Removal percentages of $SUVA_{254}$, $SUVA_{280}$ and $SUVA_{365}$ increased with decreasing molecular size fractions and expressed in the order of 30 kDa fraction> 100 kDa fraction> 0.45 μm filtered fraction fraction respectively. In addition, the removal of the specific UV-vis parameters followed the order of LLGW> HLGW> LLGWH> LLGWHIC> LLGWLIC> HLGWLIC trend respectively. A

significant order of SFI_{emis} and SFI_{sync} could not be expressed for the photocatalytic oxidation of grey water compositions with regard to irregular fluctuations observed.

Comparative evaluation of the removal of selected UV-vis parameters ($Color_{436}$, UV_{365}, UV_{280} and UV_{254}) expressed the removal perctanges in the order of LLGW> LLGWHIC> LLGWLIC> HLGWLIC> HLGW> HLGWHIC respectively. It was inferred from the removal percantages of selected UV-vis parameters that impact of chosen components of grey water compositions would be either inhibitory or enhacing on photocatalytic oxidation process. Consequently, higher concentrations of anions contributed higher removal percentages of selected UV-vis parameters in low load grey water compositions while anion strength inhibited photocatalytic activity of TiO_2 in the presence of higher organic molecules. On the other hand, selecting anion concentration in the low range revealed the highest removal percentages of UV-vis parameters for HLGWLIC whereas the lowest removal percentages were achieved for LLGWLIC by inhibiting the performance of photocatalytic oxidation process. DOC removal percentages followed the order of LLGWLIC> LLGW> HLGW> HLGWLIC> LLGWHIC that was considerably different from UV_{254} removal data obtained for different grey water compoitions. Removal percentages of selected UV-vis parameters and DOC contents of grey water compositions gave the order of $Color_{436}$> UV_{365}> UV_{280}> UV_{254}> DOC respectively indicating the higher oxidative removal tendency of color forming moities and aromatic groups rather than degradation of organic matter content via photocatalysis.

Kinetic evaluation of humic acid solutions and their molecular size fractions and various grey water compositions were taken into consideration to signify the application of photocatalysis for the removal of selected parameters (UV-vis parameters, DOC and bacteria) intentionally. Pseudo first-order degradation rates for the removal of UV_{254}, UV_{280}, UV_{365}, $Color_{436}$ and DOC were determined. Humic acid solution and its molecular size fractions followed 0.45 μm filtered fraction> 30 kDa fraction> 100 kDa fraction trend for the removal of UV_{254} and UV_{280} whereas photocatalytic degradation rates of UV_{365} and $Color_{436}$ decreased in the order of 0.45 μm filtered fraction> 100 kDa fraction> 30 kDa fraction respectively. Considering the dependence of kinetics and mechanisms of oxidative degradation on solution matrix, pseudo first-order degradation rates of different grey water samples were expressed in the order of LLGW> LLGWHIC> HLGWLIC> LLGWLIC>

HLGW> HLGWHIC in terms of UV_{365}, UV_{280} and UV_{254} parameters respectively. On the other hand, $Color_{436}$ removal followed LLGW> LLGWHIC> LLGWLIC> HLGWLIC> HLGW> HLGWHIC trend respectively.

Considering the bacterial inactivation of LLGW and HLGW, the most satisfactory results for the removal of total coliforms (TC), faecal coliforms (FC) and faecal streptecocci (FS) were attined for LLGW via photocatalytic oxidation that could be attributed to impact of lower organic matter loading whereas higher organic loading lead to retardation of bacterial inactivation in HLGW. However, substantial removal of FC bacteria was achieved for both LLGW and HLGW indicating that photocatalytic inactivation of FC bacteria was irrespective of organic matter loading. Inactivation profiles of TC, FC and FS bacteria were comparatively different from each other even in the same medium. While rapid removal of TC and FC was attained in the early stages of photocatalytic oxidation process, effective removal of FS was achieved after longer periods of photocatalytic irradiation time.

In conclusion, photocatalytic oxidation process revealed the most effective results for low load grey water with microorganism and low anion content in terms of the removals of all of the selected parameters specifically. High load grey water with high anion content revealed the lowest degradation efficiency that could be explained by the retardation effects due to the presence of higher molecular size humic fractions as well as high anion contents. It could be stated that under the specified experimental conditions covering a wide range of grey water compositions, photocatalytic treatment could hold significance form practical application point of view.

REFERENCES

Alberts, J. J., Takacs, M., Egeberg, P. K., 2002. Total luminescence spectral characteristics of natural organic matter (NOM) size fractions as defined by ultrafiltration and high performance size exclusion chromatography (HPSEC). Organic Geochemistry, 33, 817-828.

Al-Jayyousi, O. R., 2003. Greywater reuse: towards sustainable water management. Desalination, 156, 181-192.

Al-Jayyousi, O. R., 2004. Greywater reuse: knowledge management for sustainability. Desalination, 167, 27-37.

Aykac, H., 2011. Semiconductor Assisted Photodegradation of Humic Acid using Fe-doped TiO_2. M.S. Thesis, Boğaziçi University.

Banu, J. R., Anandan, S., Kaliappan, S., Yeom, I., 2008. Treatment of dairy wastewater using anaerobic and solar photocatalytic methods. Solar Energy, 82, 812-819.

Bekbolet, M., 1997. Photocatalytic bactericidal activity of TiO_2 in aqueous suspensions of *E. coli*. Water Science and Technology, 35, 95-100.

Bekbolet, M., Araz, C. V., 1996. Inactivation of *Escherichia coli* by photocatalytic oxidation. Chemosphere, 32, 959-965.

Bekbolet, M., Suphandag, A. S., Uyguner, C. S., 2002. An investigation of the photocatalytic efficiencies of TiO_2 powders on the decolourisation of humic acids. Journal of Photocahemistry and Photobiology A: Chemistry, 148, 121-128.

Bekbolet, M., 2006. Photocatalytic Inactivation of Microorganisms in Drinking Water. In: Advances in Control of Disinfection By-Products, 1-21, Nove Science Publishers, Inc.

Burkhard, R., Deletic, A., Craig, A., 2000. Techniques for water and wastewater management: a review of techniques and their integration in planning. Urban Water, 2, 197-221.

Carp, O., Huisman, C. L., Reller, A., 2004. Photoinduced reactivity of titanium dioxide. Solid State Chemistry, 32, 33–177.

Challiou, K., Gérente, C., Andrès, Y., Wolbert, W., 2011. Bathroom grey water characterization and potential treatments for reuse. Water Air Soil Pollution, 215, 31-42.

Chen, F., Yang, X., Xu, F., Wu, Q., Zhang, Y., 2009. Correlation of bactericidal effect and organic matter degradation of TiO_2 Part I: observation of phenomena. Environmental Science and Technology, 43, 1180-1184.

Chick, H., 1908. Investigation of the laws of disinfection. Journal of Hygiene (British), 8, 92.

Chin, W. H., 2009. Greywater Treatment by Fenton, photo-Fenton and UVC/H_2O_2 Processes. Ph.D Thesis, School of Civil, Environmental and Chemical Engineering RMIT University, Melbourne.

Chin, W. H., Roddick, F. A., Harris, F. L., 2009. Grey water treatment with UV/H_2O_2. Water Research, 43, 3940-3947.

Chong, M. N., Jin, B., Chow, C. W. K., Saint, C., 2010. Recent developments in photocatalytic water treatment technology: A review. Water Research, 44, 2997-3027.

Christova-Boal D., Eden R.E., McFarlane S., 1996. An investigation into greywater reuse for urban residential properties. Desalination, 106, 391–397.

Christl, I., Kretzschmar, R., 2001. Relating ion binding by fulvic and humic acids to chemical composition and molecular size. Proton binding. Environmental Science and Technology, 35, 2512–2517.

Degirmenci Ilhan, E., 2010. Assessment of Molecular Size Distribution Effects on the Non Selective Oxidation of Trace Metal Humic Acid Binary System. M.S. Thesis, Boğaziçi University.

Dixon, A. M., Butler, D., Fewkes, A., 1999. ‘’Guidelines for grey water reuse: health issues’’, http://www.greywateralliance.org/guidelines-for-gw-reuse.pdf (Accessed December 2010).

Donner, E., Eriksson, E., Revitt, D. M., Scholes, L., Lützhøft, H H-C, Ledin, A., 2010. Presence and fate of priority substances in domestic grey water treatment and reuse systems. Science of the Total Environment, 408, 2444-2451.

Elmitvalli, T., Otterpohl, R., 2007. Anaerobic biodegradability and treatment of grey water in up-flow anaerobic sludge blanket (UASB) reactor. Water Research, 41, 1379-1387.

Eriksson E., 2002. Potential and Problems Related to Reuse of Water in Households. Ph.D Thesis. Technical University of Denmark.

Eriksson, E., Auffarth, K., Henze, M., Ledin, A., 2002. Characteristics of grey wastewater. Urban Water, 4, 85-104.

Eriksson, E., Auffarth, K.P.S., Eilersen, A.M., Henze, M., Ledin, A., 2003. Household chemicals and personal care products as sources for xenobiotic organic compounds in grey wastewater. Water SA, 29, 135–146.

Eriksson, E., Andersen, H. R., Madsen, T. S., Ledin, A., 2009. Grey water pollution, variability and loadings. Ecological Engineering, 35, 661-669.

Eriksson, E., Donner, E., 2009. Metals in grey water: sources, presence and removal efficiencies. Desalination, 248, 271-278.

Friedler, E., Galil, N. I., 2003. On-site grey water reuse in multi-storey buildings: sustainable solution for water saving, 2nd International Conference on Efficient Use and Management of Urban Water Supply, 2-4 April 2003, Tenerife, Canary Islands, Spain.

Friedler, E., Kovalio, R., Galil, N I., 2005. On-site grey water treatment and reuse in multi-storey buildings. Water Science and Technology, 51, 187-194.

Friedler, E., Hadari, M., 2006. Economic feasibility of on-site grey water reuse in multi-storey buildings. Desalination, 190, 221-234.

Friedler, E., Catz, I., Dosortez, C. G., 2008. Chlorination and coagulation as pre-treatments for grey water desalination. Desalination, 222, 38-49.

Fujishima, A., Rao, T. N., Tryk, D. A., 2000. Titanium dioxide photocatalysis. Journal of Photochemistry and Photobiology C: Photochemistry Reviews, 1, 1–21.

Gaya, U. I., Abdullah, A. H., 2008. Heterogeneous photocatalytic degradation of organic contaminants over titanium dioxide: a review of fundamentals, progress and problems. Journal of Photochemistry and Photobiology C, 9, 1-12.

Ghaly, M. Y., Jamil, T. S., El-Seesy, I. E., Souaya, E. R., Nasr, R. A., 2011. Treatment of highly polluted paper mill wastewater by solar photocatalytic oxidation with synthesized nano TiO_2. Chemical Engineering Journal, 168, 446-454.

Ghisi, E., Ferreira, D. F., 2007. Potential for potable water savings by using rainwater and grey water in a multi-storey residential building in southern Brazil. Building and Environment, 42, 2512-2522.

Gilboa, Y., Friedler, E., 2008. UV disinfection of RBC treated light grey water effluent: Kinetics, survival and regrowth of selected microorganisms. Water Research, 42, 1043-1050.

Goddard, M., 2006. Urban grey water reuse in at the D'LUX Development. Desalination, 188, 135-140.

Godfrey, S., Labhasetwar, P., Wate, S., 2009. Grey water reuse in residential schools in Madhya Pradesh, India-a case study of cost-benefit analysis. Resource, Conservation and Recycling, 53, 287-293.

Godinez, I. G., Darnault, C. J. G., 2011. Aggregation and transport of nano-TiO_2 in saturated porous media: Effect of pH, surfactants and flow velocity. Water Research, 45, 839-851.

Goslan, E. H., Voros, S., Banks, J., Willson, D., Hillis, P., Cample, A. T., Parsons, S. A., 2004. A model for predicting dissolved organic carbon distribution in a reservoir water using fluorescence spectroscopy. Water Research, 38, 783-791.

Gross, A., Shmueli, O., Ronen, Z., Raveh, E., 2007. Recycled vertical flow constructed wetland (RVFCW) –a novel method of recycling grey water for irrigation in small communities and households. Chemosphere, 66, 916-923.

Gual, M., Moià, A., March, J. G., 2008. Monitoring of an indoor pilot plant for osmosis rejection and grey water reuse to flush toilets in a hotel. Desalination, 219, 81-88.

Gulyas, H., 2007. Grey water Reuse: concepts, benefits, risks and treatment technologies. International Conference on Sustainable Sanitation: 'Food and Water Security in Latin America'. Fortaleza, Ceará, Brazil, 25-28 November, 2007.

Gulyas, H., Jain, H. B., Susanto, L. A., Malekpur, M., Harasiuk, K., Krawcyzk, I., Choromanski, P., Furmanska, M., 2004. Solar photocatalytic oxidation of pretreated wastewaters: laboratory scale generation of design data for technical-scale double-skin sheet reactors. Environmental Technology, 26, 501-514.

Gulyas, H., Choromanski, P., Muelling, N., Furmanska, M., 2009. Toward chemical-free reclamation of biologically pretreated greywater: solar photocatalytic oxidation with powdered activated carbon. Journal of Cleaner Production, 17, 1223–1227.

Gulyas, H., Reich, M., Otterpohl, R., 2011. Organic micropollutants in raw and treated grey water: a preliminary investigation. Urban Water Journal, 8, 29-39.

Günther, F., 2000. Wastewater treatment by grey water separation: Outline for a biologically based grey water purification plant in Sweden. Ecological Engineering, 15, 139-146.

Halalsheh, M., Dalahmeh, S., Sayed, M., Suleiman, W., Shareef, M., Mansour, M., Safi, M., 2008. Grey water characteristics and treatment options for rural areas in Jordan. Bioresource Technology, 99, 6635-6641.

Hatchard, C., G., Parker, C., A., 1956. A new sensitive chemical actinometer. II. Potassium ferrioxalate as a standard chemical actinometer, Proceedings of the Royal Society of London. Series A, Mathematical and Physical Sciences, 235, 518–536.

Henkel, J., Lemac, M., Wagner, M., Cornel, P., 2009. Oxygen transfer in membrane bioreactors treating synthetic grey water. Water Research, 43, 1711-1719.

Henriques, J. J., Louis, G. E., 2011. A decision model for selecting sustainable drinking water supply and grey water reuse systems for developing communities with a case study in Cimahi, Indonesia. Journal of Environmental Management, 92, 214-222.

Hernández Leal, L., Temmink, H., Zeeman, G., Buismann, C. J. N., 2011. Characterization and anaerobic biodegradability of grey water. Desalination, 270, 111-115.

Hoffmann , M.R., Martin, S.T., Choi, W., Bahnemann, D.,1995. Environmental applications of semiconductor photocatalysis. Chemical Reviews, 95, 69-96.

Hourlier, F., Masse, A., Jaouen, P., Lakel, A., Gerente, C., Faur, C., Le Cloirec P., 2010. Formulation of synthetic grey water as an evaluation tool for wastewater recycling technologies. Environmental Technology, 31, 215-223.

Huang, X., Leal, M., Li, Q., 2008. Degradation of natural organic matter by TiO_2 photocatalytic oxidation and its effect on fouling low-pressure membranes. Water Research, 42, 1142-1150.

Huelgas, A., Funamizu, N., 2010. Flat-plate submerged membrane bioreactor for the treatment of high load grey water. Desalination, 250, 162-166.

Jamrah, A., Al-Futaisi, A., Prathapar, S., Al-Harrasi, A., 2008. Evaluating grey water reuse potential for sustainable water resources management in Oman. Environmental Monitoring Assessment, 137, 315-327.

Jefferson, B., Laine, A., Parsons, S., Stephenson, T., Judd, S., 1999. Technologies for domestic wastewater recycling. Urban Water, 1, 285-292.

Jefferson, B., Burgess, J. E., Pichon A., Harkness, J., Judd, S. J., 2001. Nutrient addition to enhance biological treatment of grey water. Water Research, 35, 2702-2710.

Jin-hui, Z., 2012. Research on UV/TiO_2 photocatalytic oxidation of organic matter in drinking water and its influencing factors. Procedia Environmental Sciences, 12, 445-452.

Kerc, A., Bekbolet, M., Saatci, A. M., 2003a. Effect of partial oxidation by ozonation on the photocatalytic degradation of humic acids. International Journal of Photoenergy, 5, 75-80.

Kerc, A., Bekbolet, M., Saatci, A. M., 2003b. Sequential oxidation of humic acids by ozonation and photocatalysis. Ozone Science and Engineering, 25, 497-504.

Kim, R. H., Lee, S., Jeong, J., Lee, J. H., Kim, Y. K., 2007. Reuse of grey water and rainwater using fiber filter media and metal membrane. Desalination, 202, 326-332.

Kim, J., Song, I., Oh, H., Jong, J., Park, J., Choung, Y., 2009. A laboratory-scale grey water treatment system based on membrane filtration and oxidation process-characteristics of a grey water from a residential complex. Desalination, 238, 347-357.

Kraume, M., Scheumann, R., Baban, A., El Hamouri, B., 2010. Performance of a compact submerged membrane sequencing batch reactor (SM-SBR) for grey water treatment. Desalination, 250, 1011-1013.

Lesjean, B., Gnirss, R., 2006. Grey water treatment with a membrane bioreactor operated at low SRT and low HRT. Desalination, 199, 432-434.

Li, F., Wichmann, K., Otterpohl, R., 2009. Review of the technological approaches for grey water treatment and reuses. Science of the Total Environment, 407, 3439-3449.

Li, Z., Boyle, F., Reynolds, A., 2010. Rainwater harvesting and grey water treatment systems for domestic application in Ireland. Desalination, 260, 1-8.

Linsebigler, A. L., Lu, G., Yates, Jr., J. T., 1995. Photocatalysis on TiO_2 surfaces: principles, mechanisms and selected results. Chemical Reviews, 95, 735-758.

Ludwick, C. Y., Byrne, H. E., Stokke, J. M., Chadik, P. A., Mazyck, D.W., 2011. Performance of silica-titania carbon composites for photocatalytic degradation of gray water. Journal of Environmental Engineering, 137, 38-45.

Malato, S., Blanco, J. A, Vidal, A., Diego, A. O., Maldonado, M. I., Aceres, J. C., and Gernjak, W., 2003. Applied studies in solar photocatalytic detoxification: an overview.Solar Energy, 75, 329-336.

Malato, S., Fernández-Ibáñez, P., Maldonado, M. I., Blanko, J., Gernjak, W., 2009. Decontamination and disinfection of water by solar photocatalysis: Recent overviews and trends. Catalysis Today, 147, 1-59.

Mandal, D., Labhastewar, P., Dhone, S., Dubey, A. S., Shinde, G., Wate, S., 2011. Water conservation due to grey water treatment and reuse in urban setting with specific context to developing countries. Resources, Conservation and Recycling, 55, 356-361.

March, J. G., Gual, M., Orozco, F., 2004. Experiences on grey water reuse for toilet flushing in a hotel (Mallorca Island, Spain). Desalination, 164, 241-247.

March, J. G., Gaul, M., 2009. Studies on chlorination of grey water. Desalination, 249, 317-322.

Marco, A., Esplugas, S., Saum, G., 1997. How and why combine chemical and biological processes for wastewater treatment. Water Science and Technology, 35, 321–327.

Matsunaga, T., Tomoda, R., Nakajima, T., Wake, H., 1985. Photo-electrochemical sterilization of microbial cells by semiconductor powders. FEMS Microbiological Letters, 29, 211-214.

Merz, C., Scheumann, R., El Hamouri, B., Kraume, M., 2007. Membrane bioreactor technology for the treatment of grey water from a sports and leisure club. Desalination, 215, 37-43.

Milori, D. M. B. P., Bayer, C., Bagnato, V S., Mielniczuk, J., Martin-Neto, L., 2002. Humification degree of soil humic acids determined by fluorescence spectroscopy. Soil Science, 167, 739-749.

Mozia, S., 2010. Photocatalytic membrane reactors (PMRs) in water and wastewater treatment. A review. Separation and Purification Technology, 73, 71-91.

Murray, C.A., Parsons, S.A., 2004. Comparison of AOPs for the removal of natural organic matter: Performance and economic assessment. Water Science and Technology, 49, 267-272.

Mayer, P.W., DeOreo, W.B., Opitz, E., Kiefer, J., Dziegielewski, B., Davis, W., Nelson,. J.O., 1999. Residential End Uses of Water. Final Report. American Water Works Association Research Foundation. Denver, Colorado.

Nghiem, L. D., Oschmann, N., Schäfer, A. I., 2006. Fouling in grey water recycling by direct ultrafiltration. Desalination, 187, 283-290.

Nolde, E., 1999. Grey water reuse systems for toilet flushing in multi-storey buildings-over ten years experience in Berlin. Urban Water, 1, 275-284.

Ollis, D.F., 1985. Contaminant degradation in water. Environmental Science and Technology, 19, 480–484.

Ollis, D.F., Turchi, C., 1990. Heterogeneous photocatalysis for water purification: Contaminant mineralization kinetics and elementary reactor analysis. Environmental Progress, 9, 229–234.

Oschmann, N., Nghiem, L. D., Schäfer, A. I., 2005. Fouling mechanisms of submerged ultrafiltration membranes in grey water recycling. Desalination, 179, 215-223.

Ottoson, J., Strensröm, T. A., 2003. Faecal contamination of grey water and associated microbial risks. Water Research, 37, 645-655.

Pablos, C., van Grieken, R., Marugán, J., Muñoz, A., 2012. Simultaneous photocatalytic oxidation of pharmaceuticals and inactivation of *Escherichia coli* in wastewater treatment plant effluents with suspended and immobilised TiO_2. Water Science and Technology, 65, 2016-2023.

Palmquist, H., Hanæus, J., 2005. Hazardous substances in separately collected grey and black water from ordinary Swedish households. Science of the Total Environment, 348, 151-163.

Pansonato, N., Afonso, M. V. G., Salles, C. A., Boncz, M.À., Paulo, P. L., 2011. Solar disinfection for the post-treatment of grey water by means of a continuous flow reactor. Water Science and Technology, 64, 1178-1185.

Paris, S., Schlapp, P., 2010. Grey water recycling in Vietnam-application of the HUBER-MBR process. Desalination, 257, 1027-1030.

Pidou, M., Memon, F., Stephenson, T., Jefferson, B., and Jeffrey, P., 2007. Grey water recycling: treatment options and applications. Proceedings of the Institution of Civil Engineers Engineering Sustainability, 160, 119–131.

Pidou, M., Avery, L., Stephenson, T., Jeffrey, P., Parsons, S. A., Liu, S., Memon, F. A., Jefferson, B., 2008. Chemical solutions for grey water recycling. Chemosphere, 71, 147-155.

Pidou, M., Parsons, S. A., Raymond, G., Jeffrey, P., Stephenson, T., Jefferson, B., 2009. Fouling control of a membrane coupled photocatalytic process treating grey water. Water Research, 43, 3932-3939.

Rajeshwar, K., 1995. Photoelectrochemistry and environment. Journal of Applied Electrochemitry, 25, 1067-1082.

Rajeshwar, K., Ibanez, J., 1996. Environemnetal Electrochemistry: Fundamentals, Applications in Pollution Abatement. Academic Press, San Diego.

Rajeshwar, K., Chenthamarakshan, C.R., Goeringer, S., Djukic, M., 2001. Titania-based heterogeneous photocatalysis. Materials, mechanistic issues, and implications for environmental remediation. Pure and Applied Chemistry, 73, 1849-1860.

Ramon, G., Green, M., Semiat, R., Dosoretz, C., 2004. Low strength grey water characterization and treatment by direct membrane filtration. Desalination, 170, 241-250.

Revitt, D.M., Eriksson, E., Donner, E., 2011. The implications of household grey water treatment and reuse for municipal wastewater flows and micropollutant loads. Water Research, 45, 1594-1560.

Rivero, M., Parsons, S., Jeffrey, P., Pidou, M., and Jefferson, B., 2006. Membrane Chemical Reactor (MCR) combining photocatalysis and microfiltration for grey water treatment. Water Science and Technology, 53, 173–180.

Rizzo, L., Della Rocca, C., Belgiorno, V., Bekbolet, M., 2008. Application of photocatalysis as a post treatment method of a heterotrophic-autotrophic denitrification reactor effluent. Chemosphere, 72, 1706-1711.

Rodrìguez, E. M., Fernández, G., Álvarez, P. M., Hernandez, R., Beltran, F. J., 2011. Photocatalytic degradation of organics in water in the presence of iron oxides: Effects of pH and light source. Applied Catalysis B: Environmantal, 102, 572-583.

Sanchez, M., Rivero, M. J., Ortiz, I., 2010. Photocatalytic oxidation of grey water over titanium dioxide suspensions. Desalination, 262, 141-146.

Schäfer, A. I., Nghiem, L. D., Oschmann, N., 2006. Bisphenol A retention in the direct ultrafiltration of greywater. Journal of Membrane Science, 283, 233-243.

Scheumann, R., Kraume, M., 2009. Influence of hydraulic retention time on the operation of submerged membrane sequencing batch reactor (SM-SBR) for the treatment of grey water. Desalination, 246, 444-451.

Standard Methods for the Examination of Water and Wastewater, 1999. APHA, AWWA, WPCF, 20th Edition, American Water Works Association, Washington D.C., USA.

Surendran, S., Wheatley, A. D., 1998. Grey water reclamation for non-potable reuse. Water and Environment Journal, 12, 406-413.

Toifl, M., Diaper, C., O'Halloran, R., 2008. Assessing the performance of small scale grey water treatment systems under controlled laboratory conditions. IWA World Water Congress, 7-12 September 2008, Vienna, Austria.

UK Rainwater Harvesting Association, Domestic water usage chart. http://www.rainwatershop.co.uk/contents/en-uk/about.html (Accessed June 2012).

Uyguner, C. S., Bekbolet, M., 2004. Photocatalytic degradation of natural organic matter: kinetic considerations and light intensity dependence. International Journal of Photoenergy, 6, 73–80.

Uyguner, C. S., Bekbolet, M., 2005a. Evaluation of humic acid photocatalytic degradation by UV–vis and fluorescence spectroscopy. Catalysis Today, 101, 267-274.

Uyguner, C. S., Bekbolet, M., 2005b. A comparative study on the photocatalytic degradation of the humic substances of various origins. Desalination, 176, 167-176.

Uyguner, C. S., Bekbolet, M., 2007. A comparative approach to the application of a physico-chemical and advanced oxidation combined system to natural water samples. Separation Science and Technology, 42, 1405-1419.

Uyguner, C. S., Bekbolet, M., 2009. Application of photocatalysis for the removal of natural organic matter in simulated surface and ground waters. Journal of Advanced Oxidation Technologies, 12, 87-92.

Uyguner, C. S., Bekbolet, M., 2010. TiO_2-assisted photocatalytic degradation of humic acids:effect of copper ions. Water Science and Technology, 61, 2581-2590.

Uyguner Demirel, C. S., Bekbolet, M., 2011. Significance of analytical parameters for the understanding of natural organic matter in relation to photocatalytic oxidation. Chemosphere, 84, 1009-1031.

Weitao, H., Yayi, W., Jian, Y., Xu, Z., 2011. The Inherent Biodegradability Characteritics of Light Greywater for the Different Bathe Products. Energy Procedia, 11, 3122-3128.

World Health Organization, 2006. Guidelines for the safe use of wastewater excreta and grey water. http://whqlibdoc.who.int/publications/2006/9241546824_eng.pdf (Accessed January 2011).

Xiao, Y., Xu, S., Li, Z., An, X., Zhou, L., Zhang, Y., Fu, Q. S., 2010. Progress of applied research on TiO_2 photocatalysis-membrane separation coupling technology in water and wastewater treatment. Environmental Science and Technology, 55, 1345-1353.

Zhang, G., Yao, L., Wang, L., Zhang, J., Xu, L., Fan, Z., 2012. Photocatalytic membrane reactor used water and wastewater treatment. Recent Patents on Engineering, 6, 127-136.

Zhu, X., Nanny, M. A., Butler, E. C., 2008. Photocatalytic oxidation of aqueous ammonia in model gray waters. Water Research, 42, 2736-2744.

Zuma, B. M., Tandlich, R., Whittington-Jones, K. J., Burgess, J. E., 2009. Mulch tower treatment system Part 1: Overall performance in grey water treatment. Desalination, 242, 38-56.